

Université
de Toulouse

THÈSE

En vue de l'obtention du
DOCTORAT DE L'UNIVERSITÉ DE TOULOUSE

Délivré par :
Institut National Polytechnique de Toulouse (INP Toulouse)

Discipline ou spécialité :
Génie des Procédés et Environnement

Présentée et soutenue par :
Supaporn KHANGKHAM

le : jeudi 15 novembre 2012

Titre :
Catalytic degradation of poly(methyl methacrylate) by zeolites and
regeneration of used zeolites via ozonation
Dégradation catalytique du poly(méthyl méthacrylate) sur zéolithe et
régénération de la zéolithe cokée par ozonation

Ecole doctorale :
Mécanique, Energétique, Génie civil et Procédés (MEGeP)

Unité de recherche :
Laboratoire de Génie Chimique (LGC), Toulouse

Directeur(s) de Thèse :
Prof. Dr. Henri DELMAS
Prof. Dr. Somsak DAMRONGLERD

Rapporteurs :
Prof. Dr. Iordan NIKOV
Prof. Dr. Damrong KHUMMONGKOL
Dr. Sumate CHAROENCHAIDET

Membre(s) du jury :

Prof. Dr. Henri DELMAS, Dr. Carine JULCOUR-LEBIGUE, Prof. Dr. Iordan NIKOV
Prof. Dr. Somsak DAMRONGLERD, Assist. Prof. Chawalit NGAMCHARUSSRIVICHAI
Assoc. Prof. Dr. Tharapong VITIDSANT, Prof. Dr. Damrong KHUMMONGKOL
and Dr. Sumate CHAROENCHAIDET

TITLE: CATALYTIC DEGRADATION OF POLY(METHYL METHACRYLATE)
BY ZEOLITE AND REGENERATION OF COKED ZEOLITE BY
OZONATION

Ph.D. Thesis: Chemical and Environmental Engineering, INP Toulouse,
FRANCE, 2012.

Laboratoire de Génie Chimique, 4 allée Emile Monso, BP 84234, 31432
TOULOUSE cedex 4, FRANCE.

ABSTRACT:

Catalytic degradation of PMMA was successfully performed at temperatures below 300°C. The use of zeolite catalyst could reduce reaction temperature in comparison with an ordinary thermal degradation process. It was found that the product distribution obtained from batch experiment depends on zeolite acid properties whereas the composition of the liquid fraction is directly related to the shape selectivity of the catalyst. A continuous fixed bed process was designed that allowed to obtain MMA monomer as main product. The increase of reaction temperature from 200 to 270°C showed a positive effect on the liquid product yield. However, at higher temperatures, the light product was further cracked into gaseous products. Significant deactivation of ZSM-5 catalyst was observed after 120 hours of operation, resulting in a decrease in liquid product yield.

Regeneration of the coked ZSM-5 extrudates was achieved by oxidation with ozone at low temperatures, below 150°C. The effects of temperature, GHSV and inlet concentration of ozone on carbon removal efficiency were studied. Carbon removal with ozone started at 50°C and reached a maximum of 80% at 100°C. Higher temperatures were not beneficial due to the strong limitation of ozone diffusion which confines radical production then the regeneration process to the outer surface. In optimal conditions, ozonation almost fully restored the zeolite activity without damaging the texture and active sites of zeolite, as shown from the results of regenerated catalyst in PMMA cracking.

KEYWORDS: CATALYTIC CRACKING/ PMMA/ COKE/ OZONE/ ZEOLITE/
ZSM-5/ REGENERATION

TITRE: DEGRADATION CATALYTIQUE DU POLY(METHYL METHACRYLATE)
SUR ZEOLITHE ET REGENERATION DE LA ZEOLITHE COKEE PAR
OZONATION

Thèse de Doctorat : Génie des Procédés et de l'Environnement, INP Toulouse,
FRANCE, 2012.

Laboratoire de Génie Chimique, 4 allée Emile Monso, BP 84234, 31432
TOULOUSE cedex 4, FRANCE.

RESUME:

La dégradation catalytique du PMMA a été réalisée avec succès à des températures inférieures à 300°C. L'utilisation de zéolithe comme catalyseur a permis de réduire la température de réaction par rapport aux procédés classiques de dégradation thermique. On a montré que la distribution des produits de réaction obtenus en réacteur discontinu dépend des propriétés acides du catalyseur, tandis que la composition de la fraction liquide est directement liée à la sélectivité de forme du catalyseur. Un procédé continu à lit fixe a été développé qui a permis d'obtenir le monomère MMA comme produit principal. L'augmentation de la température de réaction de 200 à 270°C a montré un effet positif sur le rendement en produit liquide. Cependant, des températures de réaction supérieures ont favorisé le craquage du monomère en produits gazeux. Une désactivation significative de la zéolithe ZSM-5 a été observée après 120 heures d'opération, entraînant une diminution du rendement en produit liquide.

La régénération des extrudés de ZSM-5 cokés a pu être réalisée par ozonation à basse température - inférieure à 150°C. On a étudié les effets de la température, du débit de gaz et de la concentration en ozone sur l'élimination de carbone. Le décockage par l'ozone a débuté dès 50°C et montré un optimum à 100°C (avec une conversion de 80%). Des températures plus élevées ne se sont pas avérées bénéfiques, en raison de la forte limitation de la diffusion interne de l'ozone qui confine en surface la production de radicaux et donc le processus de régénération. Dans les conditions optimales, l'ozonation a presque complètement restauré l'activité de la zéolithe sans en endommager la texture et les sites actifs, comme le montrent les résultats de craquage du PMMA obtenus avec le catalyseur ainsi régénéré.

MOT CLES: CRAQUAGE CATALYTIQUE/ PMMA/ COKE/ OZONE / ZEOLITHE/
ZSM-5 / REGENERATION

ACKNOWLEDGEMENTS

This dissertation would not have been accomplished without the considerable assistance of the following persons and organizations:

I would like to express my sincerest gratitude and appreciation to my advisors Prof. Dr. Somsak Damronglerd and Prof. Dr. Henri DELMAS and my co-advisors Asst. Prof. Dr. Chawalit Ngamcharussrivichai, Prof. Dr. Marie-Hélène MANERO, and especially to Dr. Carine JULCOUR-LEBIGUE, who greatly contributed to this dissertation, for their providing me with insights and guidance to recognize my mistakes, giving me an invaluable suggestion and constant encouragement. I would like to sincerely appreciate to Assoc. Prof. Dr. Kejvalee Pruksathorn, for serving as the reporter and chairman of my thesis committee. Furthermore, I would like to extend my appreciation to Prof. Dr. Iordan NIKOV, Prof. Dr. Damrong Khummongkol and Dr. Sumate Charoenchaidet for their serving as the reporter and member of my thesis committee. Moreover, I would like to appreciate Assoc. Prof. Dr. Tharapong Vitidsant and Asst. Prof. Dr. Prapan Kuchonthara for their serving as member of my thesis committee. I would like to acknowledge the Office of the Higher Education Commission, Embassy of France in Thailand and Graduate School Chulalongkorn University for financial contribution to this research. In addition, I would also like to acknowledge LGC/ENSIACET-INPT, Department of Chemical Technology, Faculty of Science, Chulalongkorn University and Siam Cement Group Public Company Limited for supplying valuable materials and equipment. I would also like to acknowledge the scientists and technicians at LGC/ENSIACET-INPT and Chulalongkorn University especially to J.L. Labat, J.L. Nadalin, I. Coghe, V. Loisel and A. Müller (LGC) for technical assistance on the set-up, M.L. de Solan Bethmale, C. Rey-Rouch, G. Raimbeaux (SAP, LGC), P. Jame, A. Bonhomme (SCA, Lyon), L. Pinard and J.D. Comparot (IC2MP, Poitiers) for characterization of the zeolites. I would like to give my special thanks to the officers, my colleagues' friends in Chulalongkorn University and ENSIACET-INPT and my family for their eternal support, love and encouragement. Last but not less, I would like to give a heartfelt thanks to Mr. Sompoch Pooperasupong who is always beside me and lightens adversity by dividing and sharing it. Without him, this thesis could certainly never have become a reality.

CONTENTS

	Page
ABSTRACT (ENGLISH).....	iii
ABSTRACT (FRENCH).....	iv
ACKNOWLEDGEMENTS.....	v
CONTENTS.....	vii
LIST OF TABLES.....	x
LIST OF FIGURES.....	xi
LIST OF ABBREVIATIONS.....	xv
CHAPTER I INTRODUCTION.....	1
1.1 Background, motivations and objectives of this dissertation.....	1
1.2 Scope of the dissertation.....	3
1.3 Anticipated benefits.....	4
1.4 Outline of this dissertation.....	4
CHAPTER II THEORY AND LITERATURE REVIEW.....	6
2.1 Classification of polymer/plastic waste management.....	6
2.1.1 Landfilling.....	7
2.1.2 Mechanical recycling.....	7
2.1.3 Biological recycling.....	8
2.1.4 Thermal recycling/incineration.....	8
2.1.5 Chemical recycling.....	9
2.2 Basics of acrylic plastic or poly (methyl methacrylate) (PMMA).....	12
2.3 Basics of thermal cracking and catalytic cracking.....	14
2.3.1 Thermal cracking.....	14
2.3.2 Catalytic cracking.....	18
2.4 Catalytic system.....	21
2.4.1 Basics of a catalytic system.....	21
2.4.2 Zeolite catalyst.....	22
2.4.3 Characterization of the zeolite catalysts.....	31

	Page
2.5 Deactivation of solid catalysts.....	33
2.5.1 Causes of deactivation.....	33
2.5.2 Characterization of solid catalyst deactivation.....	35
2.5.3 Methods of coke investigation and results.....	36
2.6 Regeneration of zeolite catalyst.....	39
2.6.1 Regeneration of catalyst deactivated by coke or carbon.....	39
2.6.2 Regeneration of poisoned catalysts.....	40
2.6.3 Redispersion of sintered catalysts.....	40
2.7 LITERATURE REVIEWS.....	45
2.7.1 Thermal and catalytic cracking of plastic waste.....	46
2.7.2 Deactivation and regeneration of solid catalyst.....	49
CHAPTER III EXPERIMENTAL.....	53
3.1 Degradation of PMMA by zeolite catalyst.....	53
3.1.1 Materials.....	53
3.1.2 Experimental procedure and set-up.....	58
3.2 Regeneration of used catalyst by ozonation.....	67
3.2.1 Materials.....	68
3.2.2 Experimental procedure and set-up.....	70
CHAPTER IV DEGRADATION OF PMMA BY ZEOLITE CATALYST.....	80
4.1 Thermogravimetric /differential thermal analysis (TG/DTA) of PMMA.....	81
4.2 Catalyst Characterization.....	83
4.2.1 X-ray diffraction (XRD).....	83
4.2.2 Surface area and porosity.....	86
4.2.3 Acidity in term of acid amount and acid strength.....	87
4.3 Catalyst evaluation and screening in batch experiment.....	95
4.3.1 Effect of acidity in terms of acid strength.....	96
4.3.2 Effect of acidity in terms of amount of acid sites.....	98
4.3.3 Analysis of liquid products from batch experiments by GC-MS.....	100
4.4 Catalytic activity for the degradation of PMMA in continuous experiment.....	105
4.4.1 Effect of temperature.....	105
4.4.2 Effect of PMMA feed rate.....	107

	Page
4.4.3 Analysis of liquid and gaseous products of continuous experiment by GC-MS.....	108
CHAPTER V REGENERATION OF USED CATALYST BY OZONATION.....	112
5.1 Characterization of the zeolite.....	113
5.1.1 Surface area and porosity.....	115
5.1.2 Elemental analysis.....	117
5.1.3 Infrared and Raman spectroscopy.....	120
5.1.4 Thermogravimetry.....	124
5.2 Regeneration of the catalysts by ozonation.....	127
5.2.1 Effect of operating parameters.....	127
5.2.2 Carbon profiles in the reactor and in the particles.....	132
5.3 Activity assessment.....	135
5.3.1 Acid properties.....	135
5.3.2 PMMA degradation results.....	143
CHAPTER VI CONCLUSIONS AND RECOMMENDATIONS.....	146
6.1 Degradation of PMMA by zeolite catalyst.....	146
6.2 Regeneration of used catalyst by ozonation.....	147
6.3 Recommendations.....	148
NOMENCLATURE.....	150
REFERENCES.....	151
APPENDICES.....	165
APPENDIX A.....	166
APPENDIX B.....	167

LIST OF TABLES

TABLE	Page
2.1 Structural features of common zeolites used as catalysts in cracking	27
2.2 Deactivation of solid catalysts: origin, mechanism and typical examples.....	35
2.3 Conventional methods and representative examples of catalyst regeneration from scientific and patent literatures.....	41
3.1 Conditions of USY dealumination.....	54
3.2 Physical properties of PMMA.....	56
3.3 Specification of chemicals and gases used in part I; Degradation of PMMA...	57
3.4 Analytical techniques and applications in PMMA degradation.....	58
3.5 Operating conditions of the GC-MS for liquid and gas product analysis.....	67
3.6 Specification of chemicals and gases used in part II; Regeneration of spent zeolite.....	69
3.7 Analytical techniques and applications in coked zeolite regeneration.....	70
4.1 Physical characteristics of zeolite samples.....	86
4.2 Summary of the NH ₃ -TPD results for different zeolite samples.....	94
4.3 Composition of light fraction from PMMA degradation by zeolite in batch experiment as analyzed by GC-MS.....	101
4.4 Chemical composition of heavy fraction for various types of zeolite catalyst.....	102
4.5 Liquid product yields obtained at various temperatures.....	106
4.6 Liquid product yields at various feed rates (PMMA 250 g, 270°C).....	107
4.7 Composition of liquid and gas products from continuous catalytic PMMA degradation by zeolite in continuous experiment as analyzed by GC-MS.....	110
5.1 Physical characteristics of zeolite samples.....	115
5.2 Elemental analysis from EDX spectroscopy and carbon content from flash combustion.....	119
5.3 Summary of the NH ₃ -TPD results for fresh, used and regenerated zeolite samples and their physical characteristics.....	139
5.4 Acid properties of fresh and regenerated catalysts by pyridine adsorption method.....	142

LIST OF FIGURES

FIGURE	Page
2.1 Different routes for plastic waste management.....	7
2.2 Polymerization of methacrylate to poly (methyl methacrylate).....	12
2.3 Three step chain scissions leading to the thermal degradation of acrylic polymers.....	16
2.4 Degradation pathways for PMMA.....	17
2.5 Catalytic cracking mechanisms.....	20
2.6 Pore size of (a) chabazite 8-ring, (b) ZSM-5 10-ring, and (c) beta zeolite 12-ring.....	25
2.7 Schematic representation of the pore network of (a) MFI (b) BEA and (c) FUA zeolites. Vertices represent T atoms (Si or Al); lines between vertices are the O bridges.....	27
3.1 Photographs of zeolite catalyst.....	55
3.2 Photographs of PMMA polymer.....	55
3.3 Profiles of temperature programmed for TPD experiment (a) with and (b) without NH ₃ feeding (TPD-NH ₃ /TPD w/o NH ₃).....	61
3.4 High Pressure/High Temperature Reactors 4576, 250 mL (Parr instrument)...	62
3.5 Schematic diagram of continuous catalytic degradation unit.....	65
3.6 Liquid products from catalytic cracking of PMMA; (a) heavy fraction, (b) light fraction.....	66
3.7 Photographs of coked catalysts from continuous process; (a) ZSM-5 particles from middle-bottom of PMMA cracking reactor (ZSM5-A) and (b) ZSM-5 particles from top of PMMA cracking reactor (ZSM5-B).....	68
3.8 Profiles of temperature programmed for TPD experiment (a) with and (b) without NH ₃ feeding (TPD-NH ₃ /TPD w/o NH ₃).....	74
3.9 Schematic diagram of the set-up for the regeneration of coked zeolite.....	76
3.10 Mini bench top reactor 4560, 100 mL (Parr instrument).....	78
4.1 Dynamic TG analysis of PMMA under nitrogen atmosphere; (a) TG, DTG and DTA curve of PMMA, (b) the enlargement of DTG curve and its deconvolution peaks.....	82

FIGURE	Page
4.2 Powder XRD patterns for zeolites used in this study; (a) ZSM5-25, (b) ZSM5-1000 (c) Beta-25, (d) HUSY-6, (e) USY-30, (f) USY-63 and (g) USY-337.....	85
4.3 NH ₃ -TPD profile of fresh ZSM-5 (solid line) and blank test (dash line).....	88
4.4 NH ₃ -TPD profile (black line) and Gaussian deconvolution (green lines) with cumulative fit (red line); (a) USY-30, (b) Beta-25 and (c) ZSM5-25.....	90
4.5 NH ₃ -TPD profile of zeolite samples (black solid line) and Gaussian deconvolution (green lines) with cumulative fit (red line); (a) ZSM5-25, (b) ZSM5-1000 (c) HUSY-6, (d) USY-63 and (e) USY-337.....	92
4.6 Photo of PMMA before and after thermal degradation at 320°C.....	95
4.7 Product distribution of PMMA degradation over various types of zeolite catalyst.....	97
4.8 Product distribution of PMMA degradation over ZSM-5 and USY with different SiO ₂ /Al ₂ O ₃ ratios.....	99
4.9 GC-MS spectra of light product from PMMA degradation by zeolite in batch experiment (a) and pure MMA (b).....	101
4.10 GC-MS spectra of light product from continuous catalytic PMMA degradation at various temperatures; (a) 270°C, (b) 280°C, (c) 290°C, (d) 300°C and (e) pure MMA.....	109
4.11 GC-MS spectra of gas product from continuous catalytic PMMA degradation at reaction temperature of 270°C.....	111
5.1 Liquid product yield vs time on stream (TOS).....	113
5.2 Photographs of coked catalysts from continuous process; (a) ZSM5 particles from middle-bottom of PMMA cracking reactor (ZSM5-A) and (b) ZSM5 particles from top of PMMA cracking reactor (ZSM5-B).....	114
5.3 Evolution of BET surface areas of zeolite extrudes as a function of carbon content.....	116
5.4 SEM micrographs of the fresh zeolite and the coked zeolites: (a) zeolite particle, (b) fresh ZSM5 zeolite, (c) ZSM5-A and (d) ZSM5-B.....	117
5.5 Elemental carbon profile a on a cross-section of particle; (a) ZSM5-A and (b) ZSM5-B.....	118

FIGURE	Page
5.6 FT-IR spectra of fresh zeolite and spent zeolite; (a) fresh ZSM-5, (b) ZSM5-A and (c) ZSM5-B.....	121
5.7 Raman spectra of fresh and used catalyst with Ar laser 632 nm; (a) ZSM5-B, (b) ZSM5-A and (c) fresh ZSM-5.....	122
5.8 Raman spectra of ZSM-5 (ZSM5-B) from Raman spectroscopy with Nd:YAG (neodymium-doped yttrium aluminium garnet; Nd:Y3Al5O12), 1064 nm; (a) 180 mW Res 4.0 cm ⁻¹ No. of scans 200, (b) 180 mW Res 4.0 cm ⁻¹ No. of scans 400 and (c) 30 mW Res 16.0 cm ⁻¹ No. of scans 2000.....	123
5.9 Thermograms of coked zeolite under N ₂ , along with identification of evolved gases from IR spectroscopy: (a) ZSM5-A and (b) ZSM5-B.....	125
5.10 Evolution of carbon removal as a function of inlet O ₃ concentration for different outlet temperature (Q _G = 12.7 l•h ⁻¹ , TOS = 30 min).....	128
5.11 Evolution of carbon removal as a function of (a) time on stream and (b) outlet temperature (Q _G = 12.7 l•h ⁻¹ , C _{O₃,in} = 48 g•m ⁻³).....	129
5.12 Ozone decomposition as a function of outlet temperature (Q _G = 12.7 l•h ⁻¹ , C _{O₃,in} = 48 g•m ⁻³).....	130
5.13 Axial profiles of carbon removal (T _{outlet} = 95°C, Q _G = 12.7 l•h ⁻¹ , C _{O₃,in} = 48 g•m ⁻³ , TOS = 1 h).....	132
5.14 Photos of pellets (a) before and (b,c) after regeneration (Q _G = 12.7 l•h ⁻¹ , C _{O₃,in} = 48 g•m ⁻³ , TOS = 1 h): top pictures: T _{outlet} = 100°C, bottom pictures: T _{outlet} = 140°C.....	134
5.15 NH ₃ -TPD profile of used ZSM-5; raw TCD signal (black line) and signal from blank test (red line).....	135
5.16 NH ₃ -TPD profile of fresh zeolite, coked and regenerated samples with respect to regeneration duration; (a) fresh ZSM-5, (b) used catalyst (ZSM5-B), (c-e) regeneration duration of 1, 2 and 4 h, respectively (regeneration temperature of 95°C)	137
5.17 NH ₃ -TPD profile of fresh zeolite, coked and regenerated samples with respect to regeneration temperature; (a) fresh ZSM-5, (b-e) regenerated at 140, 105, 95 and 75°C (regeneration duration 1 h) and (f) used catalyst (ZSM5-A).....	138

FIGURE	Page
5.18 Distribution of acid sites for fresh zeolite, coked and regenerated samples A: (a) influence of regeneration duration and (b) influence of regeneration temperature.....	141
5.19 PMMA degradation yields: distribution of gas and liquid products.....	144
A-1 Ozone concentration and production at various flows rate (20°C).....	166
B-1 NH ₃ -TPD profile of amorphous silica-alumina (ASA) and its deconvolution curve.....	167
B-2 NH ₃ -TPD profile of used ZSM5; (a) used ZSM5 and its profile from blank test and (b) subtracted TPD profile and its deconvolution curve.....	168

LIST OF ABBREVIATIONS

BET	Brunauer-Emmett-Teller
BJH	Barrett-Joyner-Halenda
CHN	Carbon Hydrogen Nitrogen elemental analysis
FCC	Fluid catalytic cracking
GC-MS	Gas chromatograph and mass spectrometry
IZA	The International Zeolite Association
MMA	Methyl methacrylate
PMMA	Poly (methyl methacrylate)
SEM-EDX	Scanning electron microscopy coupled with energy dispersive X-ray spectroscopy
TCD	Thermal conductivity detector
TGA-IR	Thermogravimetry coupled with infrared spectroscopy
TG-DTA	Thermogravimetric /differential thermal analysis
TPD	Temperature programmed desorption
USY	Ultrastable Y
XRD	X-ray diffraction
XRF	X-ray fluorescence spectrometry
ZSM	Zeolite Socony Mobil

CHAPTER I

INTRODUCTION

In this chapter, a general background on both the degradation of poly (methyl methacrylate) and regeneration of spent catalyst is presented. The overall structure of this thesis along with my motivations and objectives, scope of the dissertation, anticipated benefits and outline of this dissertation are also given.

1.1 Background, motivations and objectives of this dissertation

Acrylic plastic or poly (methyl methacrylate) (PMMA) is widely used for making daily consumer products or used as a glass substitute in many applications because of its excellent toughness, transparency, easy thermoforming and good stability. In recent years, the production and consumption of PMMA have increased significantly, extensive use of this material leads to the major concern on the waste PMMA which is usually generated during the production and sheeting process. In industry, the conventional management of waste PMMA consists of mechanical recycling and thermal recycling. Among these two methods, thermal cracking/pyrolysis is the more popular since it provides MMA monomer and/or gas and liquid products which can be reutilized as chemical reagents or fuels. However, this process has two major drawbacks: high energy consumption and broad product range that requires further processing to upgrade product quality. In order to solve these problems, the alternatives to the conventional procedures of mechanical recycling and

thermal cracking of scraped PMMA are being undertaken in this study with the application of catalytic cracking process using zeolite. Zeolites have been proved to be the practical catalyst for cracking process because of their unique acid and shape-selective properties which minimize the energy consumption of this process and control the appropriate shape and size of products; moreover, they can also be easily regenerated. Therefore, PMMA degradation catalyzed by zeolites is predicted to have tremendous future potential as a viable commercial recycling process. Although more than 200 zeolitic structures were discovered, the research on new zeolites and/or modification of existing zeolites for specific purposes has still been an interesting issue (Wagner et al., 1997; Villaescusa, Barrett and Cambor, 1999). Nevertheless, the application of zeolites as catalyst for polymer cracking process also has some concerns, for instance, their cost which directly relates to their complex preparation (Van Bekkum et al., 2001), and the mass transfer limitations due to their microporous structure (Aguado et al., 1997). For this reason, only a few zeolites are suitable to be used as catalysts for commercial catalytic cracking process such as Y, Ultrastable Y, Beta and ZSM-5 (Van Bekkum et al., 2001). The spent zeolites can be easily regenerated by several methods such as high temperature combustion, or reaction with oxygen or nitrous oxide-containing mixtures (Ivanov, Sobolev, and Panov, 2003). Even if zeolite catalysts can be easily regenerated by many methods, it is still a common feature which requires efficient and low-cost regeneration techniques for the process economy. As an alternative for the regeneration of spent zeolite, ozonation is an attractive method, as the process temperature can be lower due to the high oxidizing activity of ozone (Monneyron et al., 2003). This technique is therefore

particularly interesting to preserve the structure of the zeolite catalyst and to prevent dealumination (Copperthwaite et al., 1986).

The objective of this dissertation was to investigate the catalytic degradation of scrapped PMMA over zeolites with different crystalline structures and acidic properties under both batch and continuous conditions. Moreover, to restore the catalytic activity of spent zeolite, the regeneration of coked catalyst was studied using an ozone-enriched oxygen stream at low temperatures in the range of 20 to 150°C. The suitable operating conditions for coke removal and catalyst activity restoration were also investigated. In the following, the term “coke” will be referred to as all carbonaceous materials which are located on the spent zeolite, irrespective of their chemical nature and molecular weight (Bauer and Karge, 2007).

1.2 Scope of the dissertation

In this dissertation, the influence of zeolite catalysts (ZSM-5, Beta and USY) on the yield and distribution of products obtained from the degradation of scrapped PMMA was extensively investigated. The characterization of the physicochemical properties of zeolite catalysts, such as crystallinity, $\text{SiO}_2/\text{Al}_2\text{O}_3$ ratio, porosity, morphology, acidity was done by various analytical techniques including X-ray diffraction (XRD), X-ray fluorescence spectrometry (XRF), N_2 adsorption-desorption measurement, scanning electron microscopy (SEM) and temperature-programmed desorption of NH_3 (TPD- NH_3). Thermal and catalytic degradation of PMMA was performed in both batch and continuous reactors. The reaction parameters included type of zeolite, reaction temperature and contact time. The analysis of gas and liquid products from the degradation of PMMA was carried out on a gas chromatograph

with mass spectrometry detection (GC-MS). In addition, the oxidative regeneration of spent zeolite catalyst by ozonation was investigated. The reaction parameters included ozone concentration, reaction temperature and reaction time. The physicochemical properties of spent zeolite before and after the regeneration by ozonation, such as crystallinity, porosity, morphology, acidity, and coke deposition and dispersion, were analyzed by X-ray diffraction (XRD), N₂ adsorption-desorption measurement, Hg intrusion porosimetry, scanning electron microscopy coupled with energy dispersive X-ray spectrometry (SEM-EDX), temperature-programmed desorption of NH₃ (TPD-NH₃), infrared spectroscopic study of pyridine adsorption-desorption, thermogravimetry coupled with infrared spectroscopy (TGA-IR) and CHN elemental analysis (flash combustion). The reusability of regenerated zeolite catalyst for PMMA degradation was also examined.

1.3 Anticipated benefits

1. To recover the MMA monomer and increase the commercial value of scraped PMMA by catalytic degradation.
2. To obtain the suitable conditions for restoring the activity of spent catalyst by ozonation.

1.4 Outline of the dissertation

This dissertation was formatted in a chapter form. Chapter I presents a general introduction to the subject of polymer waste recycling, overall motivations, objectives, scope and anticipated benefits of this research. Chapter II gives theoretical

information and literature review on catalysis, polymers and areas relating to catalytic degradation. Previous and current researches relevant to the thermal and catalytic degradation are brought to attention. The basic structure of poly (methyl methacrylate) (PMMA) and background of zeolites used as catalysts in this research are described. This chapter also mentions the deactivation and regeneration of solid catalyst. Experimental procedures and details of the materials and equipments used for each relevant experiment are described in Chapter III. This chapter is divided into two main parts: the degradation of PMMA by using zeolite and the regeneration of spent catalyst by ozonation. Therefore, in Chapter IV, the degradation of PMMA by zeolite catalyst is investigated. Thermogravimetric analysis of PMMA, catalyst characterization and evaluation are explained. The catalytic activity of different zeolites for the degradation of PMMA is also examined. Chapter V investigates suitable conditions for the regeneration of spent zeolite by ozonation so that to restore their catalytic activity. Finally, the overall conclusions and recommendations on the study are predicated in Chapter VI.

CHAPTER II

THEORY AND LITERATURE REVIEW

In this chapter, a short review on polymer/plastic waste management is introduced in section 2.1. The structure of poly (methyl methacrylate) (PMMA) is described in section 2.2. A brief description of thermal and catalytic degradation of polymers is given in section 2.3. Basics of the catalytic system are displayed in section 2.4, where zeolite catalysts and techniques used for their characterization are described. The deactivation and regeneration of solid catalyst and the analytical techniques used for coke characterization are described in sections 2.5 and 2.6, respectively. In the last section, literature reviews are performed.

2.1 Classification of polymer/plastic waste management

The rapid increase of polymer/plastic consumption has led to difficulties in managing the resulting wastes. The issue of polymer waste management is not only technical, but also concerns social, economic and even political aspects. This is the reason why multitudinous methods have been considered and applied to solve the problems related to polymer waste management. The alternative ways which are practical techniques for polymer/plastic waste management are displayed in Figure 2.1.

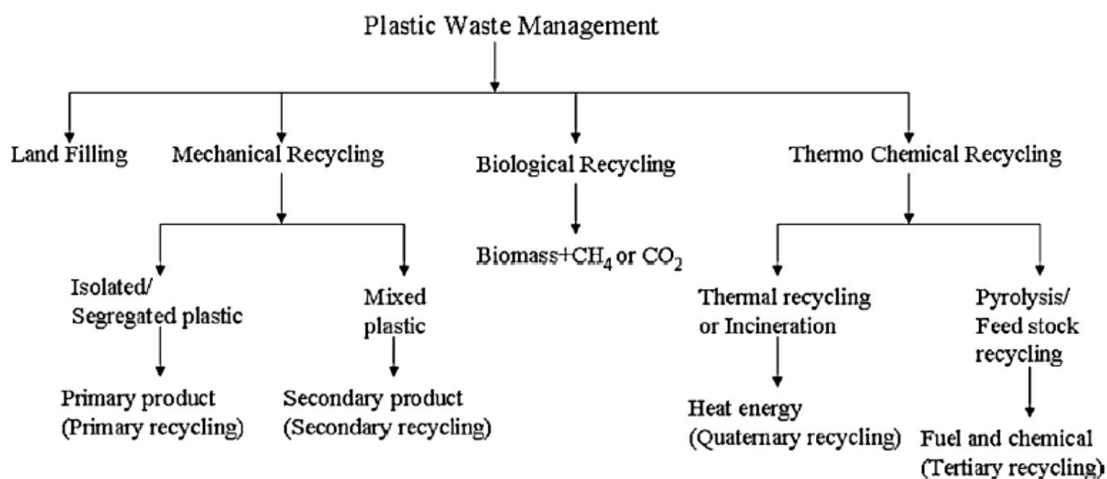


Figure 2.1 Different routes for plastic waste management (Achyut, Singh, and Mishra, 2010).

2.1.1 Landfilling

Landfilling is the main process for disposing solid waste. Most of the polymer / plastic wastes have been handled by this process. However, the disposal of solid wastes by landfill is turning into undesirable, due to legislative pressures, explosion of greenhouse gases and low biodegradability (Achyut et al., 2010).

2.1.2 Mechanical recycling

Mechanical recycling is the process for recovering polymer/plastic waste to reuse in manufacturing plastic products by means of a mechanical technique. It was encouraged and commercialized all over the world back in the 1970s (Al-Salem, Lettieri, and Baeyens, 2009). In mechanical reprocessing process, the plastic waste is fed into the elementary production process to acquire a product with has the identical specification as the original product. However, in case of the mixed polymer, the

process is restricted due to the fact that the blend of different kinds of polymers may affect the properties of polymers and therefore limit their potential to be used in the conventional applications (Ylä-Mella, 2005: online).

2.1.3 Biological recycling

Biodegradable plastics have been already successfully used. They are usually applied for packaging in food/catering industry, their photodegradation occurring in 1 to 2 months. Some non-packaging applications are also reported. Nevertheless, the biological degradation of plastics requires appropriate conditions. In addition, separation of degradable and non-degradable plastics is complicated. Furthermore, they may cause an increase of greenhouse gas emissions, namely methane, which is produced by anaerobic degradation (Achyut et al., 2010).

2.1.4 Thermal recycling/incineration

Thermal recycling/incineration is the favorite energy recovery process because selling waste plastics as fuel grants a financial income. Although its advantage is the heat generation, this process is restricted to the most developed countries due to its air pollution aspects for instance it produces greenhouse gases as well as some highly toxic pollutants. Thus this recycling process doesn't solve the waste problem, but shifts the problem to an air pollution one.

2.1.5 Chemical recycling

Chemical recycling or feedstock recycling process is purposed to reorganize polymer waste into elementary monomers or other valuable chemicals based on the degradation of plastics / polymers by applying heat, chemical agents and/or catalysts. This process can provide various products which can be applied as chemical reagents or fuels (Serrano, Aguado, and Escola, 2000). There are 3 main techniques: depolymerization, partial oxidation and cracking/pyrolysis (hydrocracking, thermal and catalytic cracking).

2.1.5.1 Depolymerization

Depolymerization is essentially the reverse of the polymerization process. In the simplest case, depolymerization consists in initiation at chain ends, depropagation, and termination. Condensation polymers such as polyamides, polyesters, nylons and polyethylene terephthalate can be depolymerized via reverse reactions. Nevertheless, addition polymers such as polyolefins cannot be certainly depolymerized into elementary monomers by reversible synthesis reactions (Achyut et al., 2010).

2.1.5.2 Partial oxidation

In comparison with the direct combustion of polymer wastes which may be detrimental to the environment due to the generation of noxious substances (NO_x) such as nitrogen oxide (NO), sulfur dioxide (SO_2) and light hydrocarbons, a partial oxidation of polymers or other carbonaceous materials known as gasification is more interesting. This technique yields a gaseous mixture consisting of carbon monoxide

(CO) and hydrogen (H₂), the so-called synthesis gas, which can be used in various chemical processes. In fact, this technique has been firstly applied to coal conversion process, and then to petroleum / natural gas processing (Serrano et al., 2000; Ylä-Mella, 2005: online). Co-gasification of biomass with polymer wastes was indicated to have a capacity to produce much hydrogen whereas less carbon monoxide. Other valuable chemical agents can be also produced by partial oxidation technique; an example is the production of acetic acid from polyolefins by nitrogen oxide and/or oxygen (Achyut et al., 2010).

2.1.5.3 Cracking/pyrolysis

Cracking process breaks down chains or macromolecules into valuable lower molecular weight compounds which can be used as fuels or chemical agents. This process can be conducted under nitrogen atmosphere, without or with catalyst, referred to as “thermal cracking” and “catalytic cracking”, respectively. It is sometime operated under hydrogen atmosphere, called “hydrocracking”, with the aim of improving the quality of products. These three different cracking processes are detailed below.

Thermal cracking

Thermal cracking or thermal degradation of the polymers is breaking up polymer molecules into smaller chemical agents by heat in the absence of catalyst. This process is typically carried out using high temperatures and pressures in oxygen-free or nearly oxygen-free environment, usually under nitrogen atmosphere. The extent of cracking reactions mainly depends on the reaction temperature and

residence time, and therefore reactor design. Major drawbacks of this process are a high energy consumption and a very broad product distribution.

Catalytic cracking

Various types of catalysts have been applied for the cracking process with the aim of amending the drawbacks of thermal cracking. The presence of a catalyst allows the cracking reactions to proceed at lower reaction temperature and to require less time. In addition, control of the product distribution is permitted by the use of shape selective catalyst, resulting in a narrow product range. From an economic point of view, this method is a very attractive polymer recycling process, especially if lesser quantities of catalysts are needed (Achyut et al., 2010).

Hydrocracking

Hydrocracking, the cracking process which takes place under a hydrogen atmosphere, is also a useful process to convert polymers into other chemical products. In case of the absence of hydrogen, products obtained from the cracking process usually contain unsaturated compounds which are often unstable and are able to further react with other species or recombine with each other. The presence of hydrogen leads to the hydrogenation of unsaturated compounds, resulting in the presence of highly saturated species concurrent with the lessening of olefins in the liquid products, therefore, making them more suitable for use as fuels. Moreover, hydrogen can also eliminate hetero atoms, such as chlorine, nitrogen and sulfur, in the form of gaseous products. Nevertheless, a major drawback is that this process has

high operating cost because high pressure hydrogen atmosphere is required (Serrano et al., 2000; Ylä-Mella, 2005: online).

2.2 Basics of acrylic plastic or poly (methyl methacrylate) (PMMA)

Acrylic plastic or poly (methyl methacrylate) (PMMA) is widely used in many applications because of its physical and mechanical properties such as high optical transmission (92% light transmission) in the infra- red and visible ranges from 380 to 780 nm, toughness, easy thermoforming and good stability. PMMA is frequently used as a light or shatter-resistant alternative to glass. The reflection angle on an internal surface is 41 to 42° which can be used for making light conductors and fiber optic filaments. Its refractive index is 1.49 which is suitable for manufacturing optical products (Gaggione Sas, 2007: online). Chemically, it is a vinyl polymer, made by free radical vinyl polymerization from the MMA monomer. This material was developed in 1928 in various laboratories, and was first brought to market in 1933 by Rohm and Haas Company, under the trademark Plexiglas.

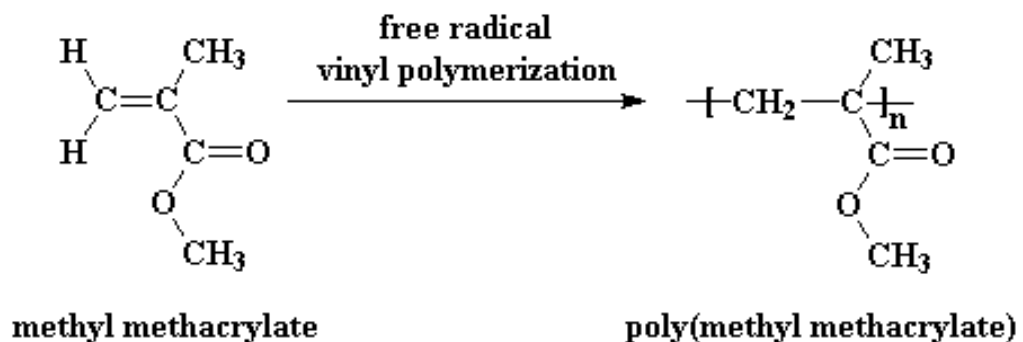


Figure 2.2 Polymerization of methacrylate to poly (methyl methacrylate) (Mathias, 2005: online).

The free radical polymerization of methacrylate is a chain-reaction (known as chain-growth or addition) polymerization across the carbon-carbon double bond of the monomer (Figure. 2.2). The polymerization can be conducted homogeneously either by bulk (mass) polymerization or by solution polymerization, or heterogeneously either by suspension polymerization or by emulsion polymerization. Conversely to other types of polymerizations, monomers with absolute dryness are not required. Nevertheless, polymerization under an oxygen-free atmosphere is absolutely recommended in order to achieve successful polymerization because oxygen is a radical scavenger by which the free radical polymerizations can be terminated.

Generally, the production of PMMA via radical initiation including living radical polymerization (LRP) is preferred, however, synthesis via anionic polymerization can also be done. Normally, approximately 2 kg (about 4.4 lbs) of petroleum is required for the production of 1 kg (about 2.2 lbs) of PMMA. PMMA can be used as a substitute for polycarbonate (PC), especially in case high strength is not a major requirement. Moreover, it is not composed of bisphenol-A, the potentially harmful species contained in polycarbonate. PMMA is one of the widely used polymeric materials because of its excellent properties, easy handling and processing, and low cost. However, the use of this material also has some limitations because it is brittle when loaded, especially under an impact force, and is scratched more easily than glass.

2.3 Basics of thermal cracking and catalytic cracking

The various recycling processes were previously introduced. This dissertation concentrates on tertiary recycling because of its great importance in future industry. Both thermal and catalytic degradation belong to the group of tertiary recycling processes. When the process temperature reaches a certain value, the structure of the polymer molecules becomes unstable. This causes the carbon chain to break into several feedstock molecules with less carbon atoms belonging to each molecule than the original. The number of carbon atoms per molecule varies, so that the cracking product shows a wide distribution of different kinds of feedstock. For this reason, a further upgrading process is necessary to filter the large molecules out of the product. By using thermal degradation as a recycling mechanism, process temperatures up to 900°C are required and the product distribution is very wide. Pilot tests of thermal cracking usually operate in kilns or fluidized beds (Toju S. Kpere-Daibo, 2009).

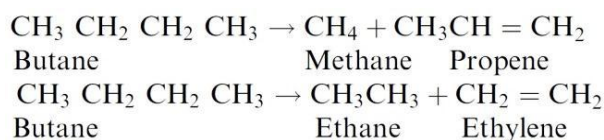
2.3.1 Thermal cracking

Thermal cracking decomposes the polymer and/or petroleum materials under temperatures of at least 350-500°C. In some cases, higher temperatures up to 700-900°C are required to achieve appropriate product yields. In this process, high molecular weight materials, e.g. polymer and long chain hydrocarbons, are broken down into smaller molecules. The mechanism of cracking reaction involves the dissociation of carbon bonds via β -scission which is thermodynamically favored only at high temperatures. In other words, the cracking reaction can produce lower boiling point (lower molecular weight) products from higher boiling point (higher molecular weight) substances. Nevertheless, some compounds, whose molecular weights are

higher than the original substances, can be also produced during cracking process by secondary reactions. The cracking reaction can yield gaseous, liquid or even solid products which are frequently categorized based on their boiling ranges such as; LPG (gas), naphtha, gasoline, kerosene, light and heavy gas oil (liquid) and coke (solid). The distribution of cracking products can be controlled by both process design and adjustment of reaction conditions.

Generally, there are two types of reactions involved in cracking:

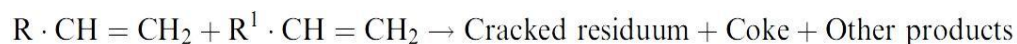
1. Primary reactions, or decomposition of large or long-chain molecules into smaller species:



2. Secondary reactions, or recombination of some of the primary products to form larger or more complex molecules:



or



Thermal cracking of an acrylic polymer, synthesized via free-radical polymerization, occurs according to a three step mechanism: the first (Figure 2.3 (1)) is initiated by dissociations of head-to-head (reverse) linkages which are causes of defects in polymer backbone. This step is the easiest and usually proceeds at a temperature of about 160°C; the second (Figure 2.3 (2)), which takes place at a temperature of about 270 °C consists in a dissociation of the chain-ends initiated from

vinylidene groups; and the last (Figure 2.3 (3)) is a random scission of the weakest bonds of the polymer chain (Wampler, 1989, Pielichowski and Njuguna, 2005).

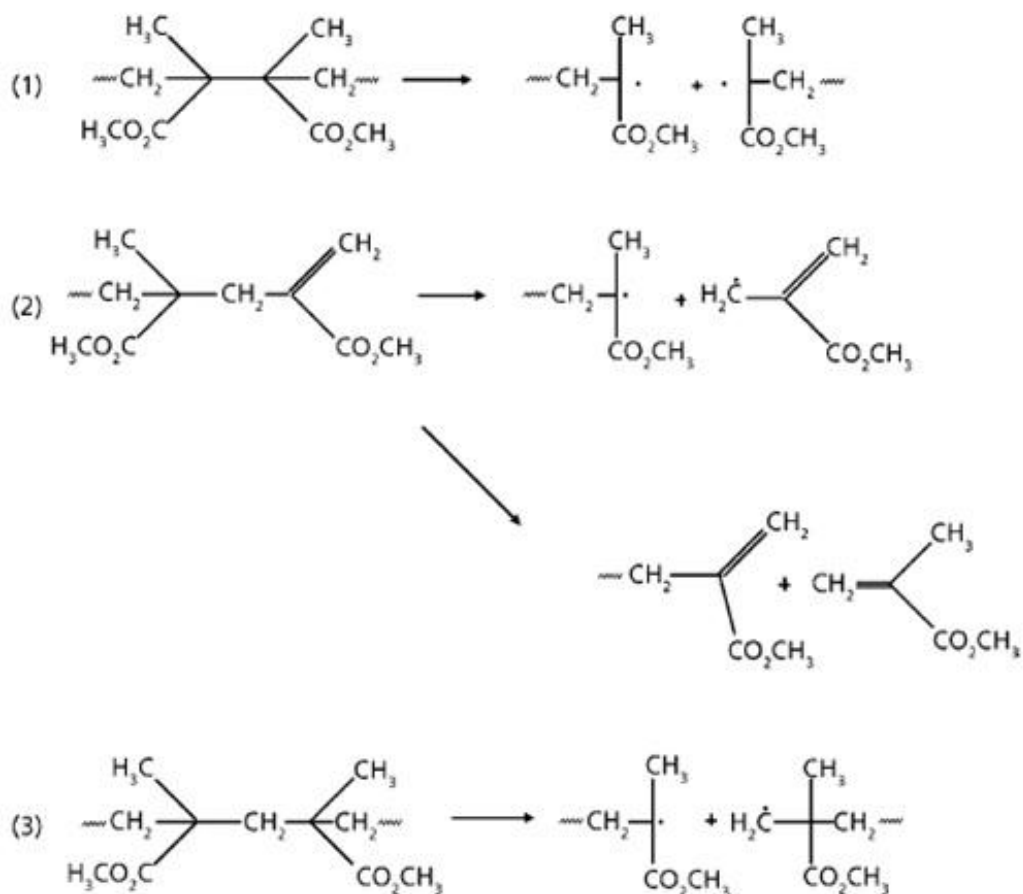


Figure 2.3 Three step chain scissions leading to the thermal degradation of acrylic polymers (Pielichowski and Njuguna, 2005).

Since PMMA polymer is widely used, e.g., in orthopedic surgery, fracture fixation, human body implantations and as filler in irregularly shaped skeletal defects or voids, a considerable amount of scientific researches on the thermal degradation of PMMA has been conducted. The rate of thermal cracking was reported to be dependent on the initial degree of polymerization, which is used for the identification

of mechanisms of thermal cracking, e.g., a radical one (Figure 2.4) (Holland and Hay, 2002 Cited in Pielichowski and Njuguna, 2005).

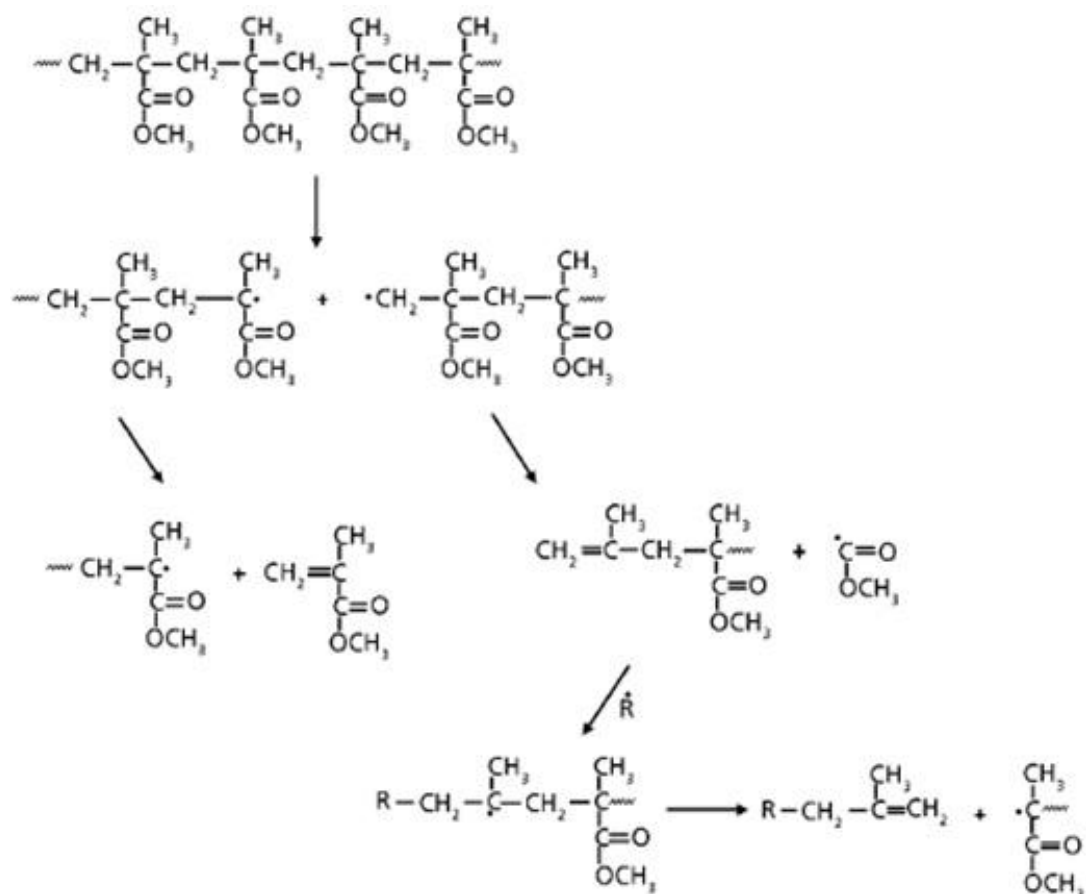


Figure 2.4 Degradation pathways for PMMA (Wilkie, 1999, cited in Pielichowski and Njuguna, 2005).

It has been reported (Peterson, Vyazovkin, and Wight, 1999, cited in Pielichowski and Njuguna, 2005; Holland and Hay, 2002, cited in Pielichowski and Njuguna, 2005) that elimination of side-groups can also take place in the degradation of polymers, resulting in the formation of unsaturated compounds. Moreover, it was predicted to be a more crucial pathway than chain scission initiation because of the possibility of efficient recombination of the caged radical chain ends (Madorsky,

1953, cited in Pielichowski and Njuguna, 2005; Arisawa and Brill, 1997, cited in Pielichowski and Njuguna, 2005; Bair, 1997, cited in Pielichowski and Njuguna, 2005).

PMMA has the same thermal stability as the polymers prepared thermally or with free-radical initiators in the absence of oxygen. Apart from unsaturated end groups and oxygen copolymerization, there is no evidence for weak links increasing the rate of degradation of PMMA (Holland and Hay, 2002, cited in Pielichowski and Njuguna, 2005). PMMA begins to decompose slowly at 220 °C, then degrades up to 40%–47% in the temperature range of 220–270 °C; a further rise of temperature to 305°C allows PMMA to completely decompose. The degradation reactions are reported to be initiated by the scission of weak links and random chain scission (Manring, 1989, cited in Pielichowski and Njuguna, 2005). The weak links can be produced by various reactions, for example combination during polymerization, head-to-head chain growing or termination by disproportionation which results in vinylidene chain ends (Pielichowski and Njuguna, 2005).

2.3.2 Catalytic cracking

Catalytic cracking is fundamentally similar to thermal cracking, except the presence of a catalyst in the process. It has been successfully applied to refining industry with aims to enhance process efficiency and improve quality of products. Nowadays, this process becomes a major application in catalysis: more than 500 million ton/year worldwide capacity. Moreover, it was the first large-scale application of fluidization, called fluid catalytic cracking (FCC) which is still retained even a modern catalytic cracking reactor is often an entrained-flow reactor.

In catalytic cracking, many reactions, for example C-C bond cleavage, dealkylation, isomerization and even condensation, proceed simultaneously. These reactions occur via positively charged hydrocarbon ions, so called carbocations. Both, carbenium and carbonium ions belong to the group of carbocations. The nature of the carbocations is a subject of debate. In case of the cracking of paraffins, carbenium ions are often assumed to be the crucial intermediates which decompose into olefins and smaller carbenium ions via beta scission. A typical reaction mechanism for catalytic cracking (and hydrocracking) under the relatively mild conditions used in FCC is shown on Figure 2.5.

The catalyst causes a 'classical' carbenium ion to be formed by acid catalyzed activation reactions. The classical carbenium ion is transformed into the key intermediate which can be described as a protonated cyclopropane structure. After some rearrangements cracking occurs. The formation of branched paraffins is very fortunate since branched paraffins have high octane numbers and the isobutane produced can be used in alkylation. The preferred products are those of which the formation proceeds via tertiary carbenium ions. Carbenium ions can also be generated by intermolecular hydride transfer reactions between alkane and carbenium ions that are not able to form tertiary carbonium ions. Under more severe conditions lower paraffins can also be cracked.

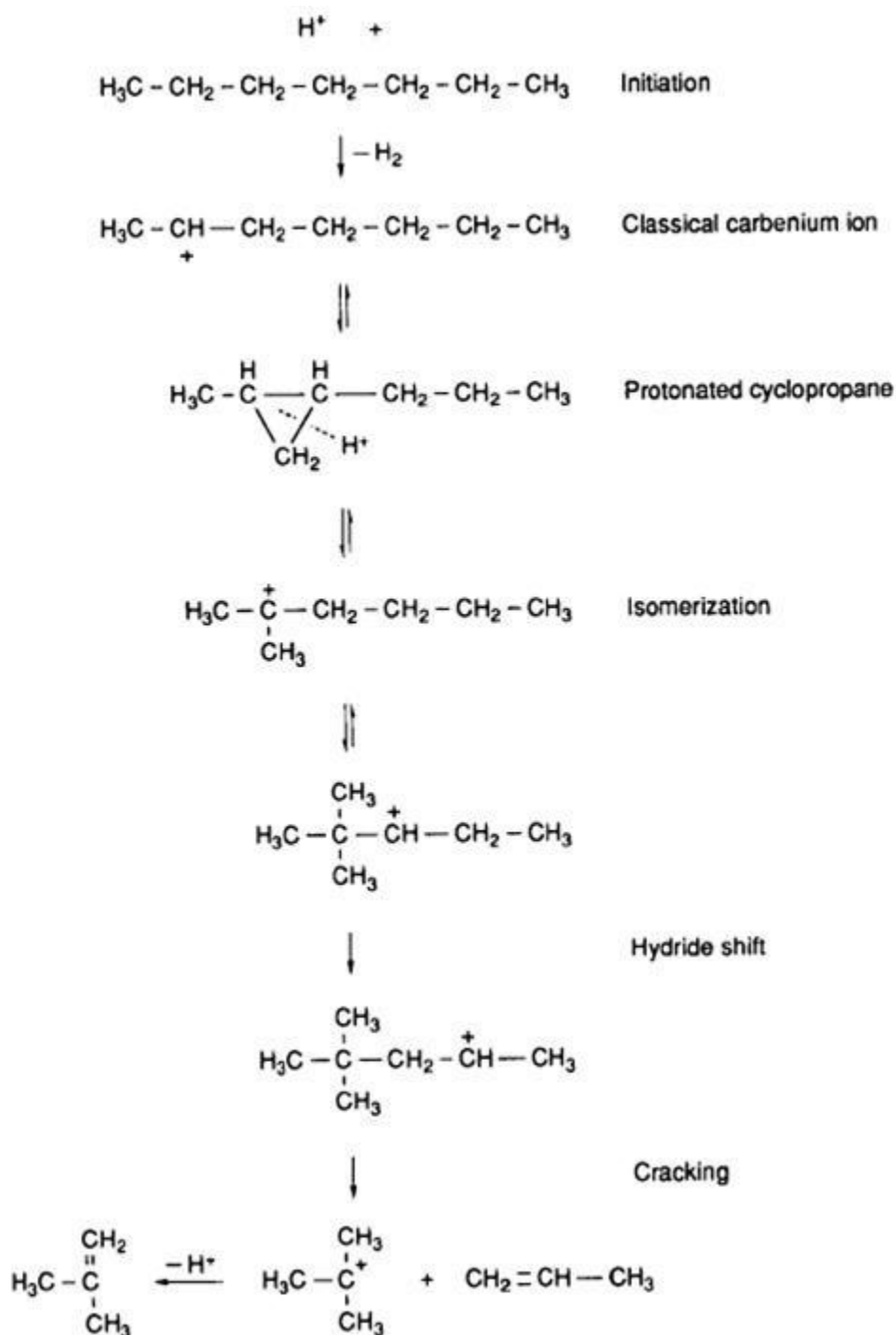


Figure 2.5 Catalytic cracking mechanisms.

Apart from the above-mentioned reactions, dehydrogenation and coking are also two important reactions involved in catalytic cracking processes. For contaminated catalysts, e.g. catalysts containing metals such as nickel and vanadium,

dehydrogenation will proceed. If the contamination of the catalyst is negligible, dehydrogenation reactions won't take place. Catalyst coke formation is a bimolecular reaction with carbenium ions or other free radicals. Yet the formation process is very little investigated. In general, coke formation is increasing with an increasing hydrogen transfer, because the products of this reaction (e.g. olefins, di-olefins, and multi-ring polycyclic olefins) are very reactive and can polymerize to form coke.

2.4 Catalytic system

2.4.1 Basics of a catalytic system

There is a lot of different types of catalysts that are used in industrial applications. These catalysts are classified into 2 broad groups; i) homogeneous catalyst and ii) heterogeneous catalyst. Homogeneous and heterogeneous systems have been used to catalyze the degradation of polymers. Generally, heterogeneous catalysts are the most popular choice since they can be easily separated and recovered from the reaction system.

In a catalytic system, the reaction normally consists of 5 major steps which can be described in the following order: i) diffusion of reactant to the active sites of catalyst, ii) adsorption of reactant, either physical or chemical adsorption, on the active sites of catalyst, iii) chemical reaction, iv) desorption of products from the active sites of catalyst and v) diffusion of products out from the catalyst. Among these steps, the slowest step always controls the rate of reaction, referred to as rate-determining step. For the catalytic degradation of polymer, the linking of the polymer to the active sites of the catalyst is usually the rate-determining step. However, the

selectivity is affected by size and shape of reactants, intermediates and products. Various kinds of heterogeneous catalysts have been applied to the catalytic degradation, which can be summarized as follows (Scheirs and Kaminsky, 2006):

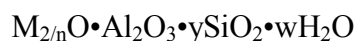
- Acid solids; zeolite, silica-alumina, alumina, fresh and spent FCC catalysts
- Mesoporous structured catalysts; MCM-41, FSM-16, Al-SBA-15
- Aluminium pillared clays
- Nanocrystalline zeolite; n-HZSM-5
- Super acid solids; $\text{ZrO}_2/\text{SO}_4^{2-}$
- Gallosilicates
- Metals supported on carbon
- Basic oxides; BaO, K_2O , etc.

Among them, zeolites have been definitely the most used catalysts for polymer degradation and this type of catalysts will be described in more details in the following paragraph.

2.4.2 Zeolite catalyst (Chester, A.W., 2009)

Zeolites are porous crystalline framework materials containing pores of molecular size (5-12 Å or 0.5-1.2 nm). The term zeolite is derived from the Greek words for “boiling stone,” from the ability of these materials to absorb water and release it upon heating. Conventional zeolites are based on silicate frameworks in which substitution of some of the Si with Al (or other metals) leads to a negative charge on the framework, with cations (usually Na or other alkaline or alkaline earth metals) within the pore structure. This leads to another important property, ion

exchange, where the metal ions in the pore structure can be replaced by other cations (e.g. metal, ammonium, quaternary ammonium). Zeolite is a crystalline microporous aluminosilicate with a well-defined 3-D framework structure and whose chemical composition can be represented by the following empirical formula (Van Bekkum et al., 2001):



Where $2 < y < 10$, n is the cation valence and w represents the amount of water contained in the apertures of the zeolite.

The zeolitic frameworks are networks composed of tetrahedral T atoms (T=Si, Al, etc.) linked by oxygen ions. Common building blocks of zeolite structures consist of 3, 4, 5, and 6 membered rings (n-MR). Each n-MR consists of n T atoms linked in a ring by O ions and thus actually has 2n atoms; thus a 6-MR has 12 total atoms. The structures are arranged such that they form larger rings that represent the molecular pores – commonly 8-, 10- and 12-MR, although structures with 9-, 14-, 18-, and 20-MR pores are known. The 8-, 10-, and 12-MR containing zeolites are commonly known as small, intermediate, and large pores. Small pore zeolites will generally allow n-paraffins to be adsorbed, while large pore zeolites allow all highly branched paraffins to be adsorbed as well. Intermediate pore zeolites allow some branched chains, but not highly branched paraffins, to be adsorbed. Thus zeolites are part of the larger class of materials called molecular sieves, which allow mixtures of molecules of differing structures to be separated.

Zeolites occur naturally and are generally formed in alkaline environments from volcanic sediments and materials. The first zeolite discovered and identified as such was stilbite; common abundant zeolites are analcime, clinoptilolite, erionite,

heulandite, laumontite, and mordenite. Many of these materials have valuable properties as sorbents and even catalysts, but the natural forms often have faults and irregularities in their structures that limit their application. It is the development of laboratory methods of synthesizing zeolites that led to the wide commercial application of zeolites.

The first synthetic zeolite was made from Na, Si, and Al at Linde's laboratories in Tonawanda, NY. It was termed zeolite A, being the first, and was found to be composed of sodalite cages arranged to give 8-MR pores. Zeolite A was capable of adsorbing water and n-paraffins as well. Its first commercial application was as a drying agent and it is still commonly used. Some time later, Linde synthesized zeolites X and Y; these zeolites had the structure of the natural zeolite faujasite and were also composed of sodalite cages arranged such that a 12-MR pore structure existed. The major difference between X and Y are their $\text{SiO}_2/\text{Al}_2\text{O}_3$ ratios in their framework. For X, this was 2–3; for Y, it was 3.5–5.5, which conferred greater hydrothermal stability, which was important in applying it to catalytic cracking. It was then found that organic “templates” could be used to make new zeolite structures. This approach was pioneered by Mobil and led to ZK-5 (from Dabco), Beta (from tetraethylammonium ion), and ZSM-5 (from tetrapropyl ammonium ion), among others. Like natural zeolites, synthetic zeolites are generally named by their inventors. Since it was mostly companies that were involved in early zeolite synthesis, most names derived from them: ZSM for Zeolite Socony Mobil, LZ for Linde Zeolite, ECR for Exxon Corporate Research, and SSZ for Standard Selective Zeolite (from Chevron). This practice has continued into the present days, with designations now based on universities as well (for example, ITQ for Instituto de Tecnologia Quimica

in Valencia). The International Zeolite Association has also developed a “Structure Code,” which is applied to particular structure types but does not indicate chemical composition. Thus, for example, zeolite A, X and Y, and ZSM-5 are known as LTA, FAU, and MFI (for Linde Type A, Faujasite, and Mobil Five), respectively. Proposals for structure codes are made by those determining the structure and are approved by the IZA. An excellent source of information on zeolites is the Web page of the IZA (<http://www.iza-online.org/>). Detailed information on the structures of all known zeolite structure types is available, plus information on catalysis, synthesis, and other aspects of zeolite science.

Different types of zeolites have different channel dimensions (Figure 2.6). For example, chabazite (CHA) has small pores formed by 8-membered rings, ZSM-5 (MFI) has medium pores (10-membered rings), and beta zeolite (*BEA) has large pores (12-membered rings). The shape selectivity of different zeolites is due to a large extent to differences in pore size. The different pore sizes allow the selective adsorption of certain reactants, or the selective desorption of certain products and can inhibit or promote different reaction intermediates in catalytic reactions. (Jang Ho Yun., 2011)

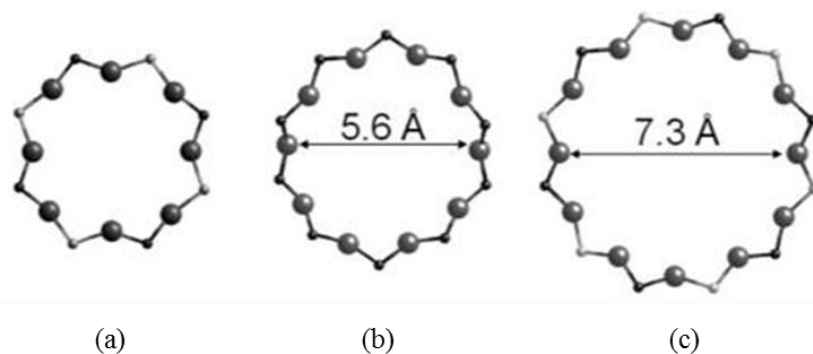


Figure 2.6 Pore size of (a) chabazite 8-ring, (b) ZSM-5 10-ring, and (c) beta zeolite 12-ring.

Zeolite framework can be classified according to various schemes (example as shown in Figure 2.7). Most of these features are defined in the *Atlas of Zeolite Framework Types* (Baerlocher et al., 2007) and then given for each framework type. The physicochemical properties and the application of zeolites are also determined to a great extent by the amount of aluminum in the framework of zeolite. The amount of aluminum in the zeolite framework is typically represented by the (atomic) Si/Al ratio. The minimum Si/Al ratio is 1 due to the Loewenstein rule, which establishes that no Al-O-Al bond exists in a zeolite. Since an alumina tetrahedron (AlO_4^-) has a negative charge while a silica tetrahedron (SiO_4) is neutral, a counter ion, such as H^+ or alkali-metal ion, must be present to balance the negative charge. The sites compensated by H^+ form bridging hydroxyl group (Si-OH-Al) that are chemically and functionally Brønsted acid sites. The Si/Al ratio affects the acidity of the zeolites: the total number of acid sites increases as the Si/Al ratio decreases but at the same time the acidity becomes weaker. Acid-base reactions, the most common class of industrial chemical reactions, and acid base catalysis can be applied to every area of the chemical industries, including the oil refining industry. Since zeolites have high acidity, high surface area as well as the ability to do shape selectivity, they are used primarily as a solid catalyst in oil refining and petrochemical industries, in processes such as hydrocracking, fluid catalytic cracking (FCC), aromatization and isomerization. MFI, BEA and FUA zeolites are probably the most important in terms of commercial development of zeolites. Their structures are illustrated in Table 2.1 and Figure 2.7. The vertices in the structures represent the T atoms (Si or Al) and the lines between vertices represent the O atom bridges. This is a conventional way to

represent zeolite structures, since showing all the oxygen atoms only produces a confused representation. (Chester, A.W., 2009)

Table 2.1 Structural features of common zeolites used as catalysts in cracking.

Zeolites	Structure	Pore size (nm)	Si/Al ratio
ZSM-5	MFI	0.53x0.56, 0.51x0.55	10-1000
Y	FAU	0.74	1.5-3
Beta	BEA	0.64x0.76, 0.55x0.55	8-1000
Mordenite	MOR	0.65x0.7	5

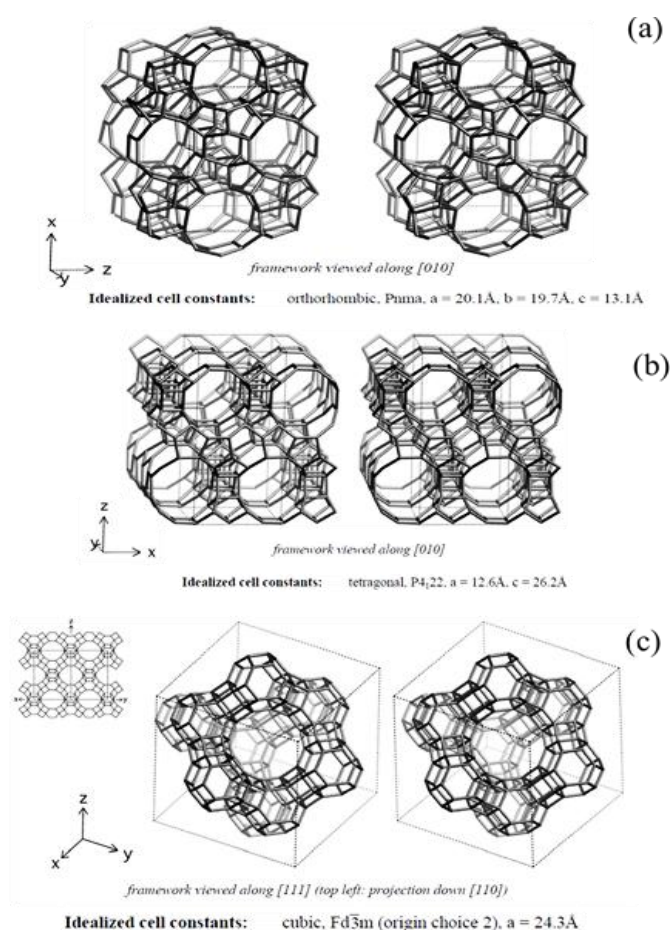


Figure 2.7 Schematic representation of the pore network of (a) MFI (b) BEA and (c) FAU zeolites. Vertices represent T atoms (Si or Al); lines between vertices are the O bridges.

Faujasite (also zeolites X or Y) is also constructed from sodalite cages, but connected through 6-MR, leading to a crystallographically cubic structure in which the sodalite cages are tetrahedrally arrayed and resulting in three large orthogonal pores of 7.4 Å diameter. Most organic molecules, with some exceptions, fit into these pores. Zeolite Y has a $\text{SiO}_2/\text{Al}_2\text{O}_3$ ratio of 4–6 and is used in very large scale catalytic cracking applications.

ZSM-5 is based on cages made of 4-, 5-, and 6-MR resulting in two elliptical pores of 5.1- 5.5 and 5.3 - 5.6 Å normal to each other. Small and intermediate organic molecules can be adsorbed, but not larger molecules. ZSM-5 has a much higher $\text{SiO}_2/\text{Al}_2\text{O}_3$ ratio than the other zeolites mentioned, anywhere from around 20 to almost infinity. It is most useful in conversion of small olefins and alcohols (particularly methanol) to gasoline range hydrocarbons, as well as in shape selective cracking applications such as dewaxing.

The definition of zeolites has undergone some changes over time. Zeolites were thought to be inherently aluminosilicates, since all known examples had that composition. In the 1970s, however, Union Carbide synthesized porous zeolites like aluminum phosphates with structures identical in some instances to known zeolites as well as new structures (AlPO_4s). Materials with silicon and other metals substituted for Al or P were also made that had acidity and catalytic activity (SAPOs and MAPOs). Because they were not aluminosilicate, carbide claimed that they were non-zeolitic molecular sieves (NZMSs) as a way to get stronger patent claims. Similarly, carbide was able to synthesize a form of ZSM-5 that they claimed had no Al and was therefore a silicate and not a zeolite (silicalite). In fact, these latter materials had Al from the silica sources used and had $\text{SiO}_2/\text{Al}_2\text{O}_3$ ratios as low as 200. Nowadays, with

the commercial interests out of the picture, all of these materials are recognized as part of zeolite science (in point of fact, carbide always published papers on AlPO_4 s, SAPOs, and silicalites in the journal *Zeolites*).

Zeolites are useful in catalysis because of their acidity. Acidity arises from the Si-OH-Al grouping formed by ion exchange with acid or, more typically, by thermal decomposition of exchanged ammonium ions to form the acid group and gaseous ammonia. Zeolitic acidity is much stronger than that formed in amorphous aluminosilicate, which is usually based on the Al-OH group.

The most important use of zeolites, particularly by volume, is in catalytic cracking, in which the Faujasite zeolites X and Y were applied by Mobil Oil in early 1960s. Prior to this, catalysts were amorphous aluminosilicate prepared by coprecipitation or cogelation, or were made from acidified natural clays. Catalytic cracking is a cyclic process in which the catalyst generates coke during the reaction and must be regenerated before reuse. Early units used swing reactors that were alternately on reaction and then on regeneration, but the more efficient cyclic units, both moving bed and fluid bed (FCC) were developed during the Second World War.

Early proposed cracking catalysts were prepared from the low $\text{SiO}_2/\text{Al}_2\text{O}_3$ zeolite X, but were hydrothermally unstable. Mobil researchers discovered that exchanging zeolite X (and later zeolite Y) with mixed rare earth ions led to higher hydrothermal stability and activity (REX and REY). Early demonstrations indicated significantly higher conversions, higher gasoline selectivities, and lower coke yields than obtained with amorphous catalysts, even though early zeolite cracking catalysts contained only 5% zeolite! Although zeolite cracking catalysts did give lower octane gasoline, this could be corrected by using higher reaction temperatures, and, within 10

years of the first demonstration, zeolites were adopted throughout the industry, with REY the dominant zeolite component at up to 25–30% of the total composition, the remainder being a matrix formulated for low activity but high binder strength and low attrition. In the late 1970s, a new component USY (for Ultrastable Y) began to be used to improve octane, although it had poorer hydrothermal stability. USY is a framework dealuminized version of Y made by decomposition of the NaNH_4 form of Y in the presence of steam at controlled temperatures. Modern catalysts generally contain rare earth-modified USY and also contain additive components for oxidizing CO to CO_2 in the regenerator, reducing S and N oxides in the flue gas and for passivating metal contaminants found in the feed (particularly residue).

The success of zeolites in catalytic cracking (including hydrocracking, jointly developed by Union Carbide and Union Oil), led to significant programs at Mobil, Union Carbide, Exxon, BP, and ICI to synthesize new zeolites with improved properties. The most significant early success, as mentioned above, was the high silica zeolite ZSM-5, which was found to have revolutionary applicability in a wide number of applications: catalytic dewaxing, improving gasoline octane in FCC, conversion of methanol to gasoline (MTG) or olefins (MTO), olefin oligomerization, xylene isomerization, ethylbenzene synthesis, toluene disproportionation, and selective toluene disproportionation (directly to p-xylene), to name the most prominent. All of the named processes – and others – have been commercialized over different forms of ZSM-5. It is currently used in FCC to generate high volumes of propylene – an offshoot of its octane enhancement properties. (Chester, A.W., 2009)

2.4.3 Characterization of the zeolite catalysts

In order to accomplish a complete characterization of each zeolite catalyst, many techniques are needed; the objective is to identify the structural properties that discriminate their efficiency. This part briefly describes the concepts of the techniques that are most frequently used for catalyst characterization. The intention is to give the new comer an idea of what these methods tell about a catalyst. There are many ways to obtain the information on the physicochemical properties of this material such as:

N₂ adsorption / desorption analysis

The N₂ adsorption / desorption analysis is the most widely used technique to determine physical characteristics of micro- and meso-porous materials, such as specific surface area, pore volume, pore diameter, as well as pore size distribution. The surface area reported may vary depending on the theoretical model used and the pressure range on which it is applied. For instance, Brunauer-Emmett-Teller (BET) equation usually holds for a relative pressure range below 0.3.

X-ray diffraction (XRD)

X-ray diffraction (XRD) is often used for identification of bulk phases and estimation of crystallite sizes. Diffraction patterns can be also used to identify the various phases in a catalyst material. The XRD patterns as well as the information about the space group and unit cell parameters of entire zeolites have been published in the book “Collection of Simulated XRD Powder Patterns of Zeolites” (Treacy and Higgins, 2001).

X-ray fluorescence spectrometry (XRF)

X-ray fluorescence spectrometry (XRF) is frequently used for identification and estimation of the elemental composition of solid or liquid samples.

Electron Microscopy and Imaging

The various specialized forms of electron microscopy are used in zeolites characterization, for example Scanning electron microscopy (SEM) and Transmission electron microscopy (TEM). These techniques allow the direct observation of the material surface and provide information on their morphology. Moreover, by coupling Energy Dispersive X-ray spectrometry (EDX) to electron microscopy, the estimation of local elemental composition is also permitted. SEM is used to observe the surface topology of a sample, while TEM delivers a two-dimensional image of the inner structure of a very thin sample (< 200 nm) at a resolution down to 0.2 nm. A STEM instrument combines the two modes of electron microscopy.

Temperature Programmed Techniques

Temperature programmed techniques, such as Temperature Programmed Reduction (TPR), Oxidation (TPO), Desorption (TPD), Sulphidation (TIS) and Reaction Spectroscopy (TPRS), are very versatile. The main idea of these techniques is the observation of the temperature-dependent behaviour of a chemical process. TPR is a simple and rapid characterization of metal catalysts, from which basic information on the phases present after impregnation and on the eventual degree of reduction are provided. In case of bimetallic or multimetallic catalysts, TPR patterns can also indicate a mixing of components. Temperature programmed desorption (TPD) is a

very useful technique and is widely used for characterization of the acid properties of solid catalysts. It allows the determination of quantity and strength of the basic/acid sites in solid catalysts which is crucial for understanding and predicting their performance. TPD of a basic molecule such as ammonia (NH_3 -TPD) is popular for determining concentrations of species adsorbed on the surfaces of single crystals and of real catalysts. In principle one can also determine the energy of the adsorption bond, however, only after applying rather complex computations (Damjanović and Auroux in Chester and Derouane 2010).

Infrared spectroscopy and Raman spectroscopy

Infrared spectroscopy is often used to identify species adsorbed on the surface of the catalyst, and also to investigate how they are chemisorbed. In addition, infrared spectroscopy is also an important technique to measure hydroxyl groups (OH) on the surfaces of oxide catalyst supports and zeolites. These species may possess either positive, zero or negative charge, known as acidic, neutral or basic, respectively.

Raman spectroscopy can give complementary information to infrared spectroscopic data for analysing the coordination environment of framework and non-framework metal ion.

2.5 Deactivation of solid catalysts (Guisnet and Ribeiro, 2011)

2.5.1 Causes of deactivation

The various causes of catalysts deactivation as well as the involved deactivation mechanisms have been already summarized by Bartholomew

(Bartholomew, 2004). The typical causes of deactivation are categorized into 5 groups (as shown in Table 2.2):

(i) Poisoning: a deactivation of catalysts due to strong chemical bonding between absorbed species and the active sites. Poisoned sites dramatically or completely lose their ability to catalyze the reaction.

(ii) Deposition of foulant (fouling) or coke (coking) on the surface of catalyst: this type of deactivation can occur by simple deposition or transformation of reactants.

(iii) Structural and chemical transformations of the catalysts: for example, sintering of metal at high temperature, sintering of sulphur-poisoned noble metal, dealumination and collapse of zeolitic structure caused by the presence of water added or formed from dehydroxylation at high temperature.

(iv) Mechanical alterations of catalyst particles because of a mechanical force including crushing, attrition, abrasion or erosion.

(v) Leaching of active species: this type of deactivation can be frequently found in the presence of a liquid phase, such as for the production of fine chemicals.

Based on their mechanisms, the causes of deactivation can be classified as: mechanical, thermal, and chemical. (i), (iii), and (v) are considered as chemical deactivation whereas (ii) and (iv) are mechanical deactivation. Brief basic mechanisms of deactivation of catalysts are provided in Table 2.2.

Table 2.2 Deactivation of solid catalysts: origin, mechanism and typical examples
(Guisnet and Ribeiro, 2011)

Origin	Mechanism	Examples
Poisoning	Chemisorption (or reaction) of feed impurities or reaction products on the active sites, limiting or inhibiting reactant chemisorption Reversible or irreversible	<i>Metals:</i> S compounds, CO, polyaromatics, coke <i>Acid oxides:</i> bases, polyaromatics, coke
Fouling and coking	Deposit of heavy compounds: feed impurities or secondary products (coke) on the active surface Only reversible by oxidative regeneration	<i>Metals:</i> coke (e.g. Pt), carbon (e.g. Ni) <i>Acid oxides:</i> FCC: deposit of heavy feed components, catalytic or thermal coke
Chemical and structural alterations	Decrease of the active surface, e.g. increase of crystal size, partial framework collapse Irreversible	<i>Metals:</i> sintering <i>Acid oxides:</i> e.g. dealumination then collapse of the zeolite framework under hydrothermal conditions
Mechanical alteration	Loss of catalyst caused by attrition or erosion. Loss of surface area by crushing. Irreversible	Fracture, erosion, e.g. in fluidized beds i) from collisions of particles with each other or with reactor walls ii) or due to high fluid velocities
Leaching	Loss of active component, e.g. by dissolution in reaction medium Most common in liquid-phase fine chemicals synthesis Often reversible	e.g. dissolution of metal framework (e.g. Cr in CrS-1) component of metallosilicate molecular sieves

2.5.2 Characterization of solid catalyst deactivation

The study on the deactivation behaviors of solid catalysts frequently encounters difficulties that might arise from the variety, complexity and intricate effects of the causes of deactivation, and even the problem of reproducing representative conditions (experimental conditions must be similar to those of the

industrial process). Toward a good or better understanding of the deactivation of solid catalysts, it is necessary to use several characterization techniques in combination to clarify the deactivating species (e.g. poisoning contaminants, foulants) and/or the changes in the physicochemical properties of catalysts (e.g. active phases, surface area, porosity) (Bauer and Karge, 2007). Various characterization techniques for example qualitative/quantitative analysis of elements, temperature-programmed analysis (e.g. oxidation, reduction, desorption), adsorption of inert probe molecule with difference in molecular size, are therefore used to observe the presence or composition of deactivating species (especially carbonaceous deposits or coke) and also their effects on the physicochemical properties of catalysts. Moreover, apart from the above characterizations, spectroscopic analysis techniques, such as Fourier transform infrared spectroscopy (FTIR), provide useful additional information. The advantages of spectroscopic analysis techniques are that they can be operated in-situ and are non-destructive, the consecutive application of several of them for the characterization of deactivated samples is therefore permitted.

2.5.3 Methods of coke investigation and results (Bauer and Karge, 2007)

This part briefly presents the concepts of the techniques that are most frequently used for coke investigation. There are many ways to obtain information on the properties of a coked material, such as:

Determination of Coke Content and H/C Ratio

To understand the nature of coke, it is necessary to know its composition even it is usually complex and may vary depending on process design and control. The

composition of carbonaceous deposits on catalyst surfaces is frequently assigned in terms of hydrogen to carbon (H/C) ratio which is a crucial parameter because it directly influences combustion reactivity; the higher the hydrogen to carbon (H/C) ratio, the higher the combustion reactivity. The determination of the hydrogen to carbon (H/C) ratio is therefore essential and is recommended to be the first step in coke characterization. Moreover, not only hydrogen and carbon, the analysis of other elements such as nitrogen, sulphur and trace elements should be also performed, especially for the large-scale process, since the presence of organic-based and trace atoms even at a few ppm levels may greatly affect the deactivation behavior.

Several techniques are used to determine H/C ratio, such as thermogravimetric analysis (TGA) and CHN analysis. In particular, CHN analysis is based on the instantaneous complete combustion (flash combustion). During the analysis, all combustible species are completely oxidized at high temperature and converted into gaseous products. The combustion gases then flow through a reduction column which converts nitrogen oxide (NO_x) into nitrogen (N_2) and absorbs all species except CO_2 , H_2O and N_2 . The gas stream leaving the reduction column is brought to a chromatographic column in which it is separated and then individual components are visualized by a thermal conductivity detector (TCD). Moreover, modern CHN analyzers can also measure sulphur and oxygen contents, as known as CHNSO. The thermogravimetric analysis (TGA) is also a very useful technique, especially when operated in combination with an online detection of gaseous products by GC-MS or IR.

Infrared and Raman Spectroscopy

Infrared and Raman spectroscopy are very useful analytical techniques for the investigation of the catalytic reaction mechanisms. They permit the observation of changes in active sites, the detection of absorbed species or intermediates, and put into evidence coke formation during hydrocarbon reactions, without sample destruction. Moreover, these techniques were successfully applied for in situ characterization, for instance the investigation of the formation of carbonaceous deposits on the surface of working catalysts.

Adsorption Measurements

Adsorption measurement is one of the most frequently used techniques for evaluation of deactivation of catalysts. Interpretation of adsorption isotherms based on theoretical models can give information on the important physical properties of catalysts, such as the specific surface area and the porosity (e.g. pore volume, pore diameter and pore size distribution) which are often affected by the presence of carbonaceous deposits. By using proper adsorbate species, this technique permits to locate coke deposits, e.g. in the pores or on the surface of catalysts. Particularly, small probe molecules - for example, nitrogen, water, ammonia, tri-methylamine, pyridine, and small paraffinic hydrocarbons - are preferred when investigating the inter- and intra-crystalline surface of zeolite-based catalysts, whereas bulky adsorbate species - e.g. methyl di-isopropyl amine, substituted benzenes, and methylene blue, whose diffusion through the particular internal pores are prohibited or restricted by their molecular sizes and/or shapes - are suitable for the examination of the external surface of zeolitic catalysts.

2.6 Regeneration of zeolite catalyst (Bartholomew, 2004)

In this section, various regeneration methods which depend naturally on the cause and rate of deactivation are discussed. There are many ways to regenerate spent catalyst, as described below.

2.6.1 Regeneration of coked catalyst

There are several methods for removing coke or carbonaceous deposits, such as oxidation with oxygen, gasification with steam, carbon dioxide, and hydrogen. The energy requirement of these reactions to remove carbon deposits at an acceptable rate depends on the gaseous reactant, the structural property and reactivity of coke or carbonaceous deposits, and also the activity of the catalysts. The regeneration of coked catalyst from many industrial processes such as hydrotreating, catalytic cracking and reforming, is typically performed by the oxidation with air which can rapidly remove coke at temperatures range of 400°C to 600°C. However, one of the major drawbacks of the regeneration with air is the occurrence of hot spots which may cause further deactivation of the catalysts. In order to avoid hot spots, the oxidation with air is therefore frequently controlled by adjustment of a diluting agent i.e. initially conducted under low oxygen concentration atmosphere, and then increasing oxygen content with increasing carbon conversion. Typical diluting agents are nitrogen and steam which are the favorite diluents at laboratory-scale and full plant-scale, respectively.

2.6.2 Regeneration of poisoned catalysts

Regeneration of poisoned catalysts, especially sulfur-poisoned catalysts used in hydrocarbons processing (nickel, copper, platinum and molybdenum), by using hydrogen, air or pure oxygen, steam, or even other inorganic oxidizing agents, has been already reported many times in the literature. However, the methods previously mentioned are partially successful because their high temperature requirement makes them suitable for steam reforming catalysts possessing a low surface area, but not for high surface area nickel catalysts which can suffer from sintering at high temperature.

2.6.3 Re-dispersion of sintered catalysts

During catalytic reforming of hydrocarbons on Pt-based catalysts, small Pt cluster of 1 nm can grow (sintering) to approximately 5 to 20 nm crystallites. In this case, the re-dispersion of the Pt phase is very important in order to recover the activity of catalyst. The re-dispersion can be done using a high temperature treatment in the presence of oxygen and chlorine, the so-called oxychlorination. A typical oxychlorination procedure is composed of exposure of the catalyst to hydrochloric or carbon tetrachloride at a temperature of 450°C to 550°C in 2 to 10% oxygen for 1 to 4 hours. During coke removal, re-dispersion of active phase can take place, leading to an increase of the dispersion coefficient (D), for instance $D = 0.25$ to 0.51 , while during re-dispersion by oxychlorination, a further increase of dispersion coefficient occurs, e.g. $D = 0.51$ to 0.81 (Franck and Martino, 1982, cited in Bartholomew, 2004). Conventional regeneration processes of poisoned, fouled, coked, and sintered catalysts and representative examples are summarized in Table 2.3.

Table 2.3 Conventional methods and representative examples of catalyst regeneration from scientific and patent literature (Bartholomew, 2004)

Deactivation mechanism/ reaction/catalyst	Problem/cause	Method(s) of regeneration/phenomena studied/conclusions
<i>Deactivation by coke, carbon</i> alkene aromatization oligomerization/zeolites, esp. ZSM-5, -22, -23, beta-zeolite, ferrierite	catalyst fouling by condensa- tion of heavy oligomers to coke	(1) ZSM-5 catalyst for light olefin oligomerization containing 2–3% coke is treated in 8–10% steam/air mixture (1300 kPa, 93°C inlet) in a fluidized bed (2) a coked crystalline alumogallosilicate is con- tacted with oxygen at a concentration of 0.05–10 vol%, 420– 580°C, and 300–4000 h ⁻¹
alkylation of isoparaffins on solid catalysts/sulfated zirconia, USY ⁺ , Nafion, silicalite, ZSM-5	rapid catalyst deactivation due to coke formation; unacceptable product qual- ity, and thermal degrada- tion of catalyst during regeneration	(1) coked zeolite is regenerated in liquid phase ($P > 3500$ kPa) fluid bed with H ₂ in two steps: (a) at reaction temperature (20–50°C) and (b) at 25°C above reaction temperature (2) coked Pd- and Pt/Y- zeolite catalysts containing 10–13% coke are regenerated in either air or H ₂ ; H ₂ treatment enables removal of most of the coke at low- moderate temperatures; higher temperatures are required for air
catalytic reforming of naphtha/ Pt/Al ₂ O ₃ promoted with Re, Sn, Ge, or Ir	poisoning and fouling by coke produced by condensation of aromatics and olefins	(1) coke on Pt bimetallic reforming catalyst is removed off-stream in a moving bed at 300–600°C, followed by oxychlorination (350– 550°C) (2) coke on Pt/zeolite is removed in halogen-free oxygen- containing gas at $T < 415$ °C (3) sintering during oxidation of coke on Pt–Ir/Al ₂ O ₃ catalyst can be minimized at low regeneration temperature (4) study of influence of heating rate, temperature, and time on structural properties of regenerated Pt–Sn/Al ₂ O ₃ (5) study of effects of Cl, Sn content, and regeneration sequence on dispersion and selectivity of Pt–Sn/Al ₂ O ₃ (6) regenerated Pt–Re/ Al ₂ O ₃ is more stable than the fresh catalyst in <i>n</i> -heptane conver- sion and more selective for toluene
dehydrogenation of propane and butane/Cr ₂ O ₃ /Al ₂ O ₃ , Cr ₂ O ₃ /ZrO ₂ , FeO/K/MgO, Pt/Al ₂ O ₃ , Pt–Sn/Al ₂ O ₃ , Pt–Sn/KL-zeolite	catalyst activity is low owing to equilibrium limitations and build-up of product H ₂ ; rapid loss of activity occurs owing to coke formation	(1) temperatures gradients were measured during burn off of coke formed on a chromia–alumina catalyst during butene dehydro- genation; data were used in developing a mathematical model for predicting temperatures and coke profiles (2) coked supported palladium catalyst used in the dehydrogenation of dimethylter- trahydronaphthalenes to dimethylnaphthalenes is reactivated with an organic polar solvent at a temperature below 200°C

Table 2.3 (Continued)

Deactivation mechanism/ reaction/catalyst	Problem/cause	Method(s) of regeneration/phenomena studied/conclusions
Fischer–Tropsch synthesis/ Co/Al ₂ O ₃	loss of activity due to blocking of sites by carbon overlayers and heavy hydrocarbons	(1) carbidic surface carbon deposited on cobalt can be largely removed in hydrogen at 170–200°C and in steam at 300–400°C (2) slurry-phase cobalt catalysts may lose 50% activity during synthesis over a period of a few days; the activity can be rejuvenated <i>in situ</i> by injecting H ₂ gas into vertical draft tubes inside the reactor
fluid catalytic cracking (FCC) of heavy hydrocarbons/USY or REO-Y ^b in silica matrix	rapid loss of activity due to poisoning of acid sites and blocking of small zeolite pores by coke	(1) process and apparatus for increasing the coke burning capacity of FCC regenerators; auxiliary regenerator partially burns off the coke at turbulent or fast fluidized-bed conditions (2) multistage fluidized-bed regeneration of spent FCC catalyst in a single vessel by incorporating two relatively dense phase fluidized beds beneath a common dilute phase region
hydrocracking of heavy naphtha/CoMo, NiW, MoW on Al ₂ O ₃ or SiO ₂ –Al ₂ O ₃ ; Pt or Pd on Y-zeolite, mordenite, or ZSM-5	loss of activity due to poisoning of acid sites and blocking of small zeolite pores by coke	(1) regeneration of noble metal/zeolite via progressive partial removal of carbonaceous deposits under controlled oxidizing conditions to maximize sorption of a probe molecule while minimizing metal sintering (2) regeneration of noble metal/zeolite in air at about 600°C, followed by a mild treatment in a aqueous ammonia to improve catalytic activity
hydrotreating of gas oil	loss of activity due to formation of types I, II, and III coke on metal sulfide and alumina surfaces and in pores	(1) TPO studies of oxidative regeneration of CoMo and NiW HDS catalysts; sulfur is removed at 225–325°C, carbon at 375–575°C. Redispersion of NiW was observed by EXAFS (2) physicochemical changes in CoMo and NiCoMo HDS catalysts during oxidative regeneration, including redispersion of Co, Ni, and Mo oxides and surface area loss, were examined (3) changes in NiMo catalyst structure and coke composition during reaction and regeneration were examined and correlated (4) properties of NiMo catalyst deactivated during shale oil hydrogenation and regenerated in O ₂ or H ₂ were examined. regeneration in 1.6% O ₂ was more effective than that in 5% H ₂ . Ni aluminate spinel was observed after burn off (5) hard and soft cokes formed on CoMo catalysts during HDS of gas oil were characterized. At low coke levels, hard coke was more easily removed in H ₂ than in O ₂ (6) spent catalysts are washed with solvent and contacted with steam at about 600°C

Table 2.3 (Continued)

Deactivation mechanism/ reaction/catalyst	Problem/cause	Method(s) of regeneration/phenomena studied/conclusions
methanol to olefins or gasoline/ silica–alumina, Y-zeolite, ZSM-5, other zeolites, and aluminophosphate molecular sieves	severe coking and deactivation of silica–alumina and Y-zeolite catalysts observed during high conversions of methanol, also substantial coking of ZSM-5, other zeolites, and aluminophosphate molecular sieves	(1) kinetics of coke burn off from a SAPO-34 used in converting methanol to olefins were studied; kinetics are strongly dependent on the nature of the coke. Kinetics are slowed by strong binding of coke to acid sites (2) ZSM-34 catalyst used in conversion of methanol to light olefins is effectively regenerated in H ₂ -containing gas; this approach avoids the formation of catalyst-damaging products such as steam that would be formed during burn off in air
<i>Poisoning</i> FCC of residues/USY or REO-Y in silica matrix	(1) poisoning of acid sites by N- containing compounds. (2) deposition of Ni and V metals on acid sites which change selectivity and decrease activity	(1) organometallic solutions of Sb and Bi are added to process steam to passivate Ni by forming inactive Ni–Sb and Ni–Bi species (2) V metal deposits are trapped by reaction with magnesium orthosilicate to form an unreactive magnesium vanadium silicate (3) spent metal-contaminated catalyst is demetallized by chlorinating and washing followed by contacting with NH ₄ F and one antimony compound (4) metal-contaminated catalyst is contacted with an aqueous solution of a carboxylic acid (eg, formic, acetic, citric, or lactic acid) (5) metal-contaminated catalyst is contacted with HCl, HNO ₃ , or H ₂ SO ₄ (6) metal contaminated catalyst is contacted with reducing CO gas to form gaseous metal carbonyls that separated from the catalyst
hydrogenation or dechlorination	poisoning of metal sites by arsenic, sulfur, and other poisons	(1) regeneration of Ni/SiO ₂ catalyst poisoned by thiophene using a sequence of oxidation–reduction treatments at low PO ₂ and 1 atm H ₂ respectively (2) regeneration in dilute hypochlorite solution of a Pd/Al ₂ O ₃ catalyst deactivated during the aqueous-phase dechlorination of trichloroethylene in the presence of sulfite or HS ⁻ ions present in ground water
hydrotreating of residues/ Al ₂ O ₃ -supported Mo and CoMo	pore-mouth poisoning and blockage by Ni, V, and Fe sulfides present in feed as organometallics	(1) regeneration of catalysts containing V, Ni, or Fe by contacting with H ₂ O ₂ solution and organic acid (2) following removal of coke by air or solvent wash, catalyst is acid leached to remove undesired metals

Table 2.3 (Continued)

Deactivation mechanism/ reaction/catalyst	Problem/cause	Method(s) of regeneration/phenomena studied/conclusions
<i>Thermal degradation</i>		
Catalytic reforming of naphtha/Pt/Al ₂ O ₃ promoted with Re, Sn, Ge, or Ir; Pt/ KL-zeolite	sintering of Pt causing formation of large metal crystallites crystals and loss of active surface area	(1) redispersion of Pt–Ir bimetallic catalysts using a wet HCl/air treatment, since the conventional oxychlorination is not effective (2) redispersion of Pt/KL-zeolite using wet HCl/air treatment fol- lowed by brief calcination and reduction (3) redispersion of Pt–Re/ Al ₂ O ₃ in Cl ₂ and O ₂ (4) redispersion of supported Pt, other noble metals, and Ni in Cl ₂ and O ₂
hydrocracking of heavy naphtha/CoMo, NiW, MoW on Al ₂ O ₃ or SiO ₂ –Al ₂ O ₃ ; Pt or Pd on Y-zeolite, mordenite, or ZSM-5	sintering of noble metal caus- ing formation of large metal crystallites crystals and loss of active surface area	redispersion of noble metals on molecular sieves including silica-aluminates, ALPOS, SAPOS
hydrotreating of gas oil and residues/Al ₂ O ₃ -supported Mo and CoMo	sintering of Mo and Co sul- fides causing formation of large sulfide crystals and loss of active surface area	(1) oxidative regeneration of hydroprocessing catalyst at 600°C optimizes surface area and Mo dispersion (2) oxidative regenera- tion in several steps with a final oxidation at 500–600°C to restore residual catalyst activity

^aUSY: ultrastable Y-zeolite. ^bREO-Y: rare-earth exchanged Y-zeolite.

2.7 Literature reviews

Thermal cracking of waste carbon-based materials for example used cooking oil, waste rubber and various types of waste plastics has been an interesting issue over the past half century. In case of waste plastics, common plastics especially polyethylene (PE), polypropylene (PP) and polystyrene (PS) have been more focused than special purpose plastics such as melamine formaldehyde (MF) and poly (methyl methacrylate) (PMMA).

Due to their excellent effectiveness in cracking of plastics, polymer and petroleum derivatives, zeolites have been extensively cited in literature as effective catalysts for catalytic cracking. In addition, the spent zeolite can be easily regenerated by several methods as reviewed by many researchers such as high temperature combustion, reaction with oxygen or nitrous oxide-containing mixtures.

Over the last decade, the regeneration of catalyst has been developed in combination with ozone with the aim to lower the energy consumption of the process. It is well known that ozone (O_3), one of the most powerful oxidizing agent, may readily oxidize organic as well as inorganic compounds; it therefore can regenerate deactivated catalyst even at room temperature. This oxidizing specie shows many advantages such as;

- i) It can be easily generated on-site with various methods, for instance electrical discharge (ED), electrolysis (EL) and irradiation.
- ii) It has high oxidation activity.
- iii) It rapidly decomposes to O_2 without any trace compounds.

Many researches were conducted with the main purpose to study the catalyst regeneration performance of ozone as mentioned in particular.

In this section, thermal cracking and catalytic cracking by the numerous kinds of zeolites, such as Beta, USY, ZSM-5, HY, and REY, are mentioned. Moreover deactivation and regeneration of zeolite catalyst are described.

2.7.1 Thermal and catalytic cracking of polymers

Buekens (1998) studied the developments in plastic cracking process to convert plastic wastes into valuable chemical agents. In their research, municipal plastic wastes were both thermally and catalytically cracked. In case of thermal cracking, plastic wastes were decomposed into gaseous, liquid and solid products. The thermal cracking liquid products usually consisted in high boiling point hydrocarbons. However, in the presence of fluid cracking and/or reforming catalysts, more gasoline-range hydrocarbons, especially aromatic as well as naphthenic compounds in the C6–C8 range, could be obtained.

Chester (2007) studied the catalytic cracking of hydrocarbons to obtain a high yield of butylene and iso-butane by using zeolite MCM-68. It was found that MCM-68 was suitable to be the main catalyst. Moreover, it could be applied as an additive to a conventional cracking catalyst (molecular sieve possessing pore size larger than 7 Å).

Elordi et al. (2009) studied pyrolysis of HDPE over HZSM-5, HY and H β under nitrogen atmosphere at 500°C in a continuous spouted-bed reactor. The products were separated into 7 groups according to their phase and structures. They found that HZSM-5 yielded a large portion of light olefins, up to 58 wt.%, whereas C₅-C₁₁ non-aromatic hydrocarbons were obtained as main products when using HY

and H β . In addition, HZSM-5 was also selective to single-ring aromatic hydrocarbons and showed a better deactivation resistance than HY and H β . These observations confirmed the important influence of zeolite properties, namely pore size and acidity, on the product distribution and deactivation in cracking process.

Srinakruang (2009) studied a cracking process of plastic-derived liquid, which was obtained from a pyrolysis process of plastic waste such as polyethylene (PE), polystyrene (PS) or polypropylene (PP), to produce fuel by using a dolomite catalyst. This work found that the catalytic cracking reaction of plastic-derived liquid to produce high quality oil for fuel, which comprised mainly light and heavy naphtha, was achieved at operating temperatures lower than 320°C by using dolomite catalyst.

Kaminsky and Franck (1991) recovered the methyl methacrylate (MMA) from waste PMMA in a heated fluidized-bed at temperatures above 450°C under nitrogen atmosphere. According to their work, more than 97% PMMA conversion could be achieved, moreover, a temperature-dependence of MMA monomer yield was also reported. The analysis of products revealed the presence of methane (CH₄), ethane (C₂H₆), propene (C₃H₈), carbon monoxide (CO) and carbon dioxide (CO₂) in the gaseous product while the liquid product contained MMA monomer and methyl acrylate (MA) as a main component and impurity, respectively.

Kaminsky, Predel, and Sadiki (2004) investigated the decomposition of PMMA by pyrolysis in an indirectly heated fluidized-bed called “The Hamburg process” to obtain monomers and fuel oil. They successfully produced various products, mainly MMA monomer, aliphatic and aromatics hydrocarbons. An optimum

reaction temperature for PMMA degradation was found to be 450°C, more than 98 % of PMMA was converted to the products.

Kang (2007) studied the thermal cracking of PMMA in a fluidized-bed reactor in temperatures range of 450°C to 500°C. Their process could produce MMA monomers with greater than 97% recovery. The purity was up to 98% while methyl acrylate (MA) could be found as a contaminant. The investigation of cracking reaction kinetics was also carried out with TGA. The results confirmed that the reactions could be described by The Chatterjee-Conrad (CC) and Freeman-Carroll (FC) models whose simulated DTG curves were similar to the experimental result.

Oriňák et al. (2006) studied the MMA monomer production by co-pyrolysis of PMMA and brown coal in Coupled Pyrolysis-Gas chromatograph system. They concluded that the optimal condition which granted the maximum MMA yield of 64 wt.% was as follows: temperature of 750°C, PMMA to coal weight ratio in the range of 1:1.2 to 1:1.6. At temperature above 900°C, MMA could completely decompose. They found that presence of coal affected recombination of gaseous species and promoted MMA production at high temperature; on the other hand, it eliminated other degradation products of PMMA and coal pyrolysis.

Smolders and Baeyens (2004) worked on the thermal degradation of PMMA in fluidized-bed over a temperature range of 450 to 590°C. The results showed that almost PMMA sample was decomposed and was converted to MMA monomer with 90% to 98% yield. They found that the MMA yield was not only influenced by the operating temperature, but also by the residence time of the gas.

2.7.2 Deactivation and regeneration of solid catalyst

Al-Quraish (2010) disclosed the microwave spent catalyst decoking method as a method for regenerating petrochemical catalysts by removing coke deposited in the catalyst using a 2.45 GHz microwave oven. The spent catalyst is heated in air or pure oxygen in the presence of a susceptor. The susceptor is made of silicon carbide-based composite material that absorbs 2.45 GHz microwave energy fast and efficiently. In one embodiment, the susceptor material is formed into pellets that are preferably four to five millimeters in diameter. The susceptor pellets are mixed with the spent catalyst and loaded into a thermally shielded refractory tube that rotates about its central axis. In another embodiment, the apparatus is a thermally shielded tower or vertical tube made of refractory material that is transparent to microwave radiation and supports rows of susceptor rods that are aligned horizontally.

Boyle (1993) investigated a process for the regeneration of a coked Pt/Al₂O₃, or poly-metallic Pt reforming catalyst with ozone. The coked catalyst is contacted with a gaseous stream containing ozone in a concentration of 1-50% vol. and carbon is burned at temperatures ranging from 20°C to 200°C, especially 60°C-150°C, sufficient to considerably deplete carbon and to restore the activity of the catalyst to that of the fresh one.

Copperthwaite (1986) worked on ozone-enriched oxygen regeneration of pentasil zeolite catalysts (SiO₂/Al₂O₃ ratios 35 and 70) deactivated during methanol conversion to hydrocarbons and o-xylene isomerization. Low temperature ozone reactivation was found to restore the catalyst activity for these reactions. Moreover,

ozone reactivation was found to increase slightly the catalyst lifetime and also to reduce the initial methane yield when compared with oxygen reactivation.

Gartside and Greene (2003) investigated decoking a deactivated magnesium oxide catalyst with a flowing gas containing a dry inert gas (e.g., nitrogen) and an oxidizing agent (e.g., oxygen) at a temperature of at least 500°C to substantially remove coke from the catalyst. The regeneration is preferably carried out in steps of gradually increasing temperature and oxygen concentration.

López (2011) studied the deactivation and regeneration of ZSM-5 in catalytic cracking of mixed plastic wastes. They found that in case ZSM-5 was used as catalyst in cracking of plastic wastes, it was easily deactivated by coke deposition, resulting in the loss of activity to produce liquid and gaseous products in comparison with those obtained by using fresh zeolite. However, in terms of product quality, coked zeolite still provided the products with a better quality than that obtained with a thermal cracking. A regeneration process by oxidation of coke deposits under air flow at a temperature of 550°C could almost fully recover catalytic activity of coked zeolite as evidenced from its ability to produce liquid and gaseous products which was almost equal to that with fresh zeolite.

Lowery and Wright (1992) proposed a regeneration method of a spent magnesium oxide isomerization catalyst that involves calcining the catalyst at 425 to 590°C.

Marcilla (2005) studied the influence of regeneration conditions on the catalytic activity of HUSY and HZSM-5 for the catalytic cracking of polyethylene

(PE). The result showed that the zeolitic structure of both HUSY and HZSM-5 were damaged in case of using the high regeneration temperature (900°C), an amorphization of the catalyst and a change in micropore volume and surface area were observed.

Mariey (1996) studied the regeneration of coked HY zeolite via oxygen or ozone by using FTIR. Two different zeolites, low Si/Al ratio HY and ultrastabilized HYS, were deactivated during cyclohexene cracking at 450°C, 4 kPa. It was found that regeneration via oxygen was effective above 500°C, whereas regeneration via ozone was achieved below 180°C. This study concluded that the regeneration of coked zeolite by ozonation is attractive as it takes place at very low temperature and therefore does not damage unstable zeolitic structures, for instance HY zeolite with a low Si/Al ratio.

Montgomery (1980) described a regeneration method of olefin isomerization catalyst containing magnesium oxide. The regeneration involves purging the catalyst with an inert gas, and then treating the catalyst with an oxygen-containing gas at a maximum temperature of about 1000°F (538°C.).

Pecak (1976) proposed a method for reactivating a carbonized magnesium oxide catalyst that has become carbonized in a phenol alkylation reaction. , Regeneration comprises burning carbon from the catalyst by exposing it to heat in an oxygen containing gas, to form a partially reactivated catalyst. The improvement consists essentially in contacting the partially reactivated catalyst with a sufficient amount of water at a temperature below 300°C to restore the activity of the catalyst.

Pfeiffer, Bronxville, and Garrett (1971) disclosed a two stage catalyst regeneration process, wherein the spent catalyst is sequentially introduced to the first dense bed and second dense bed, and contacted with oxygen-containing gas stream to remove coke on the catalyst by a combustion reaction. Resulting flue gases are combined together and carry the entrained catalyst into a dilute settling section. In the first fluidized dense bed the regeneration temperature is 565°C. In the second fluidized dense bed the gas superficial velocity is maintained in the range of 0.381 to 1.83 m/s, and the regeneration temperature is maintained in the range 607-732°C. Compared with a single stage regeneration process, the catalyst inventory in the regenerator is decreased by about 40 %, and the coke content is below 0.1 wt % when a low coke burning rate is employed in the regeneration process.

CHAPTER III

EXPERIMENTAL

In this chapter, there are two main experimental parts; the degradation of poly (methyl methacrylate) (PMMA) by using zeolite and the regeneration of used catalyst by ozonation are established in sections 3.1 and 3.2, respectively. Materials, equipment and apparatus set-up, experiment procedure and methodology are described.

3.1 Degradation of PMMA by zeolite catalyst

This part mentions the materials, equipment, instrument and methodology used for study of the PMMA degradation. The preliminary diagnosis is thermal analysis of scraped PMMA and characterization of the zeolite catalyst to obtain the general information of material used in this study.

3.1.1 Materials

3.1.1.1 Zeolite catalyst

The catalysts used in this study were zeolites of various types and $\text{SiO}_2/\text{Al}_2\text{O}_3$ ratios provided by the Siam Cement Group Public Company Limited as described below.

- ZSM5; produced by Zeolyst International
- Beta; produced by Süd-Chemie
- HUSY; produced by Tosoh Corporation
- Dealuminated USY; synthesized via dealumination of HUSY

Dealuminated USY with various $\text{SiO}_2/\text{Al}_2\text{O}_3$ ratios were prepared by dealumination of the original HUSY sample using an aqueous solution of nitric acid (HNO_3) with various concentrations. The solid to liquid ratio was kept constant at 1:40. The dealumination temperature and time were varied to achieve zeolites with desired aluminium (Al) contents. The solid products were filtered, washed repeatedly with de-ionized water until neutrality, dried overnight at 120°C and then calcined at 500°C for 6 h (Ngamcharussrivichai et al., 2005). The conditions of USY dealumination are summarized in Table 3.1. The photograph of zeolite catalyst used in this study was shown in Figure 3.1.

Table 3.1 Conditions of USY dealumination

Catalyst	Solution	Temperature ($^\circ\text{C}$)	Time^a (h)
HUSY-6	-	-	-
USY-30	0.5 M HNO_3	25	2
USY-63	0.15 M HNO_3	80	2*
USY-337	0.5 M HNO_3	80	2*

^a Asterisk means that the treatment was repeated 2 times.



Figure 3.1 Photographs of zeolite catalyst.

3.1.1.2 Polymer material

The polymer used in this study is poly (methyl methacrylate) (PMMA), supplied by the Siam Cement Group Public Company Limited. It is made of scraped particles whose size was in a range of 3 to 5 mm as shown in Figure 3.2. Its weight-average molecular weight is approximately $100,000 \text{ g}\cdot\text{mol}^{-1}$. Its physical properties are summarized in Table 3.2.



Figure 3.2 Photographs of PMMA polymer.

Table 3.2 Physical properties of PMMA (Thai MMA Co., Ltd, 2011: online)

		Properties	ISO		
Optical		Light Transmittance	93	%	ISO 13468-1
		Haze	0.5	%	ISO 14782
		Refractive Index	1.49		
Mechanical	Tensile strength	Rupture	75	Mpa	ISO 527-2
		Elongation at rupture	5	%	ISO 527-2
	Flexural strength	Rupture	120	MPa	ISO 178
		Modules of elasticity	3.2	Gpa	ISO 178
		Rockwell hardness	100		ISO 2039-2
	Compressive strength	Impact strength	2	$\text{kJ}\cdot\text{m}^{-2}$	ISO 180
Thermal		Specific heat	1.5	$\text{J}\cdot\text{g}^{-1}\cdot\text{°C}^{-1}$	
		Temperature of deflection under load	96	°C	ISO 75-2
		Coefficient of thermal expansion	7.00E-05	°C^{-1}	
Electrical		Surface resistivity	$>1\text{E-}16$	Ω	
		Charge reduction time by half	∞	sec	
Others		Specific gravity	1.19	$\text{g}\cdot\text{cm}^{-3}$	ISO 1183
		Tabor abrader	40	Hase%	ISO 9352
		Water absorption	0.3	%	ISO 62

3.1.1.3 Chemicals and gases

The list of chemicals and gases used in the degradation of PMMA, zeolite characterization and product analysis of this part are summarized in Table 3.3.

Table 3.3 Specification of chemicals and gases used in Part I; Degradation of PMMA

Chemicals and gases	Application
Nitrogen gas, 99.99% (Praxair)	Degradation of PMMA, characterization of zeolite and product analysis
Nitrogen gas, 99.95% (Praxair)	Degradation of PMMA and product analysis
Methyl methacrylate (MMA), ≥ 99% (Sigma-Aldrich)	Product analysis
Carbon disulfide; CS ₂	Product analysis
Liquid Nitrogen	Characterization of zeolite
Helium, 99.995%	Characterization of zeolite
Ammonia gas, 10% in Argon	Characterization of zeolite
Argon, 99.995%	Characterization of zeolite and product analysis
Oxygen gas, 99.99%	Characterization of zeolite

3.1.2 Experimental procedure and set-up

The analytical techniques and applications are summarized in Table 3.4. Thermal analysis of PMMA and the degradation of PMMA by zeolite catalyst under batch/ continuous conditions and product analysis are described in particular.

Table 3.4 Analytical techniques and applications in PMMA degradation

Analytical technique	Application
Thermogravimetric /differential thermal analysis (TGA-DTA)	Thermal analysis of PMMA
X-ray diffraction (XRD)	Crystalline structure of catalyst
X-ray fluorescence spectrometry (XRF)	Elemental analysis of catalyst
Nitrogen adsorption/desorption measurement	Porosimetry analysis of catalyst
Temperature programmed desorption of NH ₃ (TPD-NH ₃)	Evaluation of catalyst acidity
Gas chromatography with mass spectrometry (GC-MS)	Analysis of PMMA degradation products

3.1.2.1 Thermal analysis of PMMA

In this part, the thermal properties of PMMA were analyzed with a thermogravimetric analyzer (TGA, Mettler Toledo TGA/SDTA 851e) under nitrogen atmosphere with a flow rate of 50 mL•min⁻¹ in a temperature range of 50°C to 1000°C with a ramp rate of 10°C•min⁻¹. The weight loss was continuously recorded as a function of increasing temperature.

3.1.2.2 Characterization of the zeolite catalyst

The objective of catalyst characterisation was to examine the physicochemical properties of catalyst that may provide substantial information about the catalyst attributes. The information from various characterisation techniques will significantly improve the understanding of how the physicochemical attributes and catalytic performances are related. This section provides a brief review of the basic concepts of various catalyst characterisation techniques, namely XRF, XRD, N₂ adsorption/desorption analysis and NH₃-TPD.

X-ray diffraction (XRD)

The crystalline structure of catalyst was analysed by XRD instrument (Bruker D8 Advance XRD system) employing CuK α radiation ($\lambda = 1.5406 \text{ \AA}$) with an X-ray power of 40 kV and 40mA. The 2θ measurement started from 5° to 70° with steps of 0.0197° and a count time of 1 second.

X-ray fluorescence spectrometry (XRF)

X-ray fluorescence spectrometry is particularly well-suited to investigate the bulk chemical analysis of major elements. The elemental analysis of zeolite samples was performed by XRF (Wavelength Dispersive, Philips model PW2400) to determine the amount of silica and aluminium in zeolite catalysts.

N₂ adsorption/desorption analysis

Textural properties of the zeolite catalyst were measured by N₂ adsorption/desorption technique at -196°C (Micromeritics ASAP 2010). Prior to N₂ sorption, the solid samples were degassed at 300°C (this temperature being selected to eliminate some moisture and volatile matter). The specific surface area was determined by Brunauer-Emmett-Teller (BET) equation. The microporous and mesoporous volumes were measured from gas porosimetry measurements according to t-plot methods and Barrett-Joyner-Halenda (BJH) (Barrett et al., 1951), respectively.

Temperature-programmed desorption of NH₃ (TPD-NH₃)

Acidity of the zeolite catalysts in this study was evaluated by temperature-programmed desorption of NH₃ (TPD-NH₃) using a chemisorption analyser (Micromeritics AutoChem II 2920). The temperature programs for TPD experiment are illustrated in Figure 3.3. Crushed fresh zeolite sample (50 mg) was degassed up to 400°C with a rate of 10°C•min⁻¹ under a continuous flow of argon (Ar) at 50 mL•min⁻¹, then cooled down to ambient temperature prior to NH₃ saturation. After removal of physisorbed NH₃, a temperature ramp rate of 10°C•min⁻¹ was applied under argon (Ar) with flow rate of 50 mL•min⁻¹ until a temperature of 700°C was reached (except for ZSM-5 that was analyzed up to 800°C). The blank test (TPD without NH₃) was also performed to establish a proper baseline and to check for the extent of dehydroxylation reaction. The free acid sites were evaluated from subtraction of TPD profile with and without the preliminary saturation of the zeolite with NH₃. To determine the total amount of acid sites of zeolite, an amorphous silica-

alumina (ASA) with known amount of total acid sites ($0.55 \text{ mmol}\cdot\text{g}^{-1}$, as reported by Ngamcharussrivichai et al., 2004) was used as reference material.

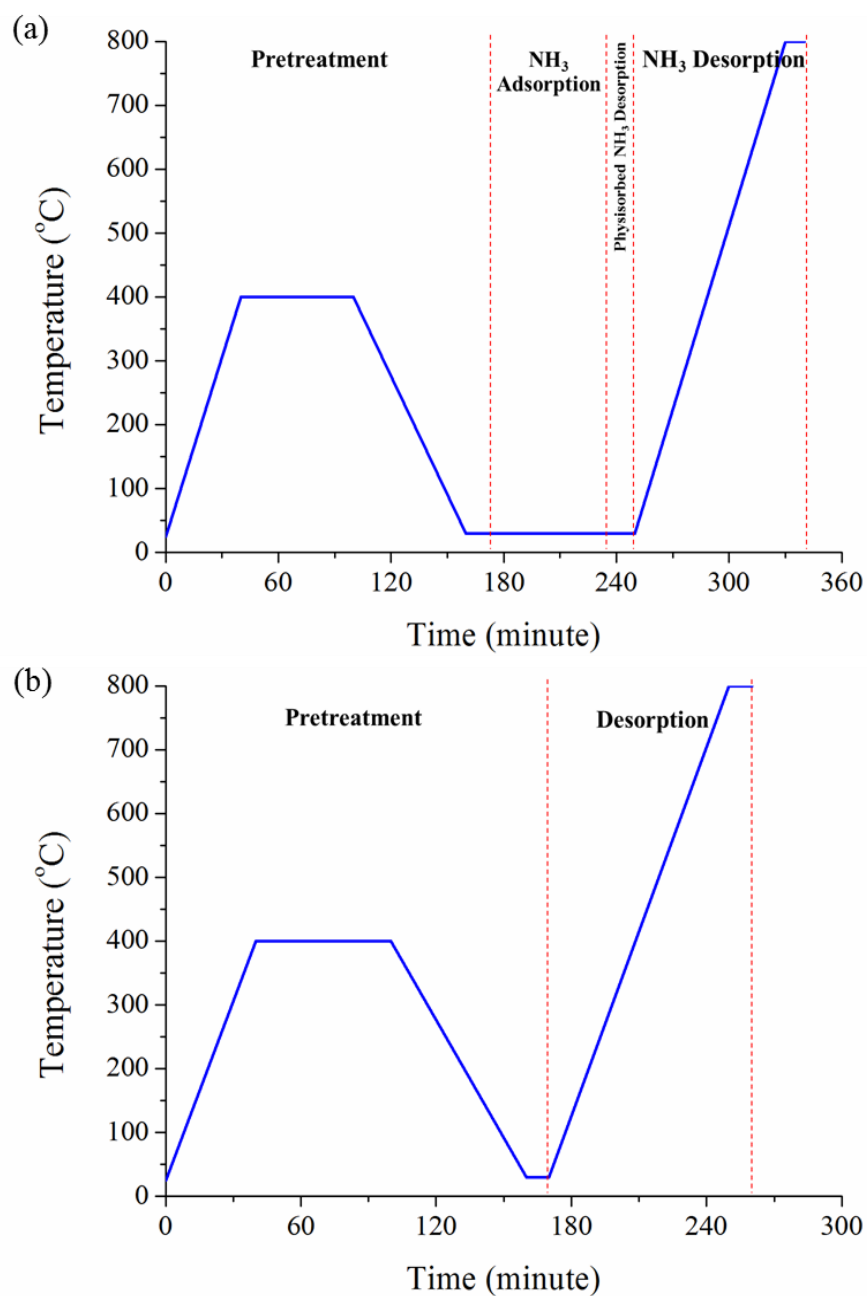


Figure 3.3 Profiles of temperature programmed for TPD experiment (a) with and (b) without NH₃ feeding (TPD-NH₃ / TPD w/o NH₃).

3.1.2.3 Degradation of PMMA by zeolite catalyst under batch conditions

The degradation experiment of PMMA was performed in a 250 mL batch reactor (High Pressure/High Temperature Reactors 4576) with 4-blade - 45° pitched blade – impeller, as shown in Figure 3.4. Vessel dimensions are i.d. 2.5” and depth 3.2”.



Figure 3.4 High Pressure/High Temperature Reactors 4576, 250 mL (Parr instrument).

In a typical experiment, 1.2 g of zeolite catalyst powder (ZSM5, Beta, HUSY or dealuminated USY) and 120 g of PMMA were used. Pure N₂ was continuously flowed through the reactor for 5 minutes in order to eliminate oxygen. Then the gas

inlet and outlet were closed and the reactor temperature was heated to 300°C. The reaction was subsequently performed at 300°C under autogenous pressure for 120 min, resulting in gas, liquid and solid products. After cooling and degassing, the reactor was weighted again to give the gas yield. The liquid and solid products were separated, liquid product being drained. After that, the solid containing trapped liquid was mixed with 100 mL of MMA, then centrifuged and dried at 80°C for 24 h to remove all interstitial liquid before weighing. The liquid product was distilled in a rotary evaporator at 95°C under vacuum pressure (200 mbar) to obtain the light fraction. The light fraction-separated liquid remaining in the rotary evaporator was classified as the heavy fraction. The experimental data were displayed in term of product yield (%) as shown in following equation:

$$Y_i (\%) = \frac{M_{Pd,i}}{M_{PMMA}} \times 100 \quad (3.1)$$

Where; Y is yield, M_{Pd} is mass of product, M_{PMMA} is mass of initial PMMA, and while i represents gas or liquid (either light or heavy) or solid.

3.1.2.4 Degradation of PMMA by zeolite catalyst under continuous conditions

The experimental set-up for PMMA degradation in continuous process consists of three main sections namely the feeding section, the reactor and gas condensing unit, which were made of stainless steel. The schematic diagram of continuous catalytic degradation unit is given in Figure 3.5.

Feeding section; the feeding section consists of a two stage conical hopper with 6 and 15 cm i.d., a vertical screw feeder placed at central axis. The hopper was

continuously purged with nitrogen (N_2) at a flow rate of $1 \text{ L}\cdot\text{min}^{-1}$ to eliminate air around PMMA particles.

Reactor; the reactor contains three sub-sections. The first one is an electrical gas preheater placed at the bottom of reactor. The second one is the reaction zone in which PMMA degradation takes place. It is a cylinder, whose dimension is 20 cm i.d., 50 cm height, equipped with an electrical heater and rock wool insulation. The last one is an expansion zone which allows vaporized heavy fraction to condense and drop back into the bed for further cracking, and also prevents catalyst particles from flying away. Before the experiment, the reactor was purged with nitrogen at a flow rate of $5 \text{ L}\cdot\text{min}^{-1}$ until the gaseous effluent has 1 ppm oxygen content or below, monitored by a fuel gas analyzer. The nitrogen flow rate was also kept constant at this flow rate along the experiment.

The gas condensing unit is composed of a condenser, a water cooler and condensate vessel. Hot gaseous stream leaving the reactor was cooled down in the condenser with a counter current flow of cooling water whose temperature was kept constant at 2°C , supplied by the water cooler. The condensed liquid product that dripped down from the condenser was retained in the liquid reservoir for product analysis, while the gaseous product leaving the condenser was vented to atmosphere.

Scraped PMMA was continuously fed via the conical hopper into the reactor with a feed rate of $250 \text{ g}\cdot\text{h}^{-1}$ and dropped freely under heated nitrogen (up-flow mode) into the bed of catalyst (100 g zeolite extrudates: 400 g alumina ball; corresponding to a fixed bed of 10 cm high, the specifications of catalyst are confidential). The bed temperature was controlled by the electric heater at a temperature range of 200°C to 300°C for 2 to 240 h of reaction duration. The added polymer melted and coated the

surface of catalyst and then diffused into the catalyst macropores (Lin et.al, 2001). The volatile products leaving the reactor were passed through the condenser column operated with 2°C cooling water. The products were collected in the sample vessel and kept for analysis.

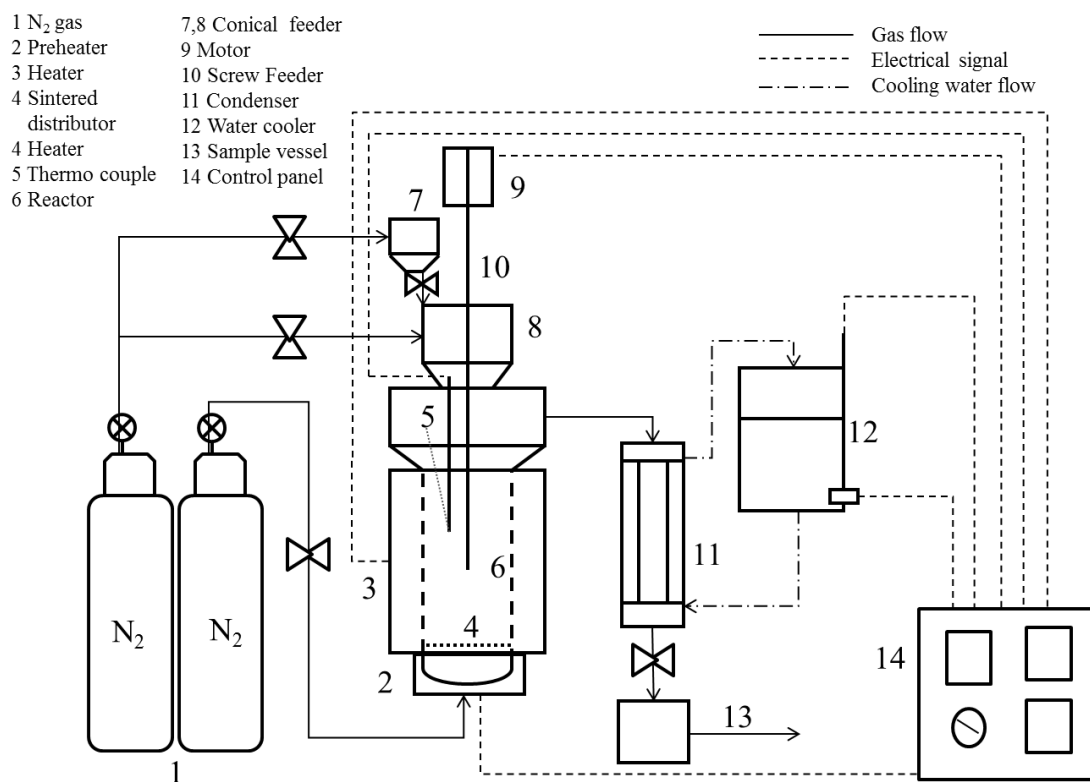


Figure 3.5 Schematic diagram of continuous catalytic degradation unit.

3.1.2.5 Product analysis

In the experiment, gas, liquid and solid products were obtained. Liquid product obtained from the batch experiment was separated into light fraction and heavy fraction (distillation residue) by a rotary evaporator under vacuum (95°C and 200 mbar). Representative liquid products are shown in Figure 3.6.



Figure 3.6 Liquid products from catalytic cracking of PMMA; (a) heavy fraction, (b) light fraction.

The distilled liquids and gaseous products were analysed by GC-MS system (model GC-MS-QP2010) using a capillary column DB-1 (0.25 mm i.d., 30 m length) and helium as the carrier gas. On the contrary, the liquid product attained from the continuous experiment was analysed without distillation. The details of GC-MS conditions used for determining the main compounds in the liquid product are given in Table 3.5. The quantity of MMA in the light fraction was roughly estimated by area percentage method, the area of an analysed peak was divided by the sum of areas for all peaks. This method assumed that the detector responds identically to all compounds.

The remaining solid that generally contained non-volatile products and coke, deposited on the catalyst after the catalytic degradation of the polymer was deemed “residues”. The amount and nature of the residues were determined by various techniques whose procedure will be described in the regeneration section.

Table 3.5 Operating conditions of the GC-MS for liquid and gas product analysis

Parameters	Analysis Operating Settings		
	Liquid product		Gas product
	Batch exp.	Continuous exp.	Continuous exp.
Column oven temperature	45.0°C	40.0°C	40.0°C
Injection temperature	180.0°C	200.0°C	200.0°C
Injection mode	Split	Split	Split
Flow control mode	Linear Velocity	Linear Velocity	Linear Velocity
Pressure	86.3 kPa	83.9 kPa	83.9 kPa
Total flow	31.6 mL•min ⁻¹	157.0 mL•min ⁻¹	8.5 mL•min ⁻¹
Column flow	1.51 mL•min ⁻¹	1.51 mL•min ⁻¹	1.51 mL•min ⁻¹
Linear velocity	44.4 cm•sec ⁻¹	44.4 cm•sec ⁻¹	44.4 cm•sec ⁻¹
Purge Flow	0.0 mL•min ⁻¹	4.0 mL•min ⁻¹	4.0 mL•min ⁻¹
Split ratio	20	100	2
Ion source temperature	200.0°C	200.0°C	200.0°C
Interface temperature	230.0°C	230.0°C	230.0°C
Solvent cut time	0 min	1.75 min	0.5 min

3.2 Regeneration of used catalyst by ozonation

This part concerns the materials, equipment, instrument and methodology used for study of the regeneration of spent zeolite catalyst by ozonation. The preliminary diagnosis is characterization of the used zeolite before and after regeneration to obtain the general information of material used in this study. The regeneration of spent zeolite by ozonation and the reusability tests are then described.

3.2.1 Materials

3.2.1.1 Zeolite catalyst

ZSM-5 zeolite (produced by Zeolyst International) was provided by the Siam Cement Group Public Company Limited in a form of ca. 3 mm X 10 mm extrudates containing 20 wt.% of aluminium oxide as binder. The pure ZSM-5 phase possesses a $\text{SiO}_2/\text{Al}_2\text{O}_3$ molar ratio of 23. The extrudates were used as the catalyst for cracking of poly (methyl methacrylate) (PMMA) in a fixed bed reactor operating at 1 bar and 270°C as described in the previous section. Regeneration experiments were conducted using coked ZSM-5 taken from different zones of the fixed bed, one from the middle-bottom and another one from the top of the fixed bed, as shown in Figure 3.7.

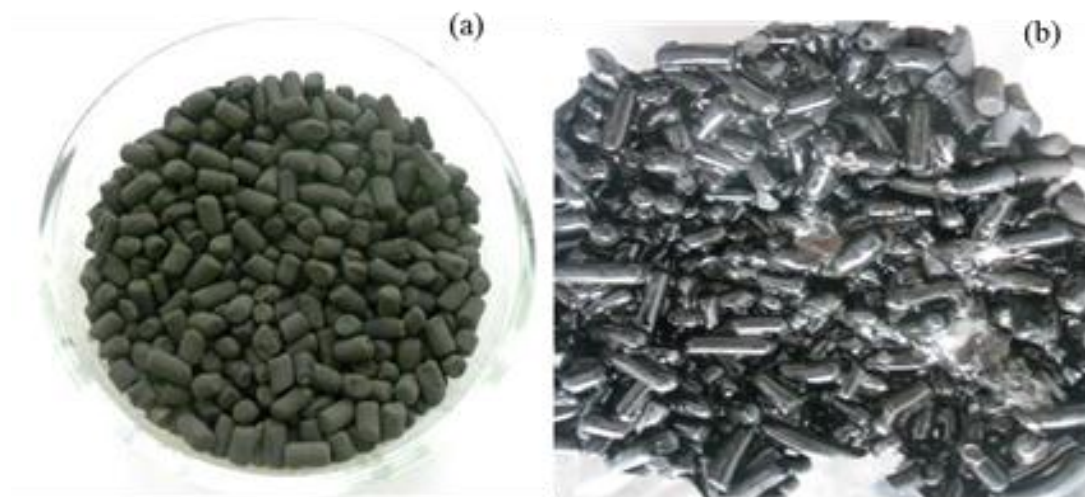


Figure 3.7 Photographs of coked catalysts from continuous process; (a) ZSM-5 particles from middle-bottom of PMMA cracking reactor (ZSM5-A) and (b) ZSM-5 particles from top of PMMA cracking reactor (ZSM5-B).

3.2.1.2 Chemicals and gases

The list of chemicals and gases used for the regeneration of spent zeolite are summarized in Table 3.6.

Table 3.6 Specification of chemicals and gases used in Part II; Regeneration of spent zeolite

Chemicals	Application
Potassium iodide; KI	Ozone determination
Sodium phosphate dihydrate; $\text{Na}_2\text{HPO}_4 \cdot 2\text{H}_2\text{O}$	Ozone determination
Potassium dihydrogen phosphate; KH_2PO_4	Ozone determination
Sodium thiosulphate; $\text{Na}_2\text{S}_2\text{O}_3$	Ozone determination
Sulfuric acid; H_2SO_4	Ozone determination
Potassium iodate; KIO_3	Ozone determination
Zinc iodide; ZnI_2	Ozone determination
Zinc chloride; ZnCl_2	Ozone determination
Potassium bromide; KBr (FTIR grade)	Characterization of zeolite
Liquid nitrogen	Characterization of zeolite
Helium, 99.995%	Characterization of zeolite
Nitrogen gas, 99.99%	Characterization of zeolite
Ammonia gas, 10% in Argon	Characterization of zeolite
Argon, 99.995%	Characterization of zeolite
Oxygen gas, 99.99%	Characterization and regeneration of zeolite

3.2.2 Experimental procedure and set-up

The analytical techniques and applications in coked zeolite regeneration are summarized in Table 3.7.

Table 3.7 Analytical techniques and applications in coked zeolite regeneration

Analytical technique	Application
Thermogravimetric analysis coupled with IR spectroscopy (TGA-IR)	Qualitative analysis of carbonaceous deposits
Scanning electron microscopy coupled with energy dispersive X-ray spectroscopy (SEM/EDX)	Morphology analysis, Elemental analysis
Flash combustion analysis	Quantification of carbon content
N ₂ adsorption/desorption measurement, Hg porosimetry	Textural properties analysis
Infrared and Raman spectroscopy	Qualitative analysis of carbonaceous deposits
Infrared spectroscopic study of pyridine adsorption	Acidity evaluation
Temperature-programmed desorption of NH ₃ (NH ₃ -TPD)	Acidity evaluation
Gas chromatography with mass spectrometry detection (GC-MS)	Activity assessment: Analysis of PMMA degradation products

3.2.2.1 Characterization of the spent zeolite catalyst before and after regeneration

For the best understanding of coke characteristics, various techniques are available for the characterization of carbonaceous compound deposited on zeolite. In this part, the physicochemical properties of the coked and regenerated catalysts were evaluated by several techniques and compared to those of fresh zeolite.

N₂ adsorption/ desorption measurement and mercury porosimetry

Textural properties of the spent zeolite catalyst before and after regeneration were measured and compared to those of fresh zeolite by N₂ adsorption and desorption at -196°C (Micromeritics ASAP 2010) and by mercury intrusion (Micromeritics AUTOPORE IV). Prior to N₂ sorption, the solid samples were degassed at 200°C (this temperature being selected to avoid coke removal). The specific surface area was determined by Brunauer-Emmett-Teller (BET) equation (Brunauer et.al., 1938). The mesoporous and microporous volumes were determined from gas adsorption measurement according to Barrett-Joyner-Halenda (BJH) (Barrett et.al., 1951) and Horvath-Kawazoe (HK) (Horvath and Kawazoe, 1983) methods respectively. The macroporous volume (50 nm < pore diameter < 30 µm) and skeletal density were evaluated from mercury porosimetry.

Thermogravimetry coupled with infrared spectroscopy (TGA-IR)

There are many techniques that can be used for the estimation of the hydrogen to carbon ratio (H/C) of coked material. The combinations of thermogravimetric analysis (TGA) with an online detection of gas-phase products such as IR is useful for

monitoring weight loss of coked sample and qualifying the nature of the carbonaceous deposit. This analysis was performed on a thermogravimetry coupled with infrared (TGA-IR) (Q50 thermobalance, TA Instruments) under nitrogen atmosphere. The samples were heated at $10^{\circ}\text{C}\cdot\text{min}^{-1}$ from 50 to 1000°C , including 60 min plateau at 120°C to remove physisorbed water.

CHN elemental analysis (CHN)

This analytical technique used for the estimation of carbon (C), hydrogen (H) and nitrogen (N) is based on the complete and instantaneous oxidation of the sample by “flash combustion”. The amount of carbon on the coked / regenerated catalysts was determined by a CHN elemental analyser (flash combustion, LECO model 2000 CHN analyser). The analysis was carried out at a temperature of $1,300^{\circ}\text{C}$ under pure oxygen atmosphere.

Scanning electron microscopy coupled with energy dispersive X-ray spectroscopy (SEM/EDX)

Scanning electron microscopy coupled with energy dispersive X-ray spectroscopy (SEM/EDX) was used to examine microscopic details of surface and cross-section of samples. In this study, the elemental profile and carbon content within the zeolite particles were observed by a Leo 435 VP scanning electron microscope coupled with an Oxford INCA 200 energy dispersive X-ray spectrometer.

Fourier transforms infrared spectroscopy and Raman spectroscopy

Fourier transforms infrared spectroscopy was performed on FT-IR PERKIN 1760 which used to investigate the nature of carbonaceous deposited laid down on the structure of zeolite catalyst. Potassium bromide (KBr) was used as the background file material. All spectra were measured from 4000 to 400 cm^{-1} with 100 scans at a resolution of 4 cm^{-1} . Raman spectroscopy was performed on FT-Raman, Perkin Elmer Spectrum GX to investigate the formation of adsorbed intermediates as well as the building up of carbonaceous deposits on the zeolite structure. The spectra were measured with Ar laser 632 nm from 4000 to 100 cm^{-1} .

Infrared spectroscopic study of pyridine adsorption

Acidity of the zeolite catalysts, which is usually correlated with their activity, was evaluated by pyridine adsorption/desorption followed by infrared spectroscopy (Nicolet NEXUS). Pyridine adsorption/desorption allowed the distinction between Brønsted and Lewis acid sites, due to the narrow character and high extinction coefficient of the typical IR bands (Martins et al., 2008). Crushed zeolite samples (10-30 mg) were pressed into thin wafers and pretreated under flowing air at 450°C overnight and then under vacuum. The wafer was saturated with pyridine vapor at 150°C and after a few minutes physisorbed pyridine was removed under vacuum for 1 h. The concentration of Brønsted and Lewis acid sites able to retain pyridine at 150°C was estimated from the surface of IR bands at 1545 cm^{-1} and 1455 cm^{-1} , respectively. Subsequent desorption analyses were performed at 250°C, 350°C and 450°C to estimate the strength of acid sites (Meloni et al., 2001).

Temperature-programmed desorption of NH_3 (TPD)

Temperature-programmed desorption of NH_3 (NH_3 -TPD) was used to measure the acid properties of spent zeolite samples and performed on a Micromeritics AutoChem II 2920 chemisorption analyser. Moreover, TPD without NH_3 of spent zeolite samples was also performed in order to observe dehydroxylation in the framework structure of zeolite and decomposition of carbonaceous deposits.

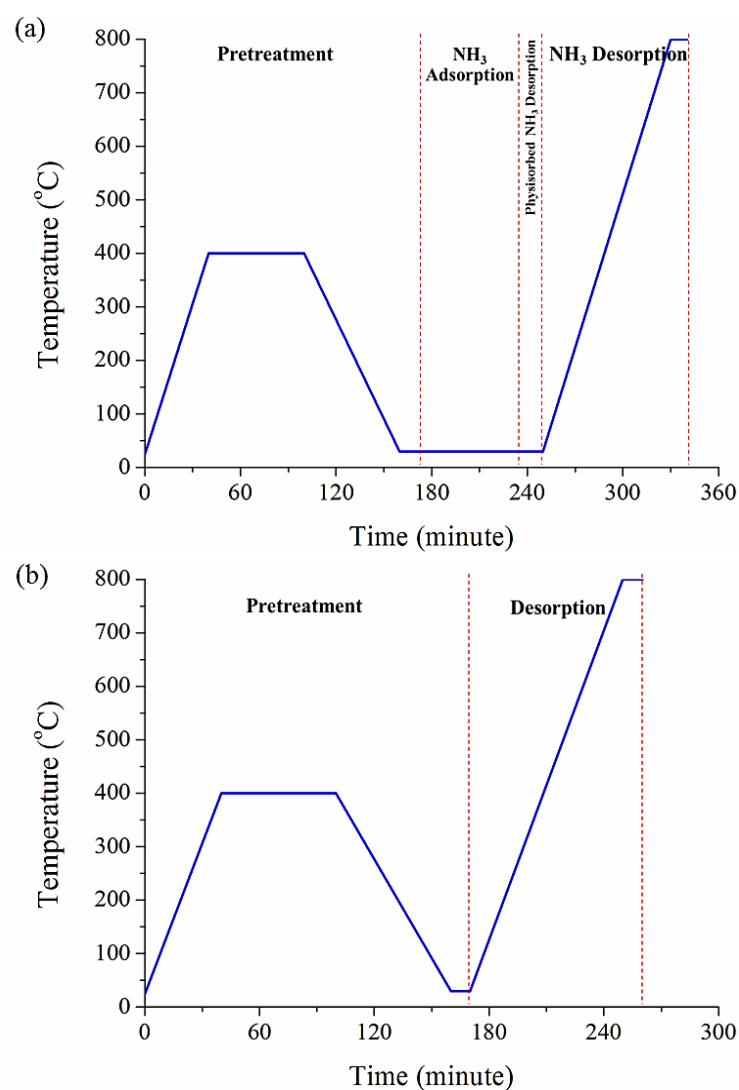


Figure 3.8 Temperature programmed profiles for the TPD experiment (a) with and (b) without NH_3 feeding (TPD- NH_3 /TPD w/o NH_3).

Figure 3.8 shows the temperature programmed profiles with and without NH_3 feeding. Crushed samples (50 mg) were degassed under argon (Ar) with flow rate of $50 \text{ mL}\cdot\text{min}^{-1}$ by heating with a rate of $10^\circ\text{C}\cdot\text{min}^{-1}$ up to 400°C , and cooled back to ambient prior to NH_3 saturation. After removal of physisorbed NH_3 , a temperature ramp rate of $10^\circ\text{C}\cdot\text{min}^{-1}$ was applied up to 800°C under argon (Ar) with a flow rate of $50 \text{ mL}\cdot\text{min}^{-1}$. The total amount of acid sites was evaluated by subtraction of TPD profile with and without the preliminary saturation of the zeolite with NH_3 .

3.2.2.2 Regeneration of spent zeolite catalyst

Ozonation of coked samples was performed in a glass tube reactor (4 mm i.d., 18 cm length) for temperatures varying from 20°C to 150°C . It was inserted in a heated stainless steel cylinder whose temperature was adjusted by a PID controller. A laboratory ozone generator (HTU-500 ozone generator, Azcozon) was used to produce ozone from pure oxygen by corona discharge. This apparatus can produce ozone in the range of 16 to $50 \text{ g}\cdot\text{m}^{-3}$. The schematic diagram of the experimental set-up is given in Figure 3.9. Coked zeolite particles of about 3 mm diameter were loaded in the reactor (after their half part were cut and kept as reference sample). The sample was first heated under oxygen flow (up-flow mode, flow rate from 12.7 to $69.9 \text{ L}\cdot\text{h}^{-1}$) until the desired temperature was reached (temperature studied in range of 25 to 150°C). Then the gas flow was switched to O_3/O_2 mixture (16 to $50 \text{ g}\cdot\text{m}^{-3}$ of ozone content) while the total flow rate was still in between 12.7 to $69.9 \text{ L}\cdot\text{h}^{-1}$. Time on stream (TOS) was varied from 0.5 h to 4 h. Inlet and outlet ozone concentrations were determined by the potassium iodide-trap method (IOA Standardized Procedure 001/96). KI solution was added to a gas washing bottle equipped with an open gas

bubbling device used to trap ozone. The determination of ozone concentration in a process gas by iodometric method is described in Appendix B. After treatment, particles were crushed and mixed for carbon analysis (same for reference half pellets). The experimental data were displayed in terms of carbon removal (%) as shown in following equation:

$$\text{Carbon removal (\%)} = \frac{C_{ref} - C_s}{C_{ref}} \times 100 \quad (3.2)$$

where C_{ref} is initial carbon content and C_s is final carbon content of zeolite samples.

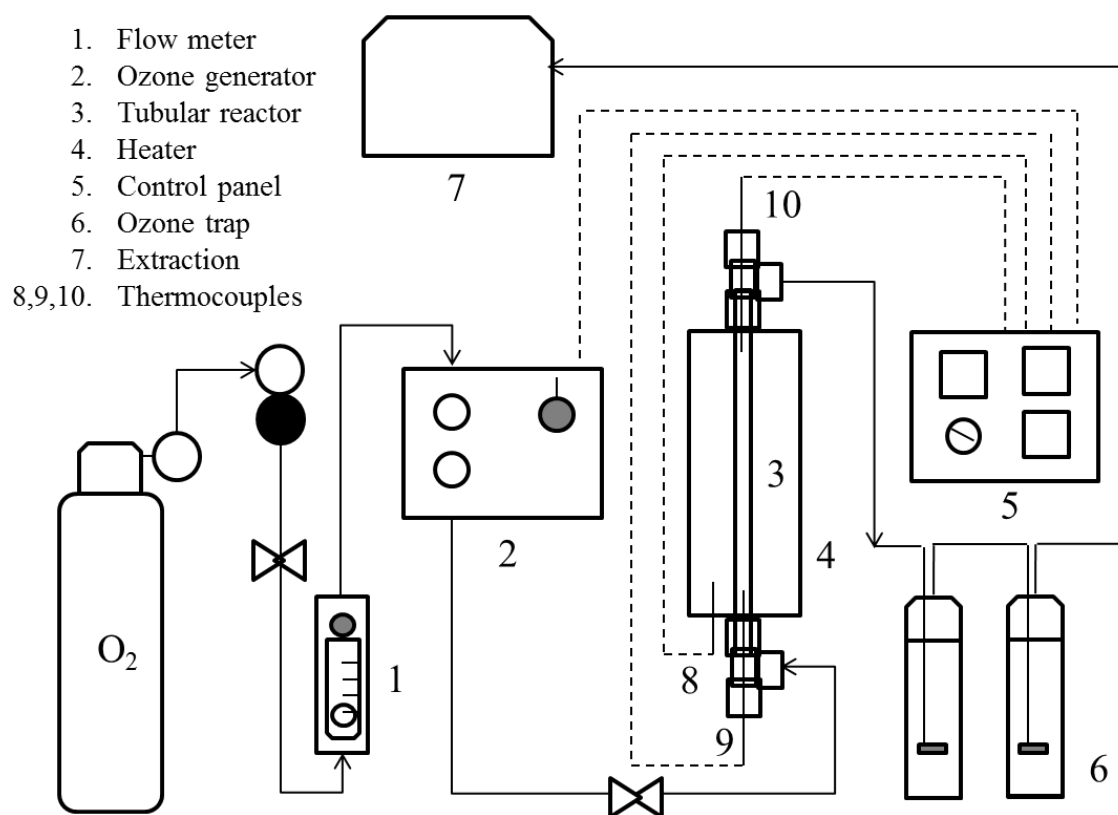


Figure 3.9 Schematic diagram of the set-up for the regeneration of coked zeolite.

3.2.2.3 Catalytic and thermal decomposition of ozone

Ozone decomposition has been extensively studied as reported in the publication and patent literature (Sidney et al. 1957; Michael 1971; Stephen and Naperville 1986; Stephen et al 1986; Krassimir 2011). Experiments on ozone decomposition under thermal and catalytic conditions were conducted to confirm the enhanced decay of ozone. For the catalytic degradation of ozone, particles of fresh zeolite (0 to 0.8 g) were loaded in the reactor and were heated under oxygen flow (up-flow mode, flow rate from 12.7 to 69.9 L•h⁻¹) until the desired temperature was reached (temperature studied in range of 25 to 150°C). Then the gas flow was switched to O₃/O₂ mixture (16 to 50 g•m⁻³ of ozone content). Inlet and outlet ozone concentrations were determined by the potassium iodide-trap method (IOA Standardized Procedure 001/96). In addition, thermal degradation of ozone was also operated with the same conditions in the empty reactor. The experimental data were displayed in terms of ozone degradation (%) as shown in following equation:

$$\text{Ozone degradation (\%)} = \frac{[O_3]_{in} - [O_3]_{out}}{[O_3]_{in}} \times 100 \quad (3.3)$$

where $[O_3]_{in}$ is inlet ozone concentration and $[O_3]_{out}$ is outlet ozone concentration.

3.2.2.4 Reusability test of regenerated catalyst

PMMA cracking tests were performed in a 100 mL batch reactor (Mini bench top reactor 4560) with 4-blade - 45° pitched blade - impeller, as shown in Figure 3.10. Vessel dimensions are i.d. 2" and depth 2".



Figure 3.10 Mini bench top reactor 4560, 100 mL (Parr instrument).

For each experiment, 0.4 g of crushed zeolite extruded and 40 g of PMMA were used. Pure nitrogen was continuously flowed through the reactor for 5 minutes in order to eliminate oxygen. Then the gas inlet and outlet were shut off and the reactor temperature was elevated to 300°C. The reaction was subsequently performed for 120 min at 300°C under autogenous pressure, while the initial pressure was 1 bar,

resulting in gas, liquid and solid products. After cooling and degassing, the reactor was weighted again to give the gas yield. Then liquid products were drained. The residual solid was washed with 50 mL of MMA, then centrifuged and dried at 80°C for 24 h to remove all interstitial liquid before weighing. The liquid product was distilled in a rotary evaporator at 95°C under vacuum pressure (200 mbar) to obtain the light fraction.

CHAPTER IV

DEGRADATION OF PMMA BY ZEOLITE CATALYST

In this chapter, the degradation of poly (methyl methacrylate) (PMMA) on various types of zeolite catalyst is investigated. The experiments were performed in batch and continuous reactors as mentioned in the previous chapter. Thermal analysis of PMMA by TG/DTA technique was done to determine the thermal stability and properties of PMMA as described in section 4.1. The characterization of catalyst is explained in section 4.2. The evaluation and screening of catalyst is described in section 4.3. The activity of zeolite catalyst in the degradation of PMMA in continuous experiment is shown in section 4.4. In details, distribution of product yields attained from the PMMA degradation over different types of catalysts (ZSM5, Beta and USY) with respect to time and temperature are provided. The characterization of catalysts with methods described in the previous chapter and their influence on cracking product are also explained. In this chapter, data analysis and graphing software “OriginPro8.5” was applied for peak deconvolution of TG-DTA and TPD curves for a better interpretation of the data.

4.1 Thermogravimetric /differential thermal analysis (TG-DTA) of PMMA

Thermogravimetric analysis (TGA) is an analytical technique used for prediction of thermal stability at temperatures up to 1000°C and for determination of the composition of materials. TGA is used to estimate the change in the mass of a sample as a function of time or temperature under a controlled atmosphere. One of the purposes of analysing PMMA by TGA was to measure the thermal stability and temperature range of PMMA degradation. PMMA sample was pyrolysed under nitrogen flowing at 50 mL•min⁻¹ and at a temperature between 50°C and 1000°C with a ramp rate of 10°C•min⁻¹. Figure 4.1 shows TG curve of PMMA polymer (green line) with corresponding DTG plot (red line) and the enlargement of DTG curve. The TGA result (Figure 4.1(a)) shows that the percentage of weight loss of PMMA sample is a function of temperature. The weight of the polymer starts changing after the first bond is broken and when the cracking products are vaporized, as previously reported by Ferriol and co-workers (Ferriol et al., 2003). It can be observed that the weight is rapidly changing with a vertical slope. PMMA polymer undergoes thermal degradation beginning at 200°C and maximum conversion is obtained at 400°C, with endothermic reaction as seen from DTA curve. From the deconvolution of DTG curve (shown by green lines), three successive degradation stages are found in Figure 4.1(b) (black line and open red circles are experimental data and fitted model, respectively).

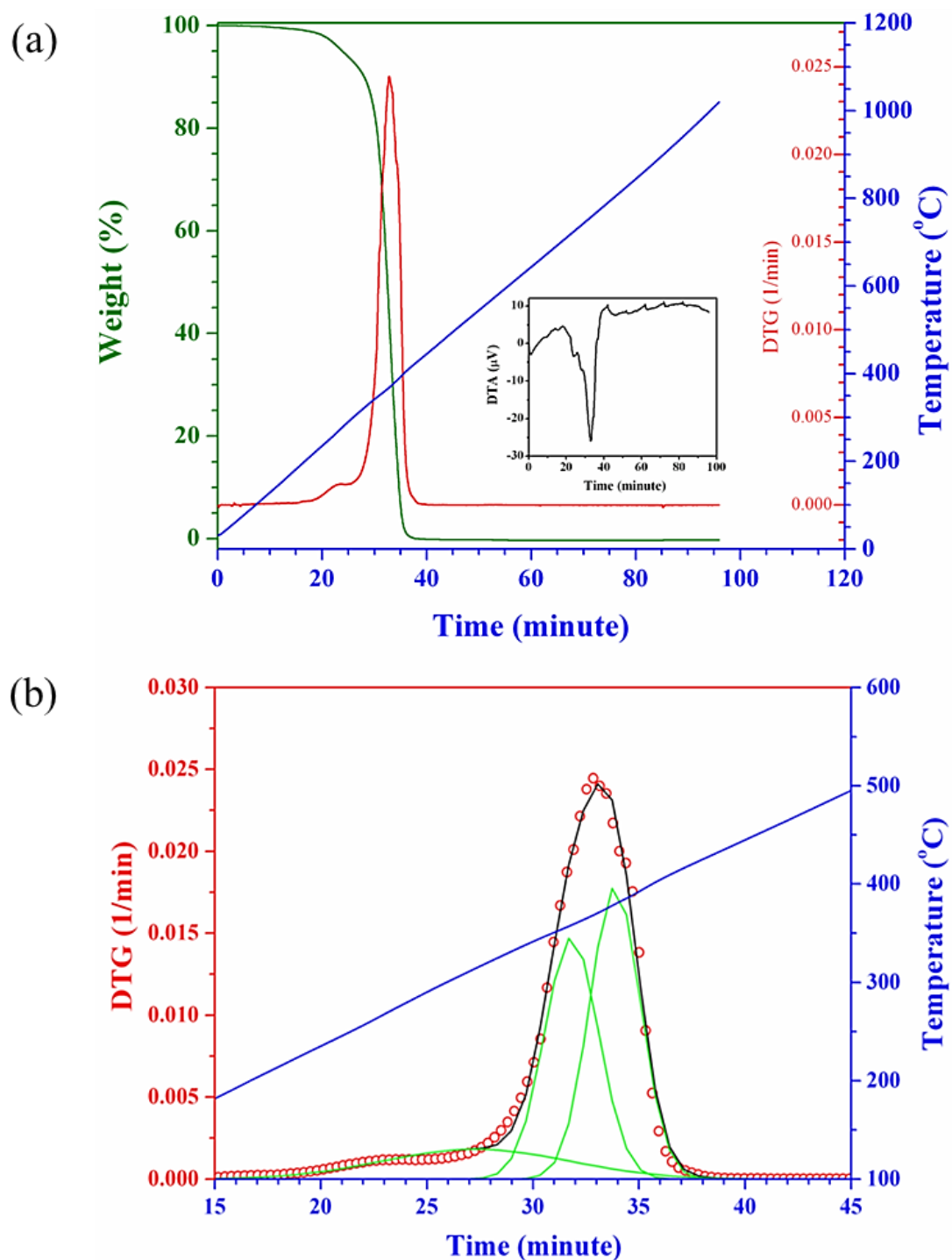


Figure 4.1 Dynamic TG analysis of PMMA under nitrogen atmosphere; (a) TG, DTG and DTA curve of PMMA, (b) the enlargement of DTG curve and its deconvolution peaks.

According to Salam and co-workers (Salam, Matthews, and Robertson, 2000), the first stage starting at 200°C corresponds to the melting of polymer, the depolymerization via the elimination of water or additive as well as residual acetone and methanol by scission of weak peroxide and hydroperoxide linkages. The second stage, starting at approximately 320°C, is ascribed to the decomposition of PMMA initiated by a mixture of chain-end and random scissions as reported by Holland and Hay (Holland and Hay, 2001, cited in Ferriol et al., 2003) while the last step starting at 350°C would be due to the depolymerization via random scissions as claimed by Kashiwaki and co-workers and Manring (Kashiwaki et al., 1986, cited in Ferriol et al., 2003; Manring, 1991, cited in Ferriol et al., 2003).

4.2 Catalyst Characterization

This part summarizes the general information of catalysts used in this study as analysed by several common characterization techniques. The catalysts are zeolites with various framework structures and SiO₂/Al₂O₃ ratios as previously described in Chapter III.

4.2.1 X-ray diffraction (XRD)

The crystalline structure of zeolite catalyst used in this study was analysed by X-ray diffraction (XRD) technique on a XRD system employing CuK α radiation ($\lambda = 1.5406 \text{ \AA}$) with an X-ray power of 40 kV, 40 mA. The 2θ measurement started from 5° to 70° with steps of 0.0197° and a count time of 1 second. The powder X-ray diffraction patterns of zeolite catalysts are shown in Figure 4.2. The results indicate

that samples exhibited either MFI, BEA or FAU typical structure when compared with the X-ray data of the corresponding standard zeolites reported by International Zeolite Association (Treacy and Higgins, 2001).

The characteristic peaks of ZSM5-25 and ZSM5-1000 (Figure 4.2 (a) and (b)) corresponded to a highly crystalline solid possessing a typical MFI zeolitic framework. Beta zeolite (Figure 4.2 (c)) exhibited a typical BEA zeolite framework. Finally, HUSY-6, USY-30 and USY-63 (Figure 4.2 (d), (e) and (f)) zeolites demonstrated the typical FAU zeolite framework. In addition, the XRD patterns of dealuminated USY zeolites with higher $\text{SiO}_2/\text{Al}_2\text{O}_3$ ratios (the exact $\text{SiO}_2/\text{Al}_2\text{O}_3$ ratios are mentioned in elemental analysis section) showed a gradual decrease in the intensities as well as a broadening of low angle XRD peaks ($2\theta = 5^\circ\text{-}30^\circ$) as increasing acuity of acid treatment (dealumination), especially for USY-337 (Figure 4.2 (g)) whose XRD pattern did not show any characteristic peaks of FAU. The decrease in the intensity of XRD peaks indicates a breakdown of the zeolite structure while the broadening of XRD peaks is due to the presence of an amorphous phase caused by a collapse of the zeolite framework. These dealumination effects are in agreement with those reported by Yan and co-worker (Yan et al., 2003). The XRD peak height of the severely dealuminated zeolite was significantly decreased from its original pattern as seen in Figure 4.2 (g).

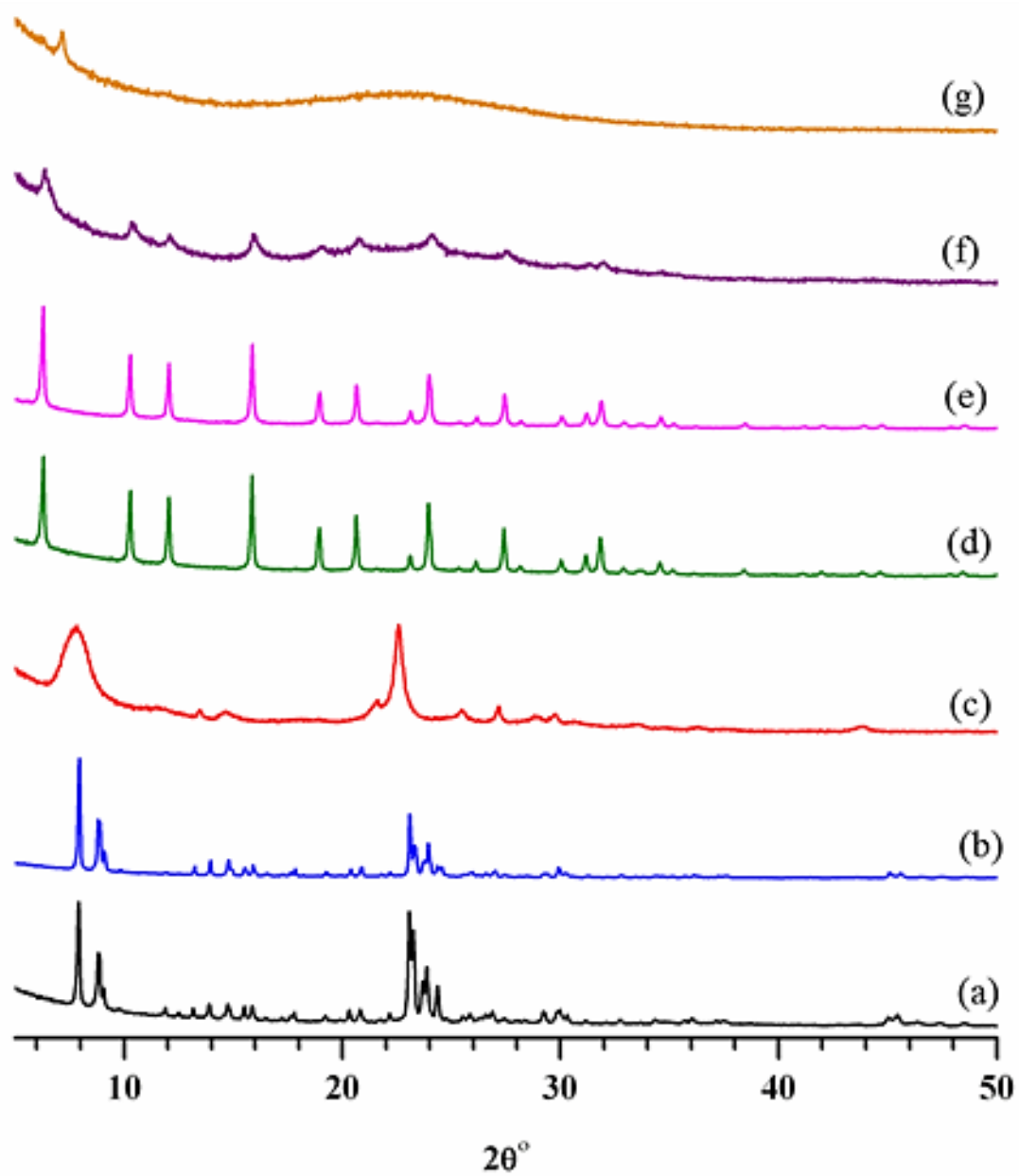


Figure 4.2 Powder XRD patterns for zeolites used in this study; (a) ZSM5-25, (b) ZSM5-1000 (c) Beta-25, (d) HUSY-6, (e) USY-30, (f) USY-63 and (g) USY-337.

4.2.2 Surface area and porosity

The textural properties and specific surface area of the zeolite catalysts were measured by N₂ adsorption/desorption technique at -196°C, then determined according to Brunauer-Emmett-Teller equation at relative pressures between 0.01 and 0.2 (Brunauer et al., 1938). The surface area depends on many parameters such as type of zeolite, type of binder used during shaping process and SiO₂/Al₂O₃ ratio (Lutz et al., 2004). The elemental composition (measured by XRF spectrometry) and physical characteristics of different zeolite samples are summarized in Table 4.1.

Table 4.1 Physical characteristics of zeolite samples

Zeolite^a	Framework structure^b	BET surface area^c (m²•g⁻¹)	BJH mesopore volume^d (cm³•g⁻¹)	t-plot micropore volume^e (cm³•g⁻¹)	BJH adsorption average pore diameter^d (Å)
ZSM5-25	MFI	361	0.18	0.08	70.38
ZSM5-1000	MFI	297	0.06	0.10	45.95
Beta-25	BEA	466	0.32	0.15	104.57
HUSY-6	FAU	901	0.18	0.25	74.37
USY-30	FAU	1010	N/A	N/A	N/A
USY-63	FAU	834	N/A	N/A	N/A
USY-337	Undefinable	410	N/A	N/A	N/A

^a Number after hyphen indicates the SiO₂/Al₂O₃ ratio, measured by XRF spectrometry.

^b Analyzed by XRD.

^{c,d,e} Measured by N₂ adsorption/desorption, then determined according to Brunauer-Emmett-Teller equation, Barrett-Joyner-Halenda equation and t-plot method, respectively.

The result shows that the BET surface area of ZSM5-25 is higher than that of ZSM5-1000. In case of USY zeolite, the result shows that BET surface area of HUSY-6 and USY-30 are significantly higher than that of USY-63 and USY-337. Moreover, in case of dealuminated USY, the surface area was found to decrease with the decrease of aluminium (Al) content. Recalling that the dealumination process partially breakdowns the zeolite structure, it results in the presence of an amorphous phase and therefore causes a decrease of surface area. This is in good agreement with the results published by Van Bokhoven et al. (2001) and Mohammed et al. (2010).

4.2.3 Acidity in terms of acid amount and acid strength

Acidity of the zeolite used in this study was determined by temperature-programmed desorption using NH_3 as basic probe molecule (TPD- NH_3) on a chemisorption analyser (Micromeritics AutoChem II 2920). The details of methodology are described in the previous chapter (Chapter III). The TPD results are presented as TCD signal which is proportional to the amount of the probe molecule (NH_3) released with change in the desorption temperature. Generally, this analysis was used to evaluate the number, type, and strength of active sites available on the surface of a catalyst. The area under TPD profile is proportional to the amount of acid sites occupied by NH_3 molecule on the surface of zeolite whereas the area under each of the mono-energetic curves is proportional to the amount of acid sites corresponding to such energy (Costa et al., 1999).

In this study, the blank test of TPD (without preliminary saturation of the zeolite with NH_3) was also established in order to create a curve corresponding to the release of structural hydroxyl groups from the zeolite framework, so called

dehydroxylation, occurring at temperatures between 600°C and 800°C. This curve was used as a baseline for the evaluation of the total number of acid sites by subtraction from original TPD curve. Figure 4.3 illustrates the NH₃-TPD profile of fresh zeolite and the blank test as shown in black solid line and short dash line, respectively. The TPD profile of the blank (short dash line) displays a small TCD signal in the 600°C to 700°C temperature range, which corresponds to the dehydroxylation of the zeolitic framework structure. It is probably negligible since it provides a very low total peak area in comparison to that of the NH₃-TPD profile.

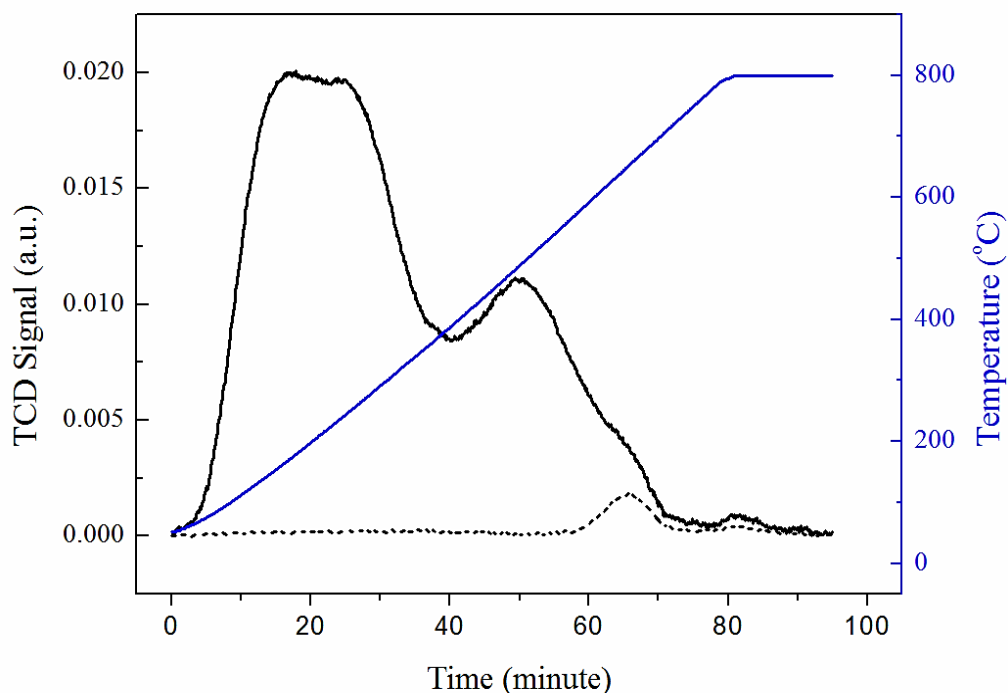


Figure 4.3 NH₃-TPD profile of fresh ZSM-5 (solid line) and blank test (dash line).

According to the TPD analysis, the NH₃ desorption shows a temperature-dependent behaviour directly related to the strength of acid sites involved in the chemical adsorption. The NH₃-TPD profiles of ZSM-5, Beta and USY zeolite are shown in Figure 4.4. A deconvolution technique was applied to the TPD curves for a better interpretation of the data. Three deconvolution peaks (green lines), each

following a Gaussian distribution, were found (black line and open red circle are experimental data and fitted model, respectively).

These three deconvolution peaks correspond to weak (low desorption temperature, $< 200^{\circ}\text{C}$), medium (200 to 400°C) and strong (high desorption temperature, $> 400^{\circ}\text{C}$) acid sites (Figure 4.4). Indeed, the higher the desorption temperature, the stronger the acid site. The temperature (T_{max}) at the maximum of NH_3 desorption from each type of acid site was recorded. To determine the amount of acid sites, an integration of the NH_3 -TPD profile has been applied, using amorphous silica-alumina (ASA) which known amount of total acid sites ($0.55 \text{ mmol}\cdot\text{g}^{-1}$, as reported by Ngamcharussrivichai et al., 2004) as the reference material. The ratio of weak to medium and strong acid sites was estimated by the ratio of areas under the corresponding peaks ($A_w/(A_m+A_s)$).

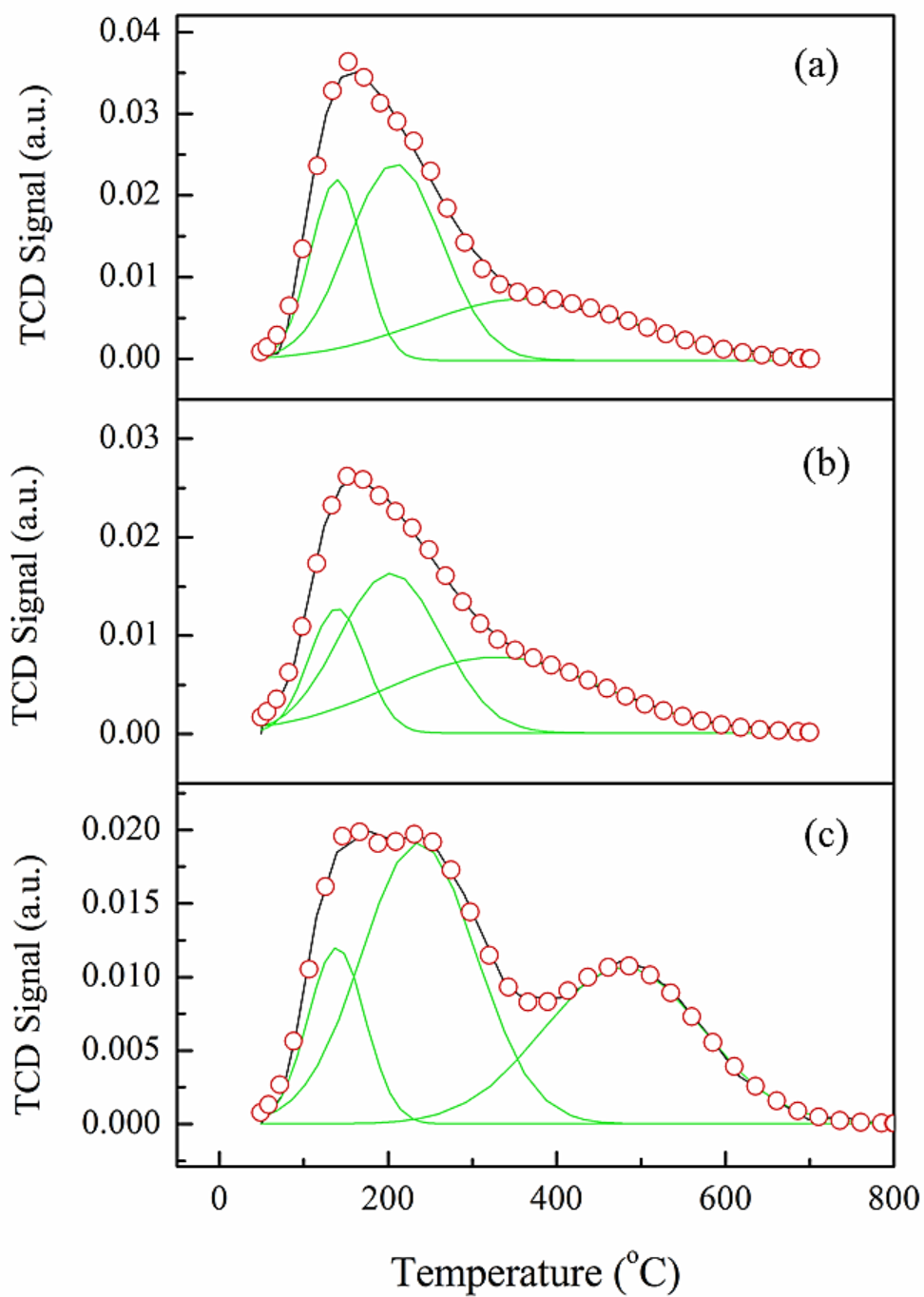


Figure 4.4 NH₃-TPD profile (black line) and Gaussian deconvolution (green lines) with cumulative fit (red line); (a) USY-30, (b) Beta-25 and (c) ZSM5-25.

The NH₃-TPD signals and deconvolution curves of ZSM-5 with SiO₂/Al₂O₃ ratios of 25 and 1000 are illustrated in Figure 4.5 (a) and (b), respectively. Recalling that the area under TPD profile was proportional to the amount of acid sites occupied by NH₃ molecules on the zeolite surface, the total amount of acid sites on ZSM5-1000 is smaller than that of ZSM5-25. The amount of acid sites is therefore directly related to the content of Al, as also reported by Martens and co-worker (Martens and Jacobs, 2001): the lower the Al content (i.e. the higher the SiO₂/Al₂O₃ ratio), the lower the number of Brønsted and Lewis sites.

In addition, the deconvolution curves of ZSM5-1000 show a down-shift of desorption temperatures when compared to those of ZSM5-25, which indicates a weaker acid strength. The relationship between the acid strength and aluminium content has been already reported by Demsey (Demsey, 1974, 1975, 1977, cited in Abbas et al., 1980) as it is directly related to the geometric distribution of the aluminium atoms. According to Demsey's works, the acid strength of a zeolite is directly associated with the number of aluminium atoms having no other aluminium atom as diagonal neighbour in four rings, which increases up to a SiO₂/Al₂O₃ ratio of 12 and thereafter decreases as the SiO₂/Al₂O₃ ratio increases (Abbas et al., 1980). Based on Demsey's observation, ZSM5-1000 would contain less aluminium atoms having no other aluminium atom as diagonal neighbour in four rings, and thus would exhibit a weaker acid strength than ZSM5-25. So, it can be concluded that an increasing of SiO₂/Al₂O₃ ratio clearly reduces the surface acidity in terms of number of acid sites and acid strength.

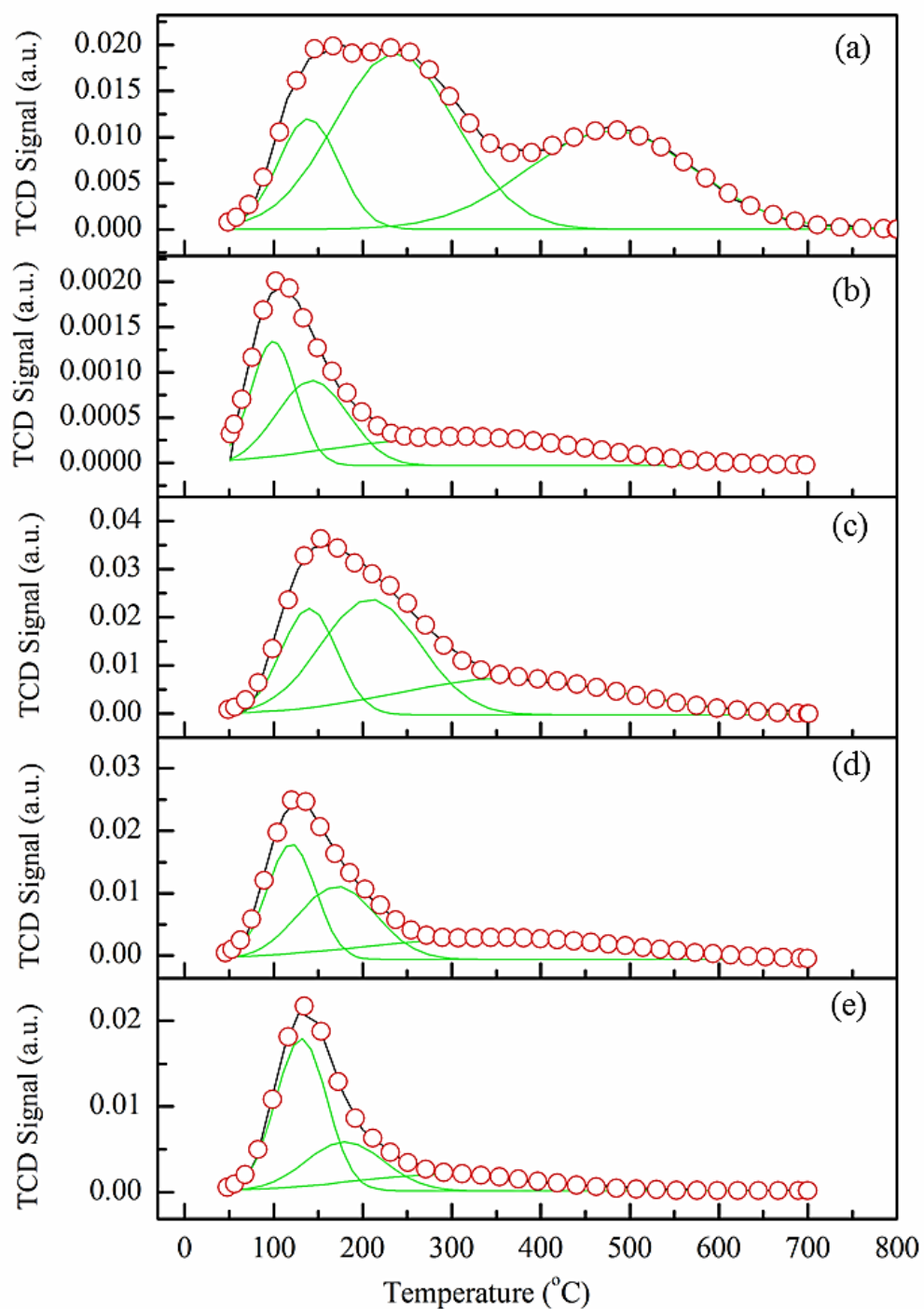


Figure 4.5 NH_3 -TPD profile of zeolite samples (black solid line) and Gaussian deconvolution (green lines) with cumulative fit (red line); (a) ZSM5-25, (b) ZSM5-1000 (c) HUSY-6, (d) USY-63 and (e) USY-337.

In case of HUSY-6 and dealuminated USY ($\text{SiO}_2/\text{Al}_2\text{O}_3 = 63$ and 337), NH_3 -TPD profiles and deconvolution curves are illustrated in Figures 4.5 (c), (d) and (e), respectively. Similarly to the results from ZSM-5, the total amount of acid sites decreases with increasing $\text{SiO}_2/\text{Al}_2\text{O}_3$ ratio as seen from the area under the TPD curve, and are in the following order; HUSY-6 > USY-63 > USY-337.

The temperature (T_{max}), at which the amount of desorbed NH_3 is maximum, is given in Table 4.2 for each type of acid site, as well as the total amount of acid sites. It is noteworthy that T_{max} of weak, medium and strong peaks of ZSM5-25 are the highest. Moreover, considering the ratio of weak acid site to medium and strong acid sites (A_w/A_m+A_s), it can be found that ZSM5-25 has the lowest ratio which means that this zeolite possesses the strongest acid strength.

Table 4.2 Summary of the NH₃-TPD results for different zeolite samples

	T_{max} (°C)			Total amount of acid sites (mmol•g⁻¹)	$\frac{A_w}{A_m + A_s}$
	(from deconvolution curves)				
	T_{m1}	T_{m2}	T_{m3}		
ZSM5-25	139	237	478	2.1	0.18
ZSM5-1000	100	143	311	0.1	0.42
Beta-25	140	203	329	2.0	0.21
HUSY-6	140	209	366	2.4	0.30
USY-30	111	160	364	1.7	0.19
USY-63	120	171	354	1.2	0.49
USY-337	131	180	294	0.8	1.14

T_{max} is the temperature at the maximum NH₃ desorption from each type of acid site (weak, medium and strong).

A_w is area under the peak corresponding to weak acid sites.

A_m is area under the peak corresponding to medium acid sites.

A_s is area under the peak corresponding to strong acid sites.

4.3 Catalyst evaluation and screening in batch experiment

According to the TG/DTA result, the thermal degradation of PMMA occurs in the range of 300 to 400°C. Thus, a reaction temperature of 320°C was used for thermal degradation of PMMA in the batch experiment. For the catalytic degradation experiment, since the catalyst was supposed to significantly reduce the temperature and time of the reaction, the reaction temperature was set to 300°C in order to screen an appropriate catalyst for degradation of PMMA.

In a preliminary experiment, a batch reaction was run in the absence of zeolite (thermal degradation) at 320°C for 2 h under autogenous pressure. It was found that the products were non-condensable gases and jelly-like solid residue, no liquid product could be recovered. This result indicates that this condition is not suitable for the PMMA thermal degradation. The photo of thermally degraded product obtained at 320°C is shown in Figure 4.6.

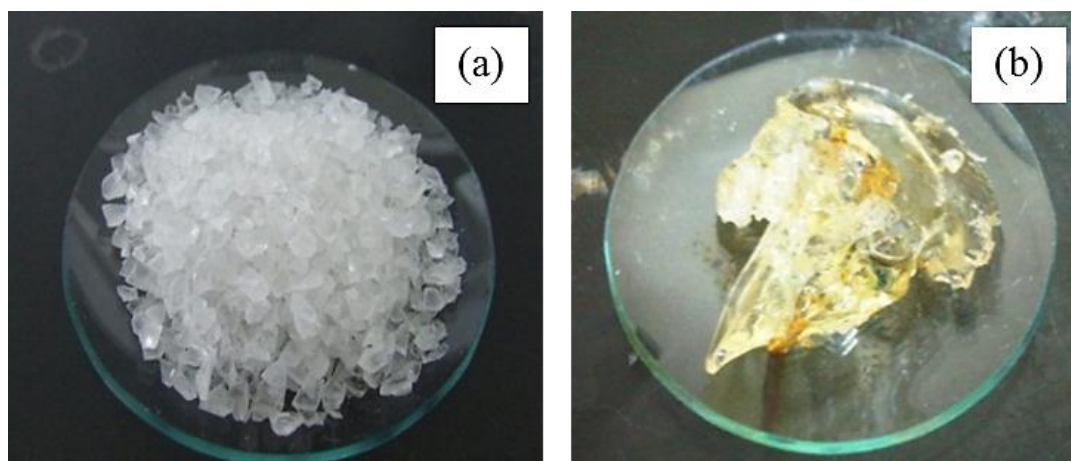


Figure 4.6 Photo of PMMA before and after thermal degradation at 320°C.

For the catalytic degradation of PMMA in batch experiment, zeolite catalyst and PMMA were fed into the cracking reactor with a catalyst/PMMA mass ratio of 1%. As claimed by Arthur and co-workers (Arthur et al., 2004), it was found that for certain mixtures of PMMA and zeolite catalyst at temperatures around 300°C (reaction duration of 2 h), the molten PMMA begins to coat on surface or diffuse into macropores of zeolite where it is cracked by the external active sites and hence becomes lower molecular weight materials which can either diffuse into mesopores and micropores of zeolite for further cracking reaction or diffuse out of zeolite through the polymeric film as products. In each experiment, gas, liquid and solid products were obtained. The liquid product was separated into two fractions, light fraction and heavy fraction, by a rotary evaporator under vacuum (95°C and 200 mbar). The liquids and gaseous products were analysed by a GC-MS system using a capillary column DB-1 (model GCMS-QP2010), and with helium (He) as the carrier gas.

In this section, the effect on PMMA degradation of the chemical properties of the zeolite catalyst (in terms of acidity) has been investigated. The acidity of a zeolite can be expressed according to; i) the acid strength and ii) the total amount of acid sites.

4.3.1 Effect of acidity in terms of acid strength

In this part, the effect on PMMA degradation of the zeolite acidity expressed in terms of acid strength has been studied by using zeolites which have a similar level of acid amount ($\text{SiO}_2/\text{Al}_2\text{O}_3$ ratio representing the acid amount), but differ from the acid strength (acidity of each zeolite was previously reported in Section 4.2.3).

Figure 4.7 shows the catalytic cracking product distribution (gas, liquid (light and heavy fraction) and solid) obtained from the PMMA degradation over USY, Beta and ZSM-5 zeolite in batch experiment at 300°C for 2 h under autogenous pressure. The percentage of gas yield, as well as solid yield decrease when using zeolites with lower acid strength, as shown by the following order: ZSM5-25 > Beta-25 > USY-30. Subsequently, the total liquid yield increases significantly when using zeolites with lower acid strength. It can be concluded that the higher the acid strength, the higher the gas and solid yields, and the lower the liquid yield. From the product distribution of PMMA degradation over various zeolite catalysts, it is noteworthy that not only the acid properties of zeolite catalyst affect the product distribution, but also the shape-selectivity and structure of zeolite play an important role in the degradation of PMMA and selectivity to monomer (see an explanation in Section 4.3.3).

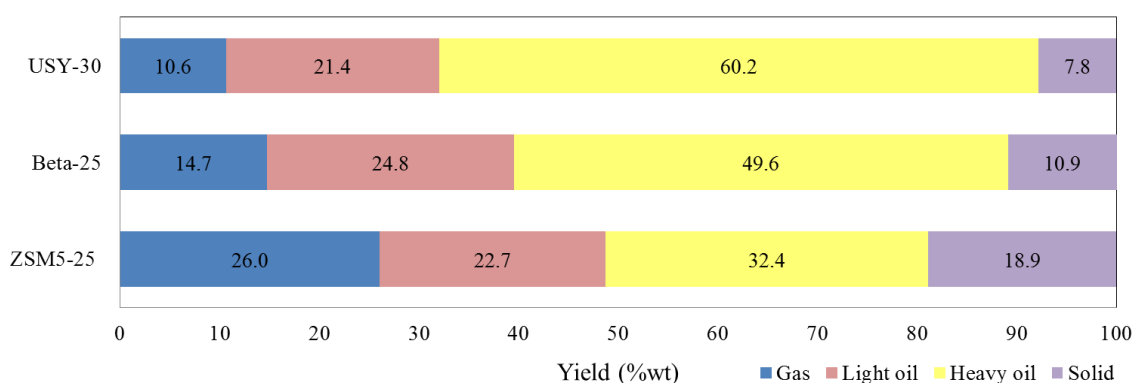


Figure 4.7 Product distribution of PMMA degradation over various types of zeolite catalyst.

4.3.2 Effect of acidity in terms of amount of acid sites

In this part, the effects on PMMA degradation of the acidity of zeolite expressed in terms of amount of acid sites have been studied. USY and ZSM5 zeolites with various $\text{SiO}_2/\text{Al}_2\text{O}_3$ ratios were applied to the reaction system (batch experiment at 300°C for 2 h under autogenous pressure) in order to study the effects of acid site content on product distribution. The result shows that zeolites with lower $\text{SiO}_2/\text{Al}_2\text{O}_3$ ratio, which implies higher amount of acid sites and higher surface area (textural properties are previously presented in Table 4.1), provide higher gas and solid products as illustrated in Figure 4.8, showing the following order: (for ZSM5) $\text{ZSM5-25} > \text{ZSM5-1000}$ and (for USY) $\text{HUSY-6} > \text{USY-30} > \text{USY-63} > \text{USY-337}$. As a consequence, the liquid yield increases significantly when using zeolites with higher $\text{SiO}_2/\text{Al}_2\text{O}_3$ ratio. It can be concluded that the lower the $\text{SiO}_2/\text{Al}_2\text{O}_3$ ratio (or the higher the amount of acid sites), the higher the gas and solid yields, and the lower the liquid yield.

Noticeably high solid contents were obtained for all experiments in this part. As these solid products were mainly formed on the wall of the reactor they might be the result of a non-well-mixed system. Indeed, the reactants that did not contact with the catalysts should have undergone thermal cracking which usually causes the formation of solid product on the wall of the reactor.

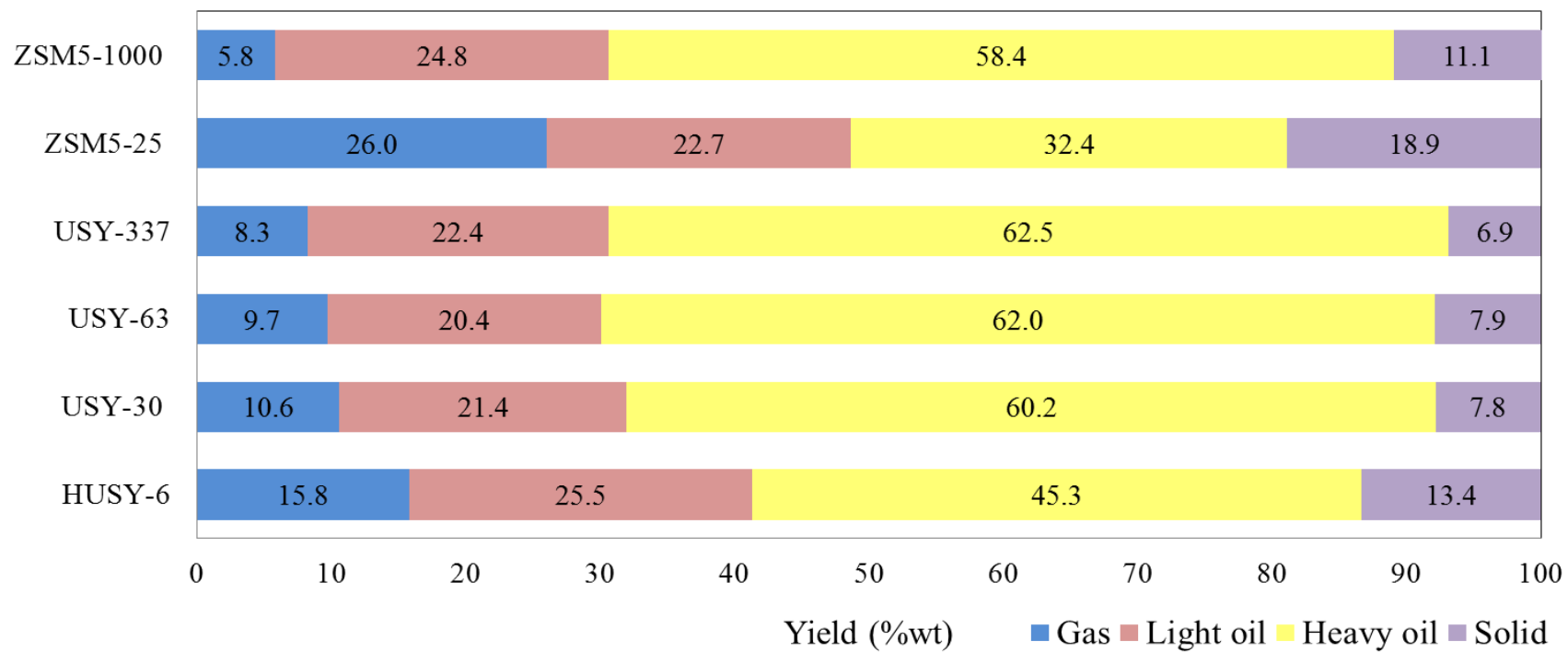


Figure 4.8 Product distribution of PMMA degradation over ZSM-5 and USY with different SiO₂/Al₂O₃ ratios.

4.3.3 Analysis of liquid products from batch experiments by GC-MS

The characteristics of light and heavy fraction obtained from the catalytic degradation of PMMA in the batch experiment using various zeolites have been investigated. The chemical composition of the liquid products has been analysed by GC-MS via the comparison of mass spectra of detected compounds with standard chromatogram data. In case of light fraction, the result obtained from the PMMA degradation over ZSM5-25 in the standard batch experiment is given as an example in Figure 4.9 which reveals MMA monomer as the main product, as evidenced by a sharp peak at a retention time of 1.66 min. In order to verify the exact specie of this component, comparisons of retention time and mass spectra were conducted concurrently. The identification of light fraction from PMMA degradation by GC-MS analysis with respect to the retention time is reported in Table 4.3. The quantitative analysis of light fraction was roughly done by comparison of the integrated areas with that of standard MMA (methyl methacrylate (MMA), $\geq 99\%$ (Sigma-Aldrich)). It was found that the MMA content in the light product from the PMMA degradation over ZSM5-25 in the batch experiment was up to 81.3 wt.%. These results led to the conclusion that the light fraction obtained by this process was mainly MMA monomer as confirmed by the same retention time (for all experiments) as well as the identical mass spectra with 97% similarity to standard MMA monomer, while C5-C6 esters or oxygenates were also detected as side products.

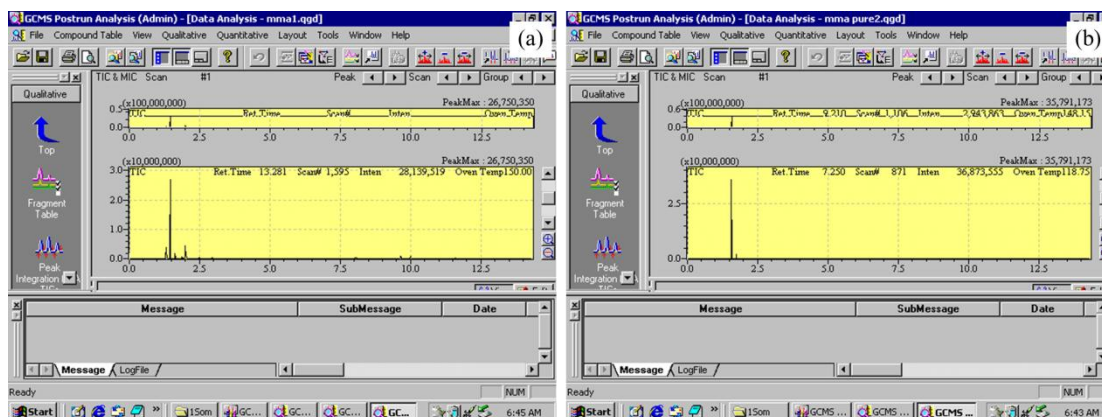
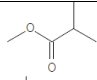
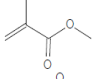
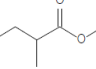


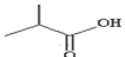
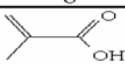
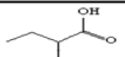
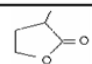
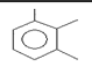
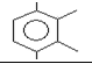
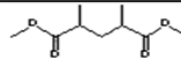
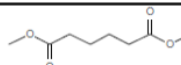
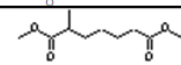
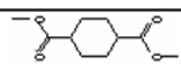
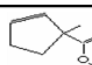

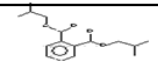
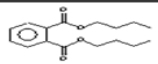
Figure 4.9 GC-MS spectra of light product from PMMA degradation over ZSM5-25 in the batch experiment (a) and pure MMA (b).

Table 4.3 Composition of light fraction from PMMA degradation by zeolite in batch experiment as analyzed by GC-MS

Retention time (minute)	Compound	Formula	Content (wt.%)
1.574	C ₅ H ₁₀ O ₂		15.6
1.664	C ₅ H ₈ O ₂ (MMA)		81.3
2.119	C ₆ H ₁₂ O ₂		3.1

Concerning the heavy fraction obtained from PMMA degradation over each zeolite in the batch experiment, the GC-MS analysis showed that this heavy fraction product consisted of 14 compounds as shown in Table 4.4.

Table 4.4 Chemical composition of heavy fraction for various types of zeolite catalyst

Compound	ZSM5-25	ZSM5-1000	Beta-25	HUSY-6	USY-30	USY-63	USY-337
C ₄ H ₈ O ₂ 							
C ₄ H ₆ O ₂ 							
C ₅ H ₁₀ O ₂ 							
C ₅ H ₈ O ₂ 							
C ₉ H ₁₂ 							
C ₁₀ H ₁₄ 							
C ₉ H ₁₆ O ₄ 							
C ₈ H ₁₄ O ₄ 							
C ₁₀ H ₁₈ O ₄ 							
C ₁₀ H ₁₆ O ₄ 							
C ₈ H ₁₂ O ₂ 							
C ₁₄ H ₃₀ 							
C ₁₆ H ₂₂ O ₄ 							
C ₁₆ H ₂₂ O ₄ 							

From Table 4.4, it can be seen that the product range was typically between C4 and C16 oxygenates. In details, the heavy fraction obtained from PMMA degradation over USY zeolites mostly consisted in aliphatic and alicyclic C9-C10 which seem to be structurally related to methyl methacrylate (MMA). These compounds have been already reported by Manring (Manring, 1991) as the products of PMMA degradation and originated from disproportionation, recombination as well as reaction of carbonium ion with MMA monomer forming R-MMA. For Beta zeolite, the heavy fraction contained more different products, for instance C14 alkane and C16 aromatic compounds. In case of ZSM-5 zeolite, the heavy fraction contained a wide variety of products, for example butyric acid, methacrylic acid, aliphatic, alicyclic and aromatic compounds.

The product distribution as well as the catalytic activity can be explained on the basis of microporous/ mesoporous structure and acidity of zeolite. In this case, the presence of various types and distinctive patterns of products in the heavy fraction when using ZSM-5 is directly related to the zeolitic structures of ZSM-5 itself. In general, on the Brønsted acid sites of ZSM-5, the carbenium ions are readily cyclized or isomerized and become cycloalkanes because of its shape selectivity. Simultaneously, the carbenium ions also undergo β -scission to give aliphatic compounds. In the pseudo-equilibrium between cycloalkanes and carbenium ions, the cycloalkanes can be dehydrogenated and lead to aromatics or can turn back to be carbenium ions by protonation. Practically, in case of catalyst with high hydrogen transfer activity, the hydride previously released by the dehydrogenation of cycloalkanes can be easily accommodated, leading to the formation of aromatics as reported by Liu and co-workers (Liu et al., 2004). When comparing ZSM5-25 and

ZSM5-1000, it can be seen that ZSM5-1000 provided less aromatic hydrocarbons due to its higher $\text{SiO}_2/\text{Al}_2\text{O}_3$ ratio. By increasing the $\text{SiO}_2/\text{Al}_2\text{O}_3$ ratio from 25 to 1000, hydrogen transfer, cyclization and aromatization reactions are decreased as confirmed by Abrevaya (Abrevaya, 2007). ZSM5-25 can provide an acid product which is probably a secondary product from C9-C10 aliphatic compounds due to its shape selectivity and acidity. From overall results, it was found that the shape-selectivity, acid properties and structure of zeolite played a very important role in the decomposition of PMMA and selectivity to monomer. It is also worth noting that the product distributions reflect features in association of porous systems of the zeolites. The different pore sizes allow the selective adsorption of certain reactants, or the selective desorption of certain products and can inhibit or promote different reaction intermediates in catalytic reactions. Over the large pore zeolites, USY and Beta, alkanes are the main products with less alkenes and aromatics compound. ZSM-5 gives significantly more aliphatic and aromatic compounds. In term of product yield, USY zeolite provides more liquid product due to its textural properties (supercage structure). In case of Beta zeolite, it also provide large portion of liquid product because of its large pores (12- membered rings). Conversely ZSM-5 (medium pore zeolite) gives significantly more gaseous product.

It can be conclude that the variety of products obtained depends on the characteristics of selected zeolite, ensuring catalytic degradation process to become a practical method for waste PMMA recycling.

4.4 Catalytic activity for the degradation of PMMA in continuous experiment

4.4.1 Effect of temperature

Temperature is one of the most important operating variables for the cracking reaction of polymer materials. In this part, the effect of reaction temperature was investigated in a continuous experiment by using extruded Beta (BETA-E1 and BETA-E2) and ZSM-5 (ZSM5-E1) zeolites (with bentonite as binder) at different temperatures in the range of 200°C to 300°C maintaining constant conditions with a feed rate of 250 g•h⁻¹.

From the catalytic degradation results shown in Table 4.5, it was found that increasing reaction temperature from 200°C to 270°C led to a huge raise of liquid product yield - 5.1, 13.0 and 23.5 at 200, 250 and 270°C, respectively - and also shortened the time at which the first drop of condensed liquid product appeared. Moreover, in case of a reaction temperature of 200°C, there was a small portion of molten PMMA coating the surface of the catalyst at the bed top which disappeared at 250°C and above. The temperature-dependence of liquid yield indicated a kinetic-controlled reaction. A further increase in reaction temperature from 280°C to 300°C conducted to a liquid product yield decrease - 9.4, 4.8 and 6.2 at 280, 290 and 300°C, respectively. Thus, it can be deduced that the main portion of product was gaseous. Due to the fast reaction rate, the light product may further react at external surface or in the pores of the catalyst. From this section, it is clearly seen that the temperature is a crucial parameter for cracking process. The reaction temperature of 270°C appeared to be the most convenient for PMMA degradation since it provided the highest

percentage of liquid recovered. The liquid product yield at various temperatures is given in Table 4.5.

Table 4.5 Liquid product yields obtained at various temperatures

Temperature (°C)	Zeolite	Liquid yield (wt.%)
200	BETA-E1	5.1
250	BETA-E1	13.0
	BETA-E2	11.7
	ZSM5-E1	13.1
270	BETA-E1	23.5
	BETA-E2	22.0
	ZSM5-E1	23.8
280	BETA-E1	9.4
	BETA-E2	8.4
290	BETA-E1	4.8
300	BETA-E1	6.2

Here, there are two points that should be elucidated;

i) Condensed liquid product is light fraction (no heavy fraction contained) because the reactor was designed to have a cold zone which permits the vaporized macromolecule to condense then drop down and further react with catalyst until macromolecule was transformed into a lower molecule or non-condensable gas.

ii) This process provides a quite low liquid yield in comparison with the thermal process proposed by Kaminsky (Karminsky et al., 2004) in which up to 50% of liquid product could be achieved. This is not because of the inadequate catalyst activity but it is due to the deficient performance of the condensing unit. A large

portion of MMA vapor was not condensed, and remained in gas phase. This will be seen later from the analysis of out gases by GC-MS.

4.4.2 Effect of PMMA feed rate

In this section, the study of the feed rate from 0.2 to 0.8 $\text{g}\cdot\text{gcat}^{-1}\cdot\text{h}^{-1}$ with constant total mass of PMMA input is presented. The liquid product yield at various feed rates is given in Table 4.6.

Table 4.6 Liquid product yields at various feed rates (PMMA 250 g, 270°C)

Feed rate ($\text{g}\cdot\text{gcat}^{-1}\cdot\text{h}^{-1}$)	Liquid product yield (%)
0.2	25.7
0.4	26.2
0.6	26.6
0.8	26.8

It is found that the feed rate of PMMA does not significantly affect the product yield. It can be referred that this process is well workable over a wide range of PMMA feed rates.

4.4.3 Analysis of liquid and gaseous products of continuous experiment by GC-MS

The composition of light fraction obtained from the catalytic degradation of PMMA at various temperatures using extruded Beta zeolites in continuous reactor was investigated by GC-MS and is summarized in Figure 4.10. It reveals that, in the temperature range of 270°C to 300°C, condensed product was single-component light fraction as seen from a single sharp peak with retention time of 2 minutes. In order to verify the exact component, comparisons of retention times and mass spectra were conducted concurrently. The quantitative analysis of the liquid product was also roughly done by comparison of the integrated areas with that of standard MMA as the same method as in batch experiment. It can be found that MMA content in the light product from zeolite catalysed PMMA degradation in continuous experiment is up to 93% wt. This result leads to the conclusion that the liquid product obtained by this process is MMA monomer as confirmed by the same retention time as well as the identical mass spectra with 96% similarity to standard MMA monomer. The composition of liquid and gas products from continuous catalytic PMMA degradation as analyzed by GC-MS is summarized in Table 4.7.

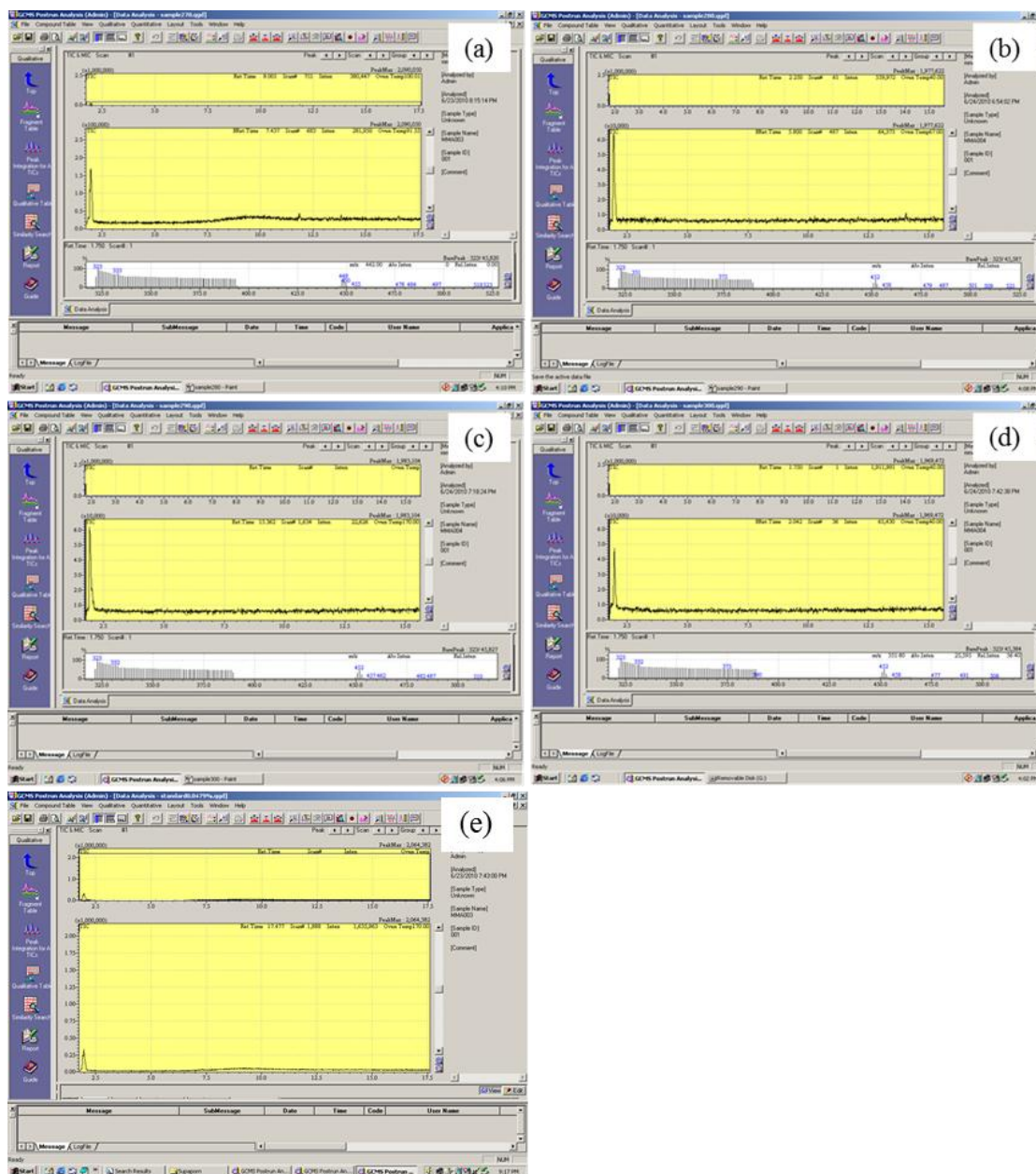


Figure 4.10 GC-MS spectra of light product from continuous catalytic PMMA degradation at various temperatures; (a) 270°C, (b) 280°C, (c) 290°C, (d) 300°C and (e) pure MMA.

Table 4.7 Composition of liquid and gas products from continuous catalytic PMMA degradation as analyzed by GC-MS

	Temperature (°C)	Zeolite	Yield (wt.%)	MMA content (%)
Liquid	270	BETA-E1	23.5	93.7
	280	BETA-E1	9.4	93.4
	290	BETA-E1	4.8	93.3
	300	BETA-E1	6.2	93.7
Gas	270	BETA-E1	N/A	60.7

The GC-MS composition of gaseous product obtained from the catalytic degradation of PMMA using extruded Beta zeolites in continuous reactor is shown in Figure 4.11. Unexpectedly, it was found that the gaseous product was concentrated with MMA vapour which should be in liquid state after passing through a gas condensing unit. The presence of a large portion of MMA vapour in the outlet gas (up to 60.7 %) proves the inadequate performance of the condenser, and this is the reason of the quite low liquid yield in comparison with the thermal process proposed by Kaminsky (Karminsky et al., 2004). Figure 4.11 shows example from GC-MS analysis of gas product from PMMA degradation by zeolite ZSM5-E1 in continuous experiment at a reaction temperature of 270°C. It reveals that at 270°C gaseous product was mainly containing MMA vapour as seen from a sharp peak with retention time of 2 minutes.

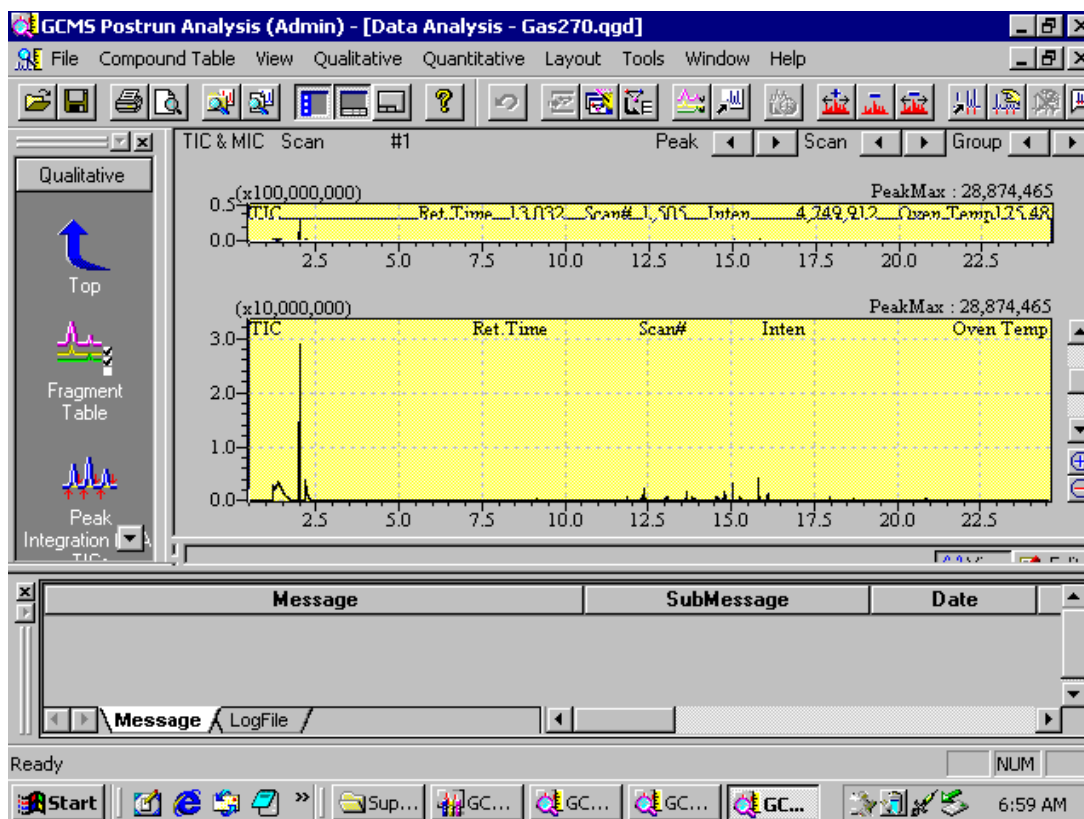


Figure 4.11 GC-MS spectra of gas product from continuous catalytic PMMA degradation at reaction temperature of 270°C.

CHAPTER V

REGENERATION OF USED CATALYST BY OZONATION

This chapter is devoted to the regeneration of spent zeolite which has been used as catalyst for cracking of poly (methyl methacrylate) (PMMA) in the previous chapter. The experiments were performed by ozonisation in the experimental set-up previously shown in Chapter III. Characterization by many techniques was done to evaluate properties of the fresh and regenerated zeolites as explained in section 5.1. Surface area and porosity measurement, elemental and thermogravimetry analyses are described. Effect of operating parameters and carbon profiles in the reactor and in the particles are investigated in section 5.2. Activity assessment, according to acid properties and PMMA degradation results, is also examined. In details, the results are presented in terms of carbon removal and reusability of regenerated zeolite. The effects of reaction temperature and time-on-stream (TOS) on the regeneration of coked zeolite are discussed. The decomposition of ozone with/without zeolite, so called catalytic and thermal decomposition of ozone, is also investigated in this study. The characteristics of zeolite before and after regeneration are also diagnosed. Moreover, the performance of regenerated zeolite for PMMA degradation is also investigated.

5.1 Characterization of the zeolite catalyst

In this part, the spent zeolite was coming from the continuous catalytic cracking of poly (methyl methacrylate) (PMMA) in a fixed bed reactor operating at 1 bar and 270°C with PMMA feed rate of $0.6 \text{ g} \cdot \text{g}_{\text{cat}}^{-1} \cdot \text{h}^{-1}$, as mentioned in the previous chapter. The liquid product yield obtained from the continuous unit with respect to time on stream is displayed in Figure 5.1.

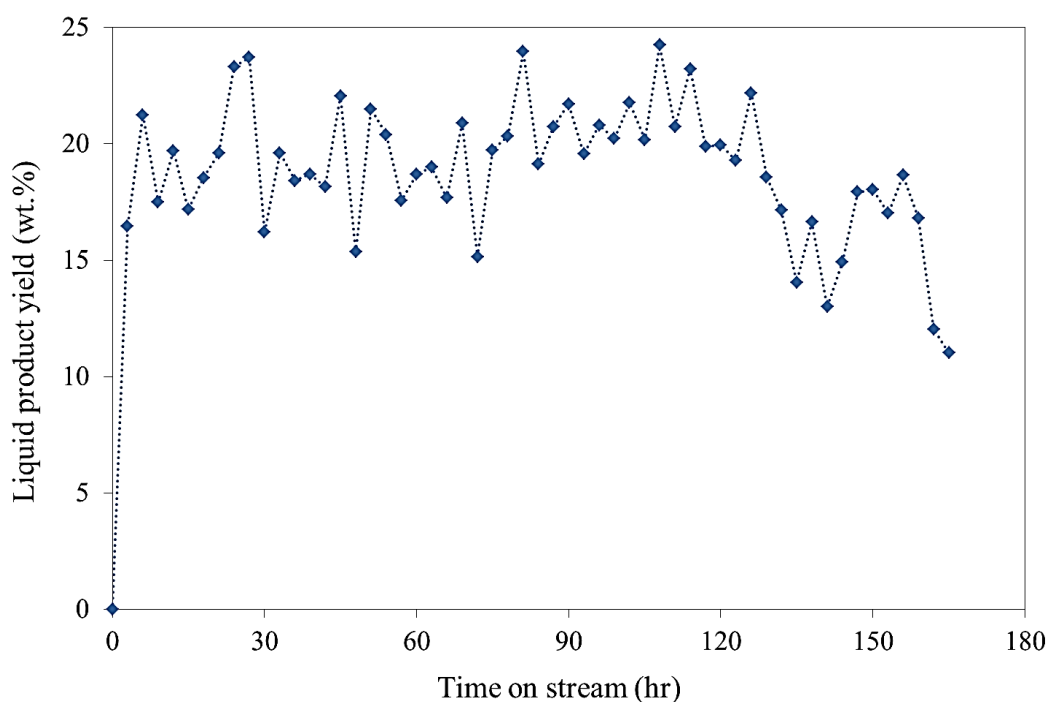


Figure 5.1 Liquid product yield vs time on stream (TOS).

This figure shows that a significant deactivation occurred after 120 hours of operation, resulting in a decrease of liquid product yield. Distribution of coke deposit varied axially along the bed, with a higher amount at the top of the reactor close to the PMMA feed. In case of longer times on stream, the catalyst lost its activity. For example, at TOS 160 h and 180 h the catalyst activity dropped by 25% and 50%, respectively.

As mentioned in chapter III, the regeneration experiments were performed on two different lots of coked ZSM-5 extrudes as shown in Figure 3.6: particles from the top layer of catalyst bed were coated with a dense, shiny black, layer that eventually stuck them together (b), while particles from bottom of reactor displayed a dark grey colour and kept well separate. Particle samples from both locations were collected for regeneration tests.



Figure 5.2 Photographs of coked catalysts from continuous process; (a) ZSM-5 particles from middle-bottom of PMMA cracking reactor (ZSM5-A) and (b) ZSM-5 particles from top of PMMA cracking reactor (ZSM5-B).

Figure 5.2 (a) shows ZSM-5 bottom particles from PMMA cracking reactor (ZSM5-A), containing 2% to 4% of carbon and Figure 5.2 (b) shows ZSM-5 top particles (ZSM5-B), containing 9% to 11% of carbon. Before carrying on regeneration experiments, the spent zeolites were characterized by many techniques. All characteristics of coked catalyst are described below.

5.1.1. Surface area and porosity

The typical textural properties of coked and regenerated samples were measured by N₂ adsorption / desorption at -196°C (Micromeritics ASAP 2010) and mercury porosimetry. The specific surface area was estimated from BET plot for relative pressures between 0.01 and 0.2 (Brunauer et al., 1938). The mesoporous and microporous volumes were estimated from N₂ adsorption/ desorption measurement according to Barrett-Joyner-Halenda (BJH) (Barrett et al., 1951) and Horvath-Kawazoe (HK) (Horvath and Kawazoe, 1983) methods, respectively. The macroporous volume (50 nm < pore diameter < 30 µm) and skeletal density were evaluated from mercury porosimetry. Typical textural properties of coked and regenerated samples are given in Table 5.1 and compared to those of fresh zeolite.

Table 5.1 Physical characteristics of zeolite samples.

	Fresh zeolite extrudate	ZSM5- A	ZSM5- B
Carbon content ^a (wt.%)	-	2.5	9.9
BET surface area ^b (m ² •g ⁻¹)	361	283	28
Microporous volume ^c (cm ³ •g ⁻¹)	0.13	0.11	0.01
Mesoporous volume ^d (cm ³ •g ⁻¹)	0.18	0.15	0.09
Macroporous volume ^e (cm ³ •g ⁻¹)	0.19	0.18	0.18
Skeletal density ^f (g•cm ⁻³)	2.1	2.1	1.9

^a Analysed by CHN elemental analyser.

^b Measured by N₂ adsorption/desorption then determined according to Brunauer-Emmett-Teller equation.

^c Measured by N₂ adsorption/desorption then determined according to Horvath-Kawazoe equation.

^d Measured by N₂ adsorption/desorption then determined according to Barrett-Joyner-Halenda equation.

^{e,f} Measured by mercury porosimetry.

Coke deposition was found to occur in both micro- and meso-pores, resulting in a sharp, almost linear, decrease of the surface area with respect to carbon content (Figure 5.3). The most severely coked sample exhibited nearly no microporosity. Interestingly the BET surface area of the partially regenerated samples aligns with the data on Figure 5.3, showing that the ozone treatment restores the textural properties of the zeolite, without any significant structural modification.

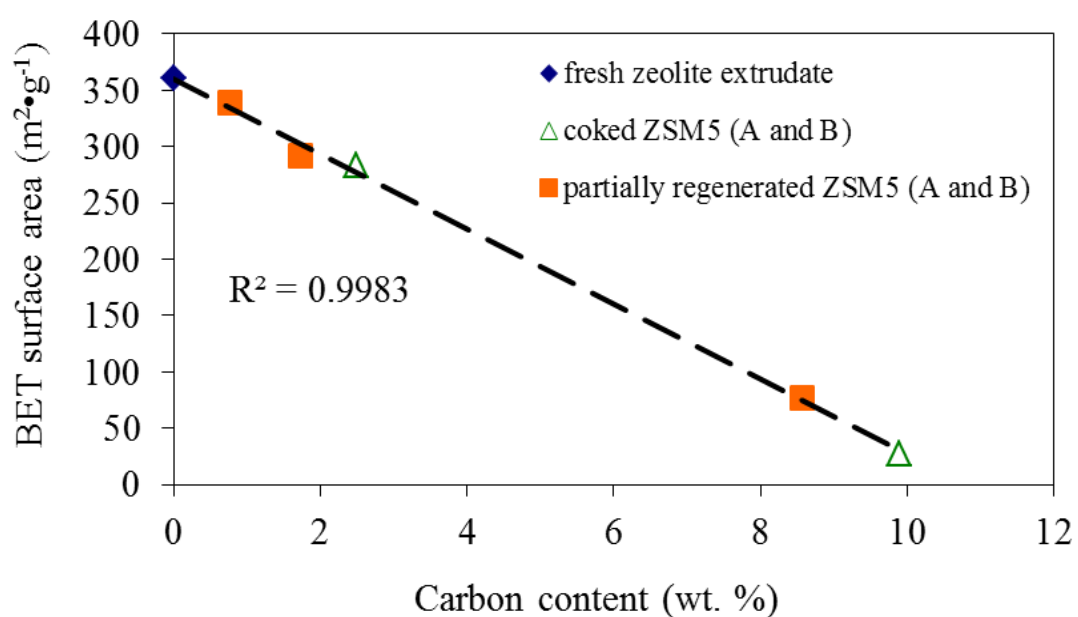


Figure 5.3 Evolution of BET surface areas of zeolite extrudates as a function of carbon content.

5.1.2. Elemental analysis

The morphology of fresh and coked zeolites was studied by Scanning Electron Microscopy (SEM). Microscopic features of the interior surface of zeolites are shown in Figure 5.4. As SEM images of fresh and coked samples did not exhibit much difference, elemental analysis by Energy Dispersive X-ray (EDX) was therefore conducted to put into evidence deposited species.

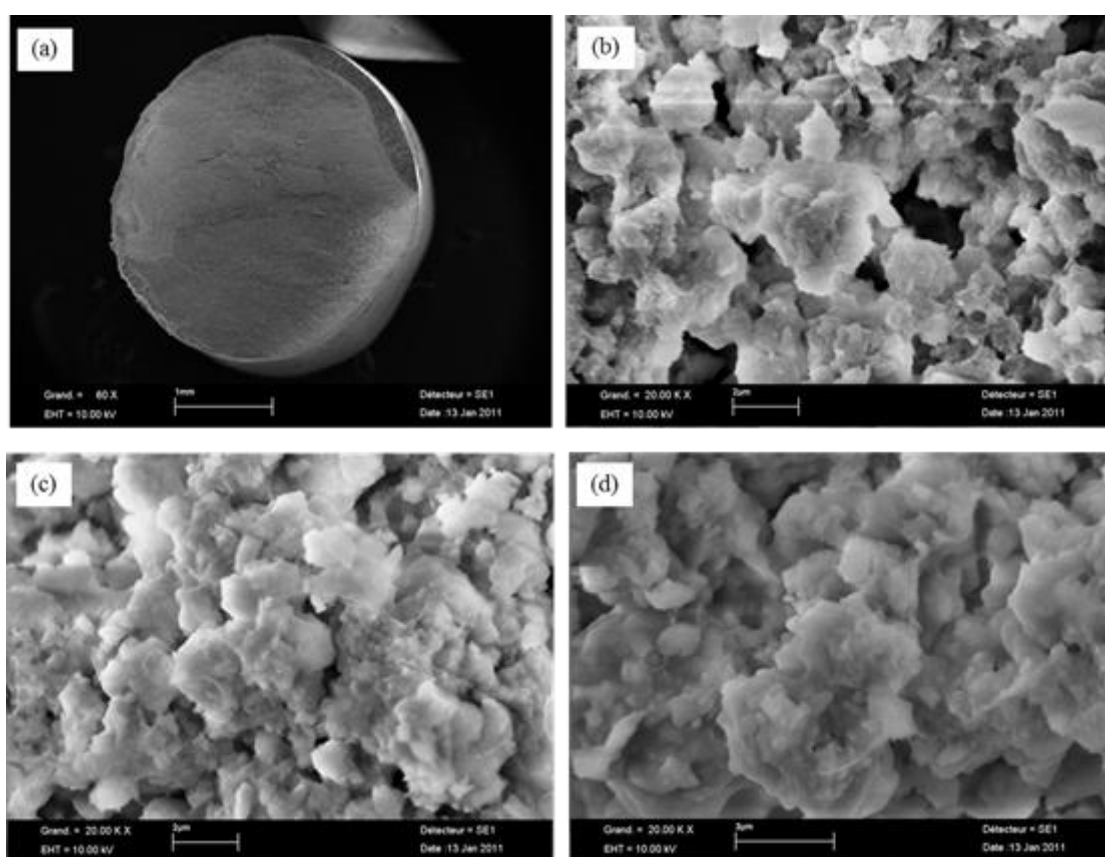


Figure 5.4 SEM micrographs of the fresh zeolite and the coked zeolites: (a) zeolite particle, (b) fresh ZSM5 zeolite, (c) ZSM5-A and (d) ZSM5-B.

The elemental profile along the cross sectional area of the particles was obtained by Scanning Electron Microscopy coupled with Energy Dispersive X-ray (SEM/EDX) for both coked samples (ZSM5-A and ZSM5-B) as shown in Figure 5.5.

The carbonaceous deposits were found well distributed across the extrudate, with the exception of a narrow zone of higher concentration at the very outer surface (depth < 50 μm). From the results, it can be briefly confirmed that a change of zeolite textural properties takes place due to the coke deposition onto zeolite surface and pores.

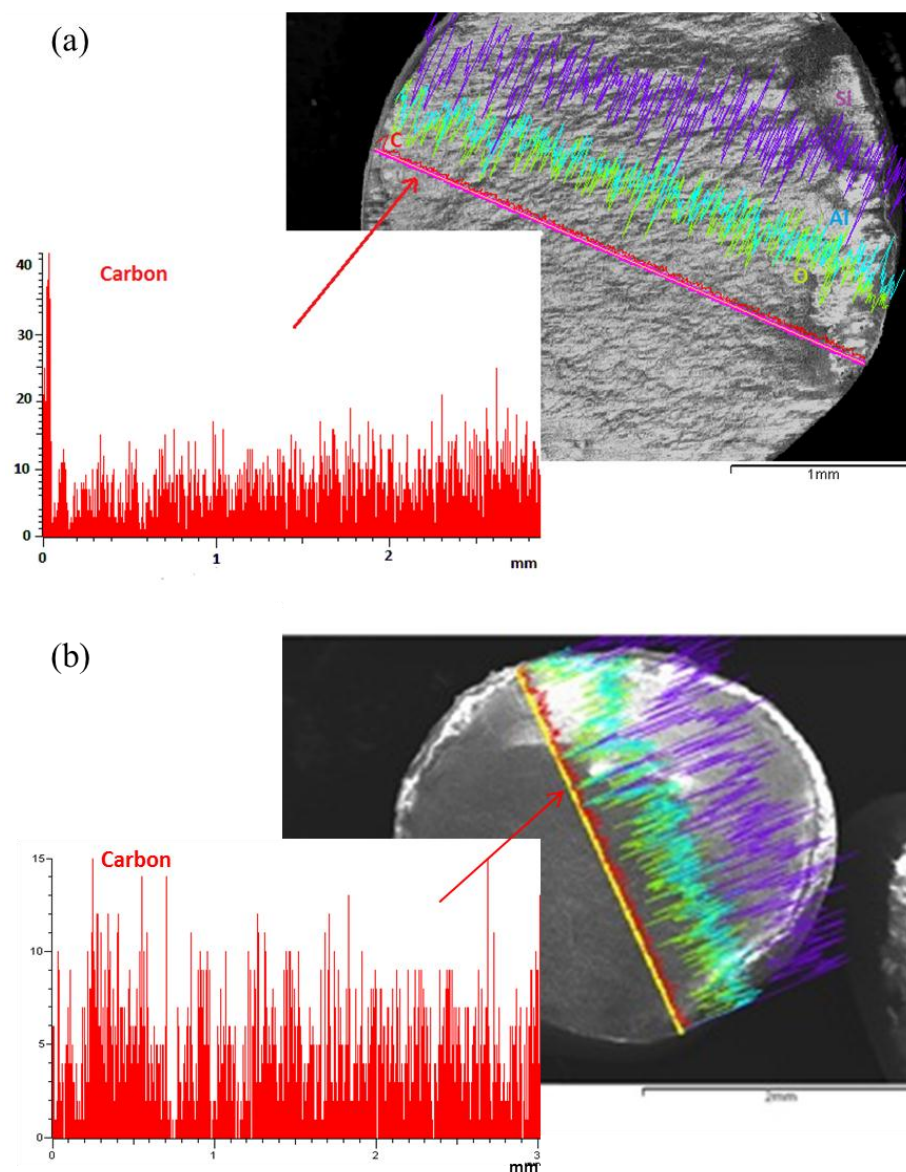


Figure 5.5 Elemental carbon profile a on a cross-section of particle; (a) ZSM5-A and (b) ZSM5-B.

The mean carbon contents estimated from EDX spectroscopy were in accordance with those determined from flash combustion of the materials (Table 5.2), with a much higher value for coked ZSM5-B. The Si/Al atomic ratio of about 2.5 also agreed well with the theoretical value (accounting for the presence of alumina binder) and kept unchanged after regeneration (no dealumination).

Table 5.2 Elemental analysis from EDX spectroscopy and carbon content from flash combustion

	Fresh ZSM5	ZSM5-A	ZSM5-B	(Partially) regenerated ZSM5-A^c
Elemental analysis from EDX ^a (wt.% / % at.)				
C	-	3.7 / 6.0	9.2 / 14.6	**
O	50.1 / 63.6	51.7 / 62.8	46.4 / 55.0	51.9 / 65.2
Al	14.0 / 10.5	12.7 / 9.1	12.8 / 9.0	13.5 / 10.0
Si	35.9 / 25.9	31.9 / 22.1	31.6 / 21.4	34.6 / 24.8
Carbon content from flash combustion ^b (wt.%)	-	3.0	9.9	0.8

^a Analysed by EDX spectroscopy.

^b Analysed by CHN elemental analyser.

^c Operating parameters ; temperature $\sim 100^{\circ}\text{C}$, TOS 2 h, $Q_G = 12.7 \text{ l}\cdot\text{h}^{-1}$ and $C_{\text{O}_3, \text{in}} = 48 \text{ g}\cdot\text{m}^{-3}$

**Asterisk means below the limit of detection.

5.1.3 Infrared and Raman spectroscopy

Fourier transform infrared spectroscopy

IR spectroscopy has many advantages for the investigation of coke deposited on zeolite because it is not destructive and can be done without a complex sample preparation. However, the study on the nature of coke by this technique still has a major drawback because it is hard to assign the exact IR bands to coke species and therefore obtained information is limited (Bauer and Karge, 2007). In this study, FT-IR spectra of fresh and spent catalysts and their enlargement for the wavenumber range 1300-1500 cm^{-1} are illustrated in Figure 5.6. As summarized by several articles, typical coke show FT-IR spectra bands in 1300-1700 cm^{-1} range (excluding wavenumber of 1640 cm^{-1} corresponding to adsorbed water) (Jolly, Saussey, and Lavalley, 1994; Bauer and Karge, 2007). In details, they can be classified in the following sub-ranges;

- i) 1340–1470 cm^{-1} can be assigned to CH_3 and CH_2 groups in side chains of polyaromatic coke species,
- ii) 1545–1550 cm^{-1} correspond to $\text{C}=\text{C}$ stretches of conjugated olefins,
- iii) 1600–1635 cm^{-1} correspond to polyolefinic and polyaromatic species.

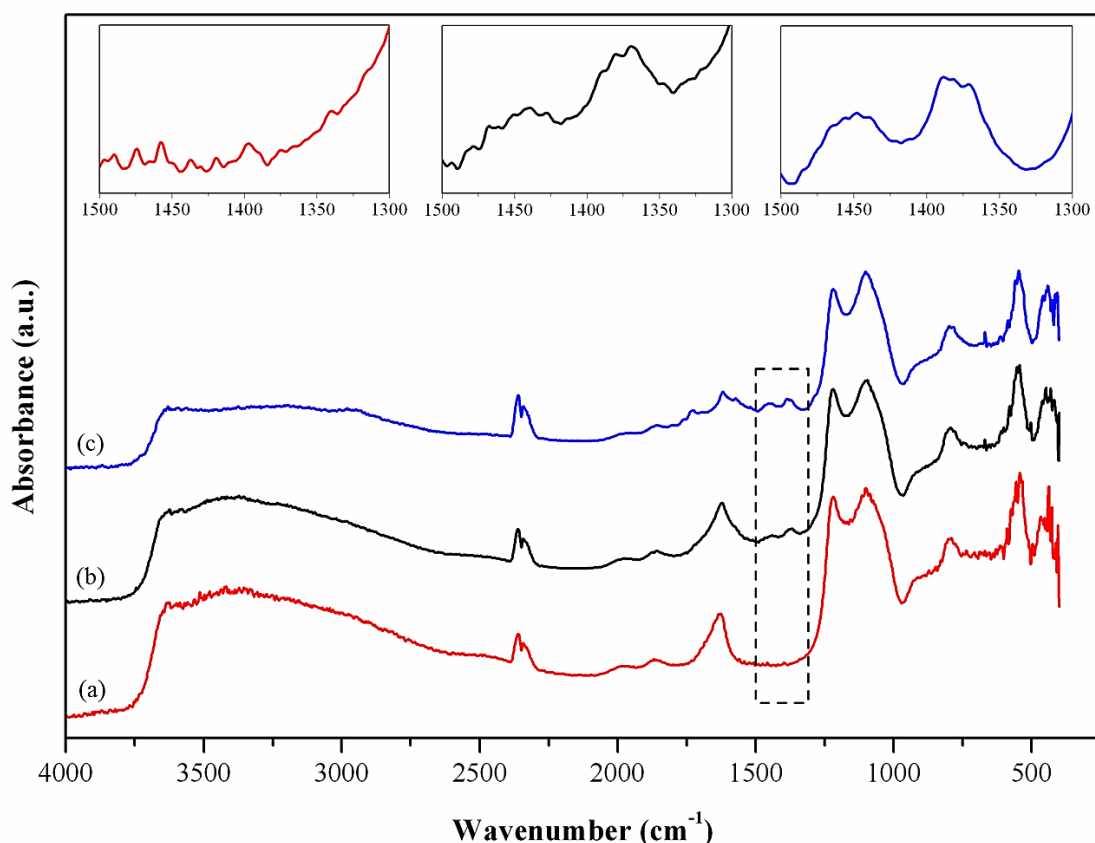


Figure 5.6 FT-IR spectra of fresh zeolite and spent zeolite; (a) fresh ZSM-5, (b) ZSM5-A and (c) ZSM5-B.

From figure 5.6, it is found that all spectra show a strong absorption at 3500 to 3750 cm^{-1} , corresponding to SiOHAl Brønsted acid sites, OH groups attached to non-framework Al species and terminal Si–OH groups (Bauer and Karge, 2007). The FT-IR characteristic bands of carbonaceous deposits do not appear on fresh ZSM-5, but on ZSM5-A and ZSM5-B. Especially for ZSM5-B, FT-IR bands of coke become more dominant which agrees with TG/IR and SEM/EDX results as it contains a much larger amount of carbon deposits.

Fourier-Transform Raman spectroscopy

The quality of the coke deposited on the catalyst surface, in terms of the carbon crystallinity was evaluate using a Fourier transform Raman spectrometer (FT-Raman, Thermo Scientific DXR Smart Raman) with a 632 nm laser.

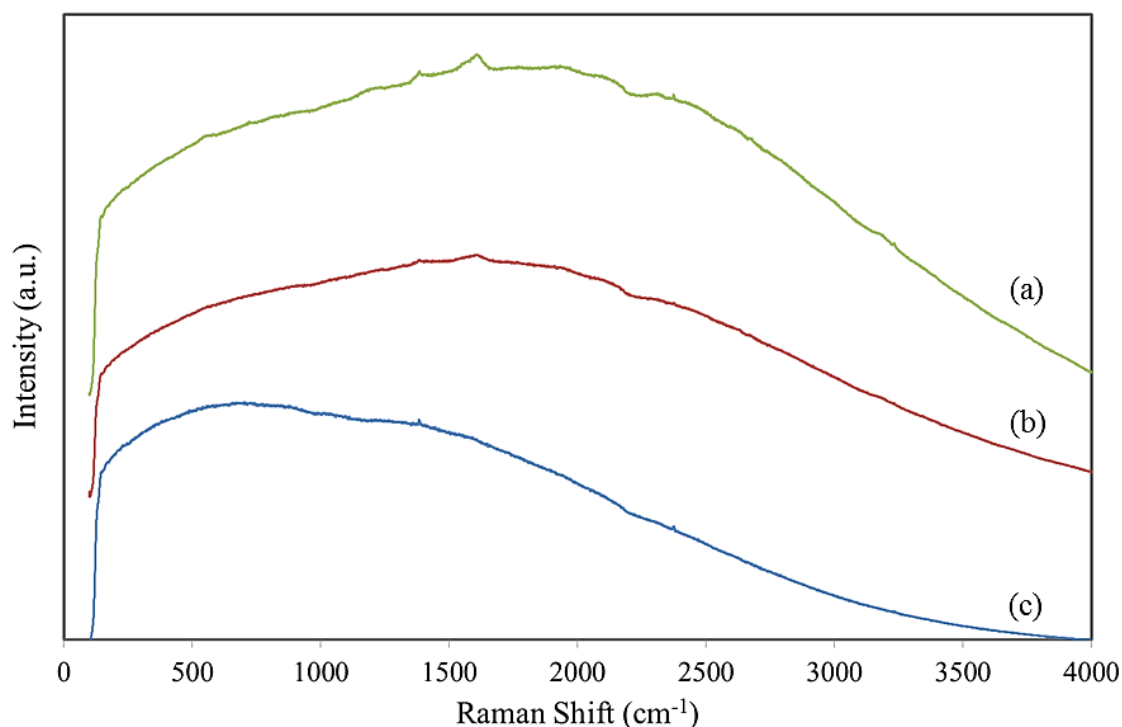


Figure 5.7 Raman spectra of fresh and used catalyst with Ar laser 632 nm; (a) ZSM5-B, (b) ZSM5-A and (c) fresh ZSM-5.

Figure 5.7 shows Raman spectra of fresh and coked catalysts. This is a typical fluorescence phenomenon caused by the zeolite itself and also the carbonaceous deposits. The surface fluorescence of sample seriously restricts the detectability of the signals, as previously explained by Vogelaar and co-workers (Vogelaar et al., 2006).

The second set of IR analysis was then performed by using a Raman spectrometer with a higher wavelength (1064 nm) as suggested by Amornsit and co-workers (Amornsit et al., 2011), as it can diminish the fluorescence effect.

Unfortunately, this analysis was not convenient due again to a strong contribution of fluorescence as shown in Figure 5.8.

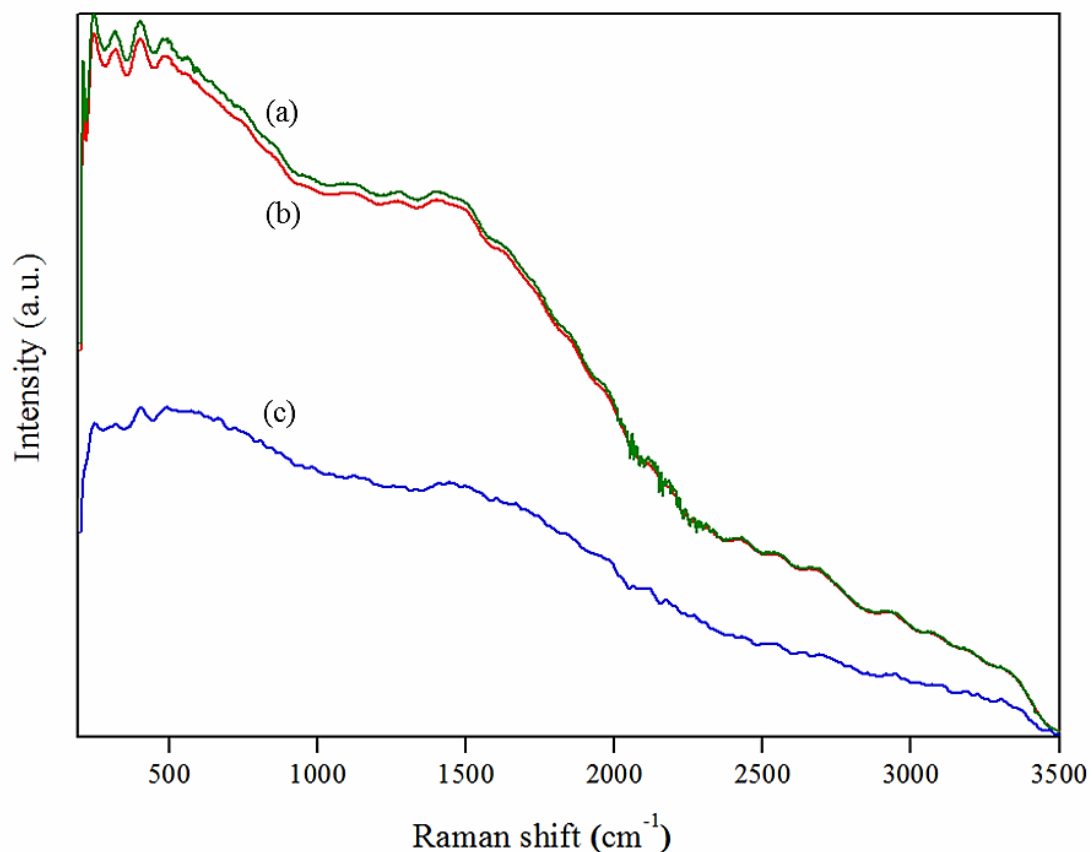


Figure 5.8 Raman spectra of ZSM-5 (ZSM5-B) from Raman spectroscopy with Nd:YAG (neodymium-doped yttrium aluminium garnet; $\text{Nd:Y}_3\text{Al}_5\text{O}_{12}$), 1064 nm; (a) 180 mW Res 4.0 cm^{-1} No. of scans 200, (b) 180 mW Res 4.0 cm^{-1} No. of scans 400 and (c) 30 mW Res 16.0 cm^{-1} No. of scans 2000.

Another method to avoid the fluorescence effect is the use of ultraviolet Raman with wavelength below 260 nm (Bauer and Karge, 2007), not only the intensity of the Raman signals is enhanced, but the background fluorescence is also avoided. However, in this work, UV-Raman analysis is disregarded since it requires a complex modification of the laser source.

5.1.4 Thermogravimetry

The thermograms of coked samples (realized under nitrogen atmosphere), as well as the identification of evolved gases from IR spectroscopy are given in Figure 5.9. The samples were heated at $10^{\circ}\text{C}\cdot\text{min}^{-1}$ from room temperature to 1000°C , including 60 min plateau at 120°C to remove physisorbed water. The amount of physisorbed water decreased logically from fresh zeolite (9.5 wt.%) to ZSM5-A (5.8%) and ZSM5-B (3.2%) Then three distinct stages were observed for coked samples after the 120°C plateau.

A first weight loss of less than 1% was observed from 120°C to $250\text{-}300^{\circ}\text{C}$ corresponding mainly to the release of water: it might be due to coordinated water, as it was also observed on the fresh zeolite. CO_2 emission then started to increase with a maximum intensity observed between 400°C and 600°C , and was detected up to the end. CO release came later, mainly after 600°C . Some compounds were only detected for ZSM5-B, namely MMA (with a narrow peak around 405°C), methanol (around the same temperature), methane (385 to 665°C) and ethylene (425 to 585°C). This difference might be attributed to a PMMA rich layer coating the top particles. It should be also noticed that the corresponding rate of weight loss (from 300°C to 450°C) was much higher than that of other stages. Some complementary TG analyses were also carried out under air. They showed that the sample weight decreases up to 700°C , with a total weight loss after the 120°C plateau of 6.5% and 17.3% for ZSM5-A and B, respectively (for a respective carbon content of 4.1% and 11.5%).

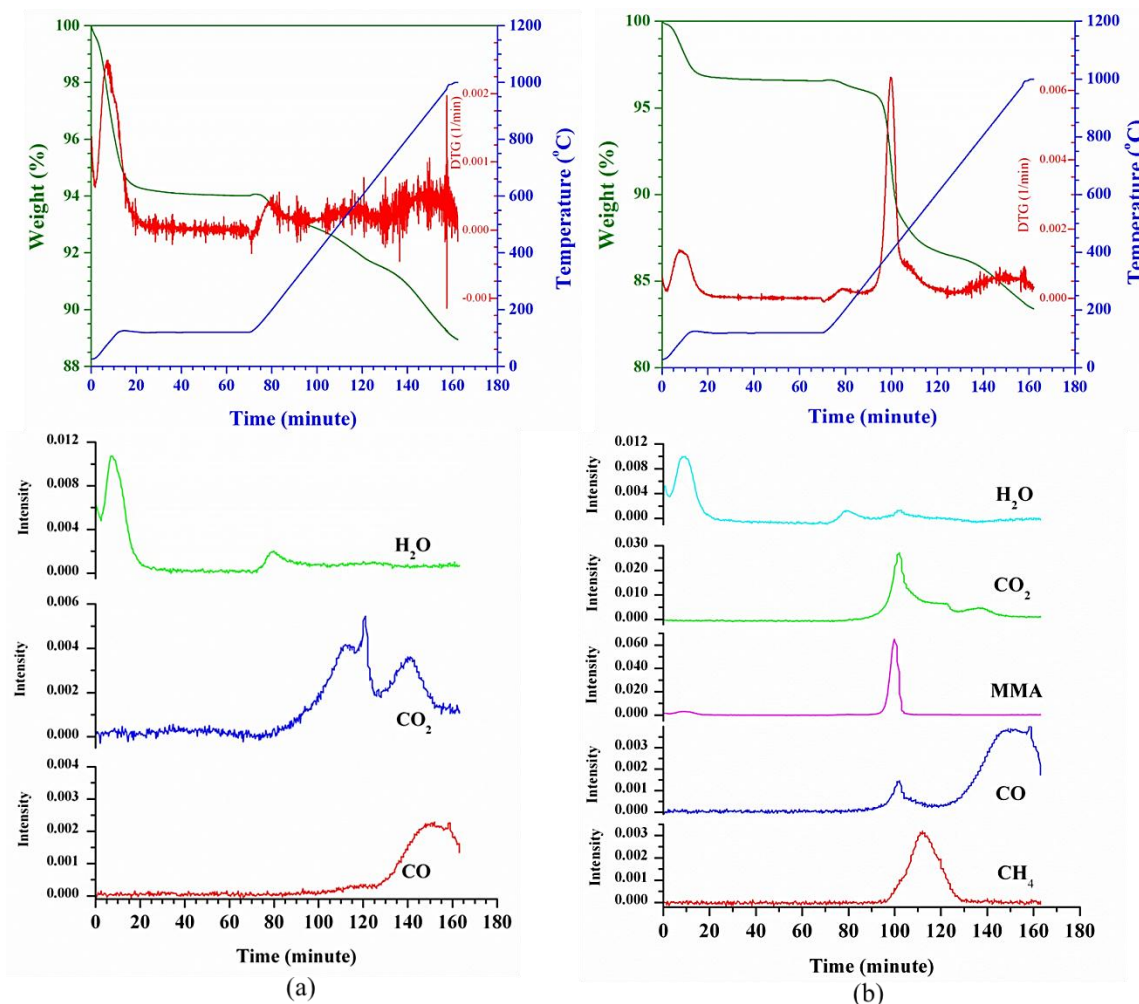


Figure 5.9 Thermograms of coked zeolite under N₂, along with identification of evolved gases from IR spectroscopy: (a) ZSM5-A and (b) ZSM5-B.

The coke deposit is usually qualified as “soft coke” or “hard coke”, depending to its ability to be volatilized / decomposed under nitrogen and oxygen. Following the work of Wang and Manos (Wang and Manos, 2007), the amount of coke precursors or “soft coke” can be roughly estimated from the weight loss observed between 250°C to 300°C and 600°C under N₂, resulting in 1.5% and 9.5% for ZSM5-A and B, respectively. However, the direct estimation of amount of “hard coke” under N₂ is more difficult because of its high thermal stability. Therefore, in this thesis, the amount of “hard coke” is indirectly obtained from the difference between the total

weight loss under air (corresponding to the weight loss due to “soft coke” and “hard coke”) and the weight loss due to “soft coke” as previously described, and is found to be 4.2% and 7.3% for ZSM5-A and B, respectively.

According to the conclusions of Elordi and co-workers (Elordi et al., 2012) on the cracking of polyethylene, “soft coke” would be mainly deposited outside the zeolite crystals, while “hard coke” would be formed in the interior of crystalline channels. However the location of the carbonaceous deposits depends also on the hydrocarbon used as the coke-forming agent (Bauer and Karge, 2007). Here the reduction of mesopores seemed better correlated with the increase of “hard coke”, and that of micropores with the increase of “soft coke”.

5.2. Regeneration of the catalysts by ozonation

Ozonation of coked samples was performed at a temperature range of 20°C to 150°C with O₃/O₂ mixture supplied by corona discharge ozone generator with controlled concentration in the range of 16 to 50 g•m⁻³. The experimental procedure was previously described in chapter III. The result shows that for ZSM5-A, very high carbon conversion up to 80% could be achieved in the investigated conditions (see Figure 5.11). For ZSM5-B, performance was more modest (35% C removal), mainly due to the fact that the particles were coated by a low porosity PMMA rich layer, as found by TG/IR, that limits the access of ozone to the zeolite. Therefore parametric study was performed with ZSM5-A only.

5.2.1. Effect of operating parameters

To analyse carbon content in zeolite samples, particles after treatment were crushed and mixed, and same for reference half pellets. Carbon removal was found to increase almost proportionally with the inlet concentration of ozone in the investigated range, as seen in Figure 5.10. This figure illustrates the evolution of carbon removal as a function of inlet O₃ concentration (16 to 50 g•m⁻³) for different temperature when gas volume flow rate is 12.7 l•h⁻¹ and time on stream is 30 min. The error bar was propagation of error. Temperature gradients were observed along the reactor axis (see section 5.2.2), so all experiments will refer to outlet temperature.

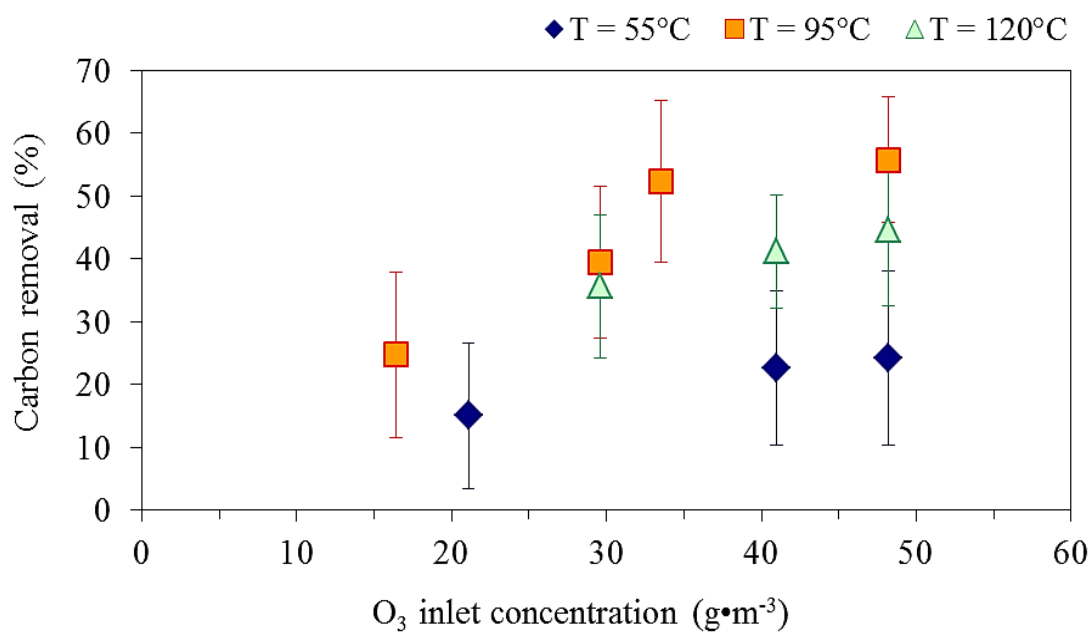


Figure 5.10 Evolution of carbon removal as a function of inlet O₃ concentration for different outlet temperature ($Q_G = 12.7 \text{ l}\cdot\text{h}^{-1}$, TOS = 30 min).

As expected, conversion was improved by increasing time on stream (TOS), but it seemed to reach a plateau after 2 h (Figure 5.11(a)). The effect of temperature, depicted in Figure 5.11(b), is more complex as an optimum was found at about 100°C regardless time on stream, due to the some competition effect between the chemical mass transport and reaction kinetics involved, as it will be explained below.

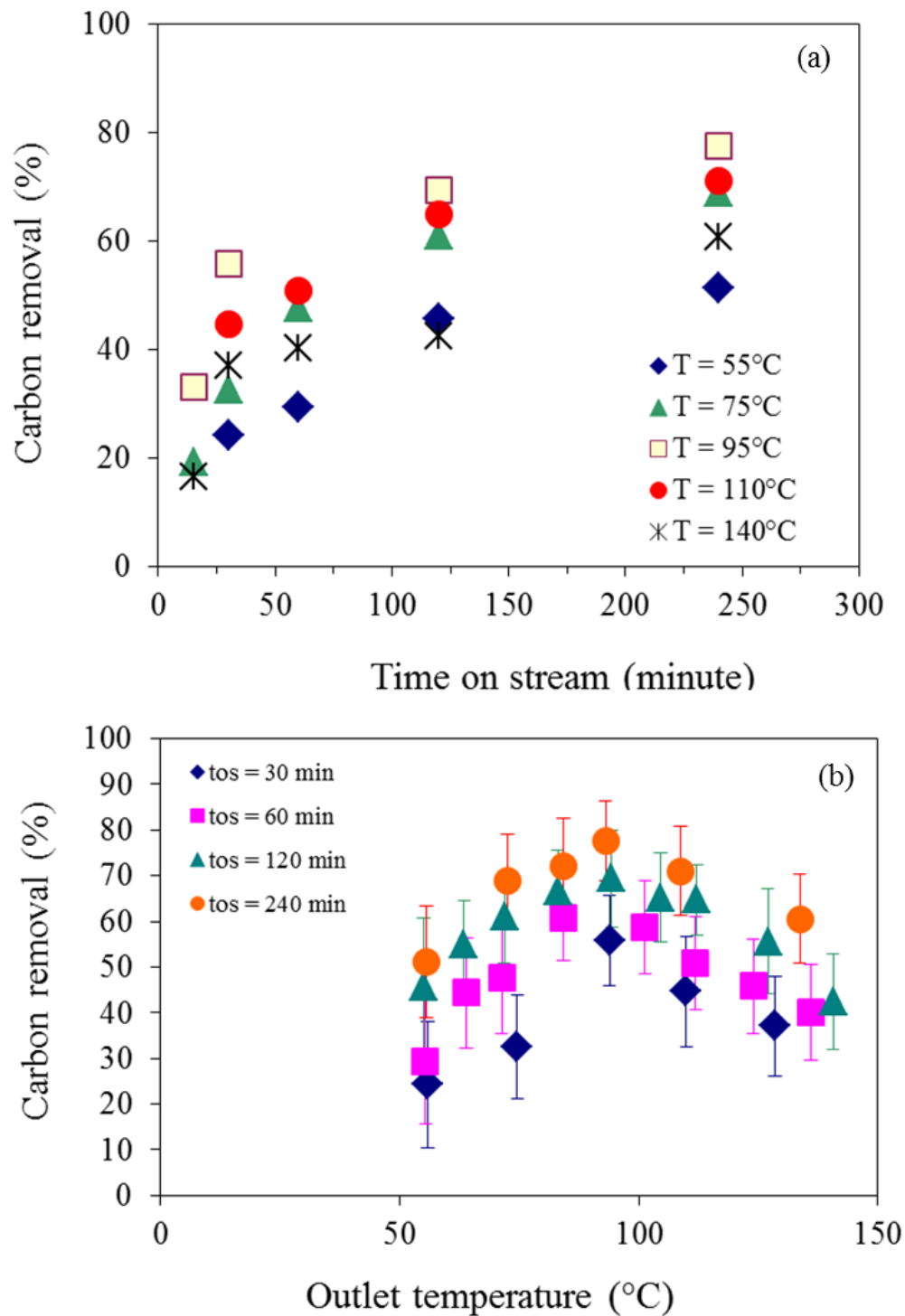


Figure 5.11 Evolution of carbon removal as a function of (a) time on stream and (b) outlet temperature ($Q_G = 12.7 \text{ l}\cdot\text{h}^{-1}$, $C_{\text{O}_3,\text{in}} = 48 \text{ g}\cdot\text{m}^{-3}$).

Thermal and catalytic decomposition of ozone were studied by varying temperature in the range of 25 to 180°C with flow rate of 12.7 l•h⁻¹ and 48 g•m⁻³ of inlet ozone concentration. The measurements of ozone concentration at the reactor outlet showed that less than 10% of ozone was thermally decomposed at 100°C (in empty tube), while over fresh extruded ZSM-5 ozone decomposition could reach more than 90% along the string reactor, as seen in Figure 5.12. Outlet ozone concentration was also analysed at the beginning of the decoking reaction (0 to 30 min): lower ozone decomposition was observed with the coked catalyst below 100°C due to its lower activity.

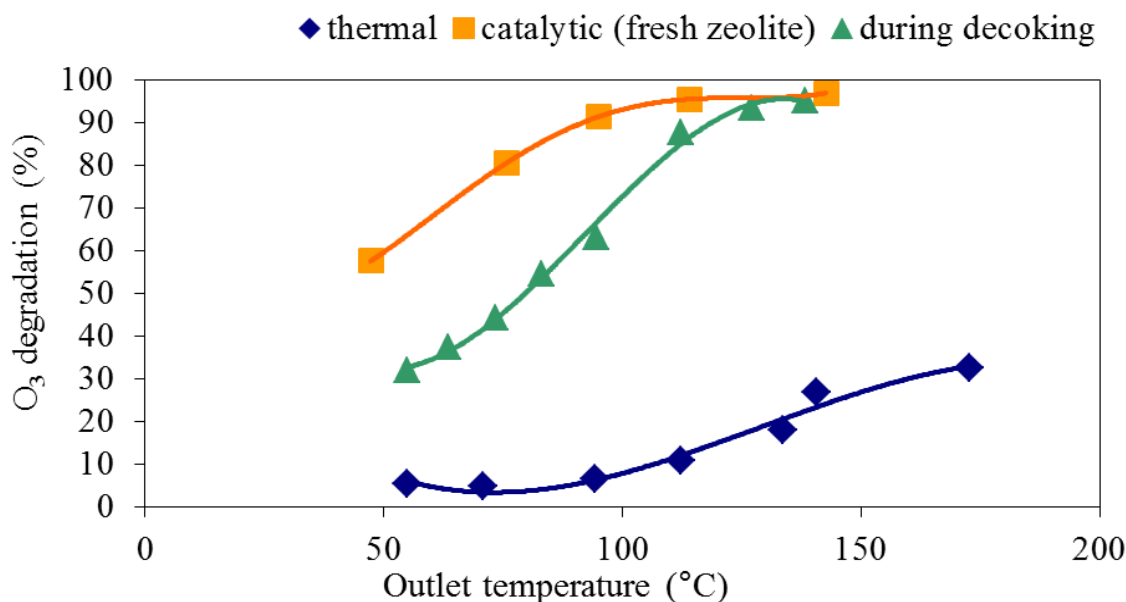


Figure 5.12 Ozone decomposition as a function of outlet temperature ($Q_G = 12.7 \text{ l}\cdot\text{h}^{-1}$, $C_{\text{O}_3,\text{in}} = 48 \text{ g}\cdot\text{m}^{-3}$).

Optimal conditions were then further investigated by varying operating parameters at about 100°C for the same amount of ozone provided to the sample. Similar results were obtained when increasing the gas flow rate from 12.7 to 45.4 l•h⁻¹ (and decreasing time on stream accordingly from 2 h to 33 min): about 40% C removal (for an inlet O₃ concentration of 19 g•m⁻³). In comparison, conversion was 24.7% for 12.7 l•h⁻¹ and 30 min TOS (other conditions being equal). Increasing the gas flow rate reduced the ozone concentration gradient inside the reactor, which compensated for the diminution of TOS. Furthermore, carbon removal was decreased when using a higher gas flow rate with lower ozone content (at same total ozone input): 55.8% for 12.7 l•h⁻¹ and 48.2 g•m⁻³ (during 30 min) against 32.9% for 41.3 l•h⁻¹ and 13.7 g•m⁻³. This confirms that the decoking rate increases with ozone concentration.

5.2.2. Carbon profiles in the reactor and in the particles

Axial coke conversion profiles were measured at about 100°C after 1 h of reaction by dividing the reactor into 5 zones (containing 3-4 pellets each) and analysing separately their residual carbon content (which was compared to that of the corresponding reference half pellets). Figure 5.13 shows that carbon conversion varied slightly along the reactor for ZSM5-A, from 59% to 50%, and from 26% to 14% for ZSM5-B. Surprisingly, the axial gradient of ozone concentration appears thus to have a rather moderate impact on the conversion. This result may be explained by the existence of a positive temperature gradient of about 10°C along the reactor (carbon removal being improved by an increase of temperature in this range). As abovementioned, the different regeneration yields of samples A and B are mainly due to the different types of carbonaceous deposit on their surface, since multiplying TOS by a factor 4 only increased the mean carbon removal of ZSM5-B to 35% conversion.

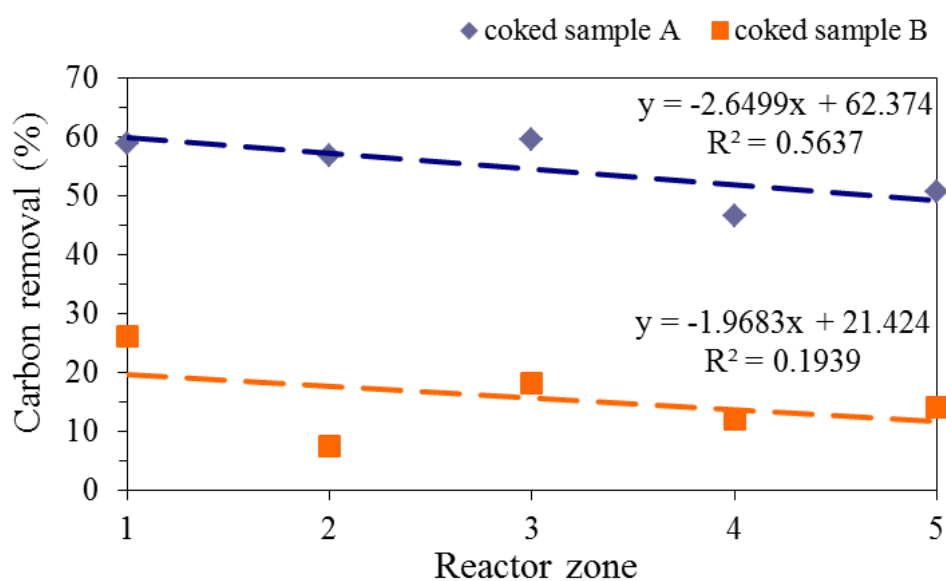


Figure 5.13 Axial profiles of carbon removal ($T_{\text{outlet}} = 95^{\circ}\text{C}$, $Q_G = 12.7 \text{ l}\cdot\text{h}^{-1}$, $C_{\text{O}_3,\text{in}} = 48 \text{ g}\cdot\text{m}^{-3}$, TOS = 1 h).

Figure 5.14 displays the photos of partially regenerated ZSM5-A for two outlet temperatures: 95°C and 140°C (after 1 h TOS). On the left are shown the reference half pellets, at the centre the outer surface of the ozonised samples and on the right their cross-section cut away. At the highest temperature, decoking takes place according to a shrinking core process as already observed by Hutchings et al. (Hutchings et al., 1987): cross-section views (c) show a black core of coked catalyst surrounded by a very white layer of regenerated catalyst. Conversely regeneration is much more uniform at 95°C as the core is less dark and much smaller.

At 140°C the rate of ozone decomposition is much faster than its diffusion rate. Radical species generated are known to have a short lifetime, and they should be consumed (either by reaction with remaining coke in the close vicinity or by radical recombination reactions) before reaching the coke deposit within the particles. This makes the overall process highly limited by diffusion. At 95°C, the smaller difference in grey level contrast between the core and the surface of the particles was due to the slower ozone decomposition rate: ozone had more time to diffuse within the particle before being converted into highly reactive species. Therefore the overall carbon removal is improved as previously shown in Figure 5.11.

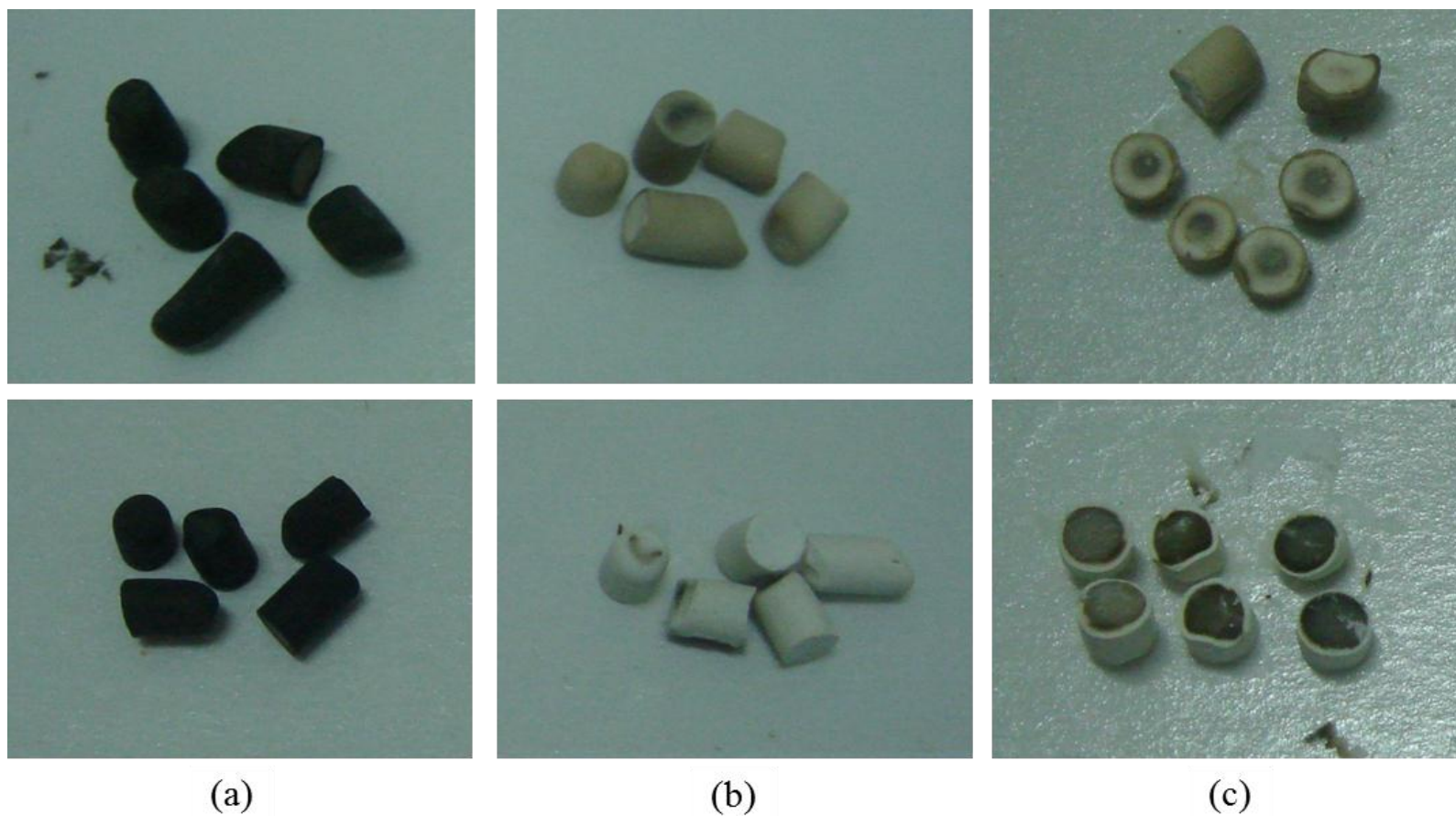


Figure 5.14 Photos of pellets (a) before regeneration and (b,c) after regeneration ($Q_G = 12.7 \text{ l}\cdot\text{h}^{-1}$, $C_{O_3,\text{in}} = 48 \text{ g}\cdot\text{m}^{-3}$, TOS = 1 h): top pictures: $T_{\text{outlet}} = 95^\circ\text{C}$, bottom pictures: $T_{\text{outlet}} = 140^\circ\text{C}$.

5.3. Activity assessment

5.3.1. Acid properties

As mentioned above, acid sites are known to promote C-C bond scission. Moreover, the strength and nature (Brønsted or Lewis) of the acid sites influence both the activity and selectivity of the cracking reaction: the stronger the sites, the lighter the hydrocarbons obtained (Serrano et al., 2000; Aguado, Serrano, and Escola, 2008).

The NH₃-TPD spectra of regenerated zeolite and its profile from blank test were shown in Figure 5.15. This figure shows a last peak on the TCD signals at 600°C to 800°C (black line from NH₃-TPD adsorption; red line from TPD without NH₃) corresponding to the dehydroxylation of the zeolite framework structure and the decomposition of carbonaceous deposits. The total free acid sites were evaluated by subtraction of TCD signals of sample with/without NH₃ adsorption.

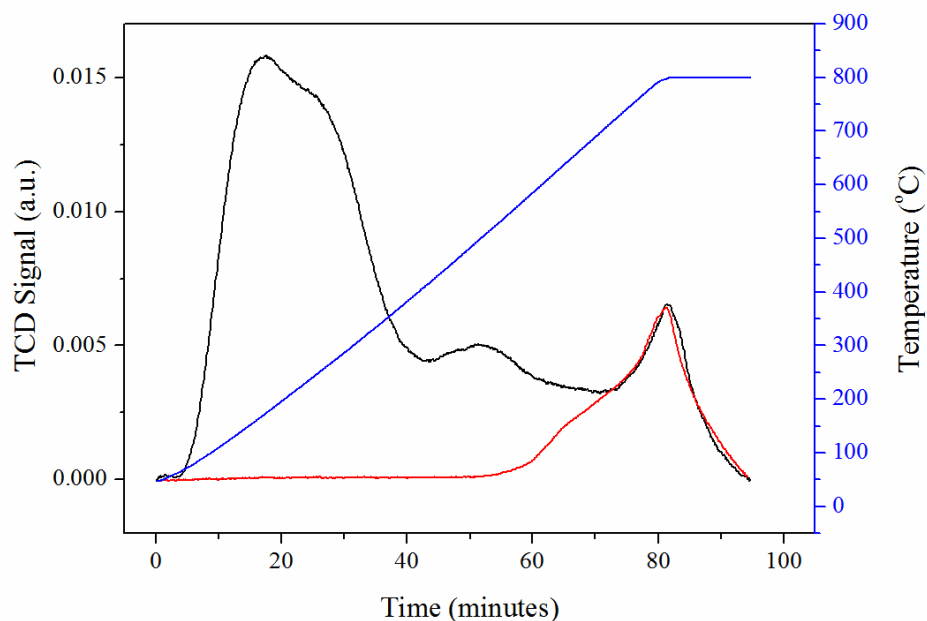


Figure 5.15 NH₃-TPD profile of used ZSM-5; raw TCD signal (black line) and signal from blank test (red line).

A distribution of the acid sites according to their strength could be provided by deconvolution of the TCD signal using a Gaussian distribution as illustrated in Figures 5.16 and 5.17. It resulted in three deconvolution peaks corresponding to the weak (low desorption temperature), medium and strong (high desorption temperature > 400°C) acid sites. Figure 5.16 shows NH₃-TPD profiles of fresh zeolite, coked and regenerated samples for several regeneration durations (1, 2 and 4 h) at a temperature of 95°C. The regeneration of coked zeolite did not affect the acid strength, as the desorption temperatures corresponding to the successive peaks were found in the same range as for the fresh zeolite. Figure 5.17 shows NH₃-TPD profile of fresh zeolite, coked and regenerated samples for different regeneration temperatures ranging from 95°C to 140°C. Similar acid strength of fresh, coked and regenerated zeolites was again observed. The desorption temperature from each type of acid site and the total amount of acid sites of all zeolite samples are summarized in Table 5.3. To determine the total amount of acid sites of zeolite, an amorphous silica-alumina (ASA) which known amount of total acid sites (0.55 mmol•g⁻¹ as reported by Ngamcharussrivichai et al., 2004) was used as the reference material.

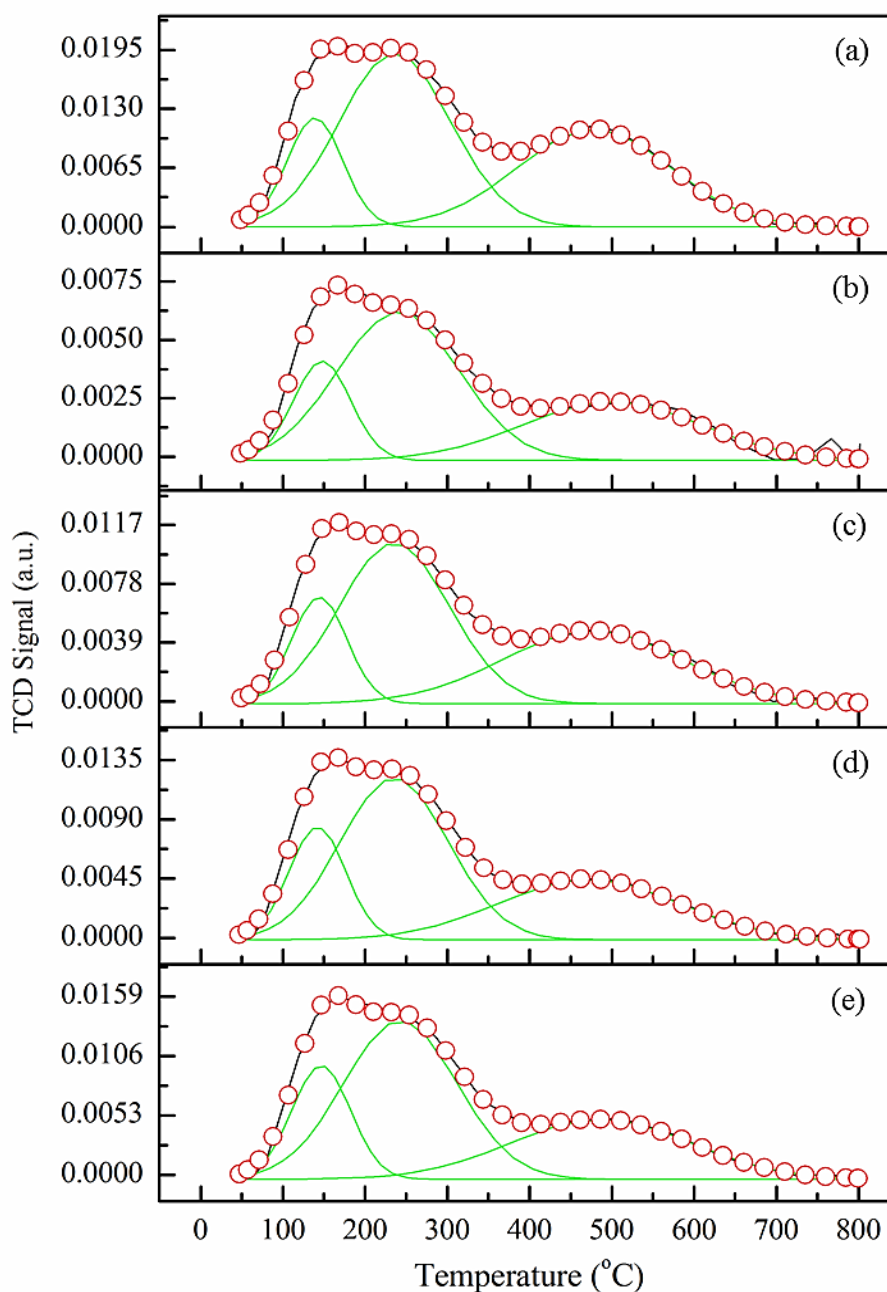


Figure 5.16 NH₃-TPD profile of fresh zeolite, coked and regenerated samples with respect to regeneration duration; (a) fresh ZSM-5, (b) used catalyst (ZSM5-A), (c-e) regeneration duration of 1, 2 and 4 h, respectively (regeneration temperature of 95°C).

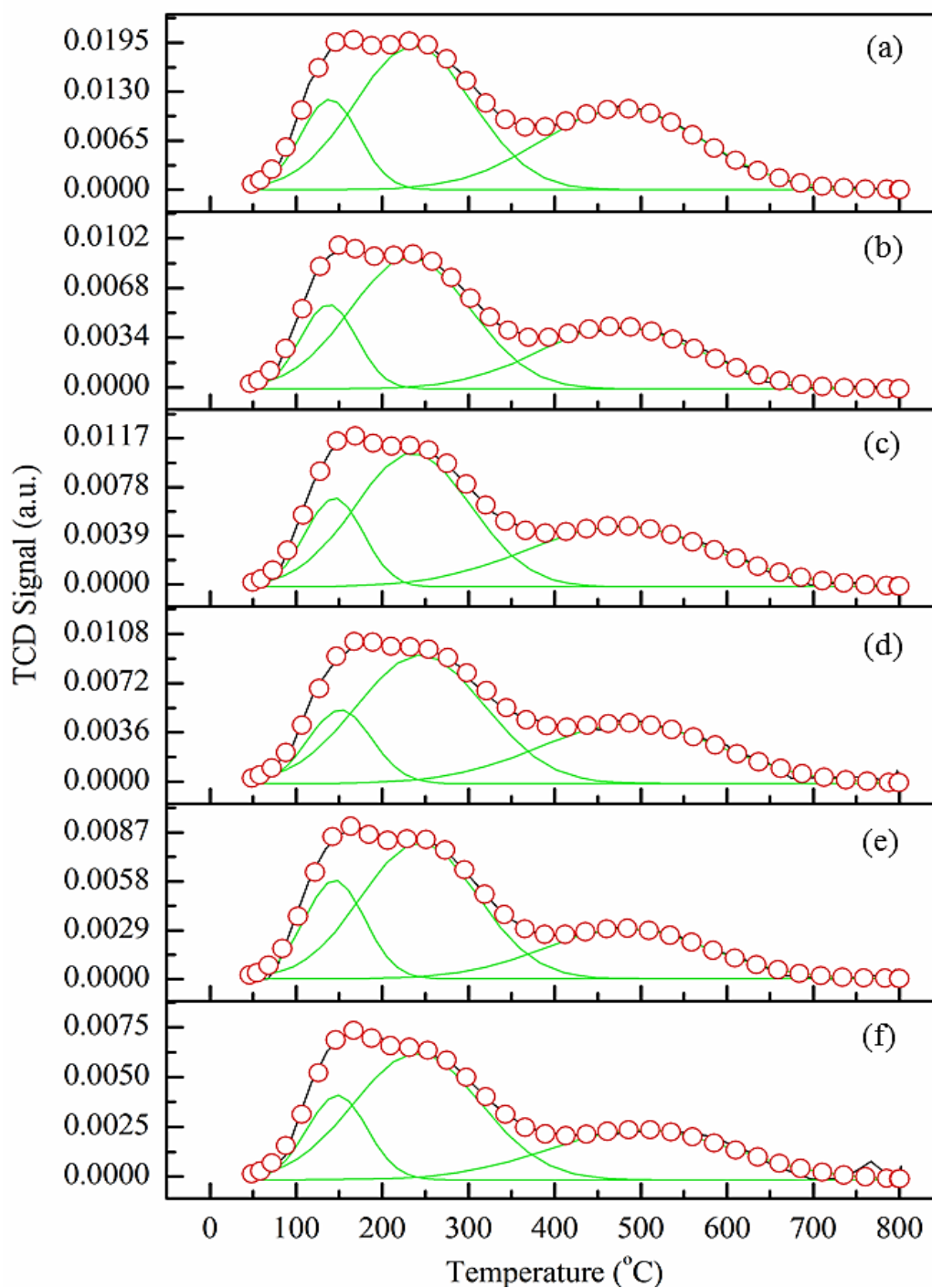


Figure 5.17 NH_3 -TPD profile of fresh zeolite, coked and regenerated samples with respect to regeneration temperature; (a) fresh ZSM-5, (b-e) regenerated at 140, 105, 95 and 75°C (regeneration duration 1 h) and (f) used catalyst (ZSM5-A).

Table 5.3 Summary of the NH₃-TPD results for fresh, used and regenerated zeolite samples and their physical characteristics

Regenerated condition		Total amount of desorbed NH ₃ •g ⁻¹ (mmol NH ₃ •g ⁻¹)	T _{max} * (°C) (from deconvolution curve)			Carbon content (wt.%)	BET surface area (m ² •g ⁻¹)	Microporous volume (cm ³ •g ⁻¹)	Mesoporous volume (cm ³ •g ⁻¹)
Temperature (°C)	Time (h)		T _{m1}	T _{m2}	T _{m3}				
95	4	1.48	147	243	487	0.6	326	0.13	0.16
95	2	1.25	142	236	472	0.8	339	0.13	0.17
95	1	1.15	144	236	476	1.2	304	0.12	0.15
75	1	1.04	138	232	475	1.4	-	-	-
105	1	1.03	151	244	487	1.6	-	-	-
140	1	0.80	145	244	482	1.7	-	-	-
Fresh ZSM5	-	2.09	139	237	478	-	361	0.13	0.18
Used ZSM5-A	-	0.68	148	241	500	2.5	283	0.11	0.15
Used ZSM5-B	-	-	-	-	-	9.9	28	0.01	0.09

*Temperature at the maximum in NH₃ desorption rate (°C) according to the strength of active site

From NH_3 -TPD analysis, a distribution of the acid sites according to their strength could be provided. Figures 5.18 reports, for different regeneration conditions, the relative amount of each category of acid sites (weak, medium and strong) with respect to the total amount of acid sites in the fresh ZSM-5 extrudate. With respect to fresh zeolite, the amount of acid sites in ZSM5-A decreased by about a factor 3, almost regardless of their strength.

As expected, the longer the regeneration, the higher the recovery of total acid sites, up to 71% of that of fresh catalyst after 4 h at 95°C (Figure 5.18 (a)). In more details, TPD profile deconvolution showed that time on stream mainly affected weak and medium acid sites, while the quantity of strong acid sites reached a quasi-plateau after 60 minutes. This level off of acidity restoration complied with the trend previously shown in Figure 5.11 (a) and Table 5.3 for carbon conversion. Thus the refractory coke fraction mainly blocked stronger acid sites, which are also known to promote oligomerization and condensation reactions (Elordi et al., 2011).

The increase of the regeneration temperature from 75°C to 100°C (Figure 5.18 (b)) improved the recovery of zeolite acidity. On the other hand, a further increase of the outlet temperature from 95°C to 140°C decreased the amount of all acid sites. Again this result matched well with the carbon removal performance.

The acidity of zeolites plays a key role in their catalytic behaviour. IR spectroscopy with adsorbed pyridine is the usual method to determine the acidity of catalysts. The lone-pair electrons of nitrogen are involved in different types of interactions with the surface acid sites. From pyridine adsorption results given in Table 5.4, it can be concluded that the sites able to retain pyridine at 350°C in fresh

catalyst were mainly of Brønsted type and they should represent the main fraction of medium and strong acid sites.

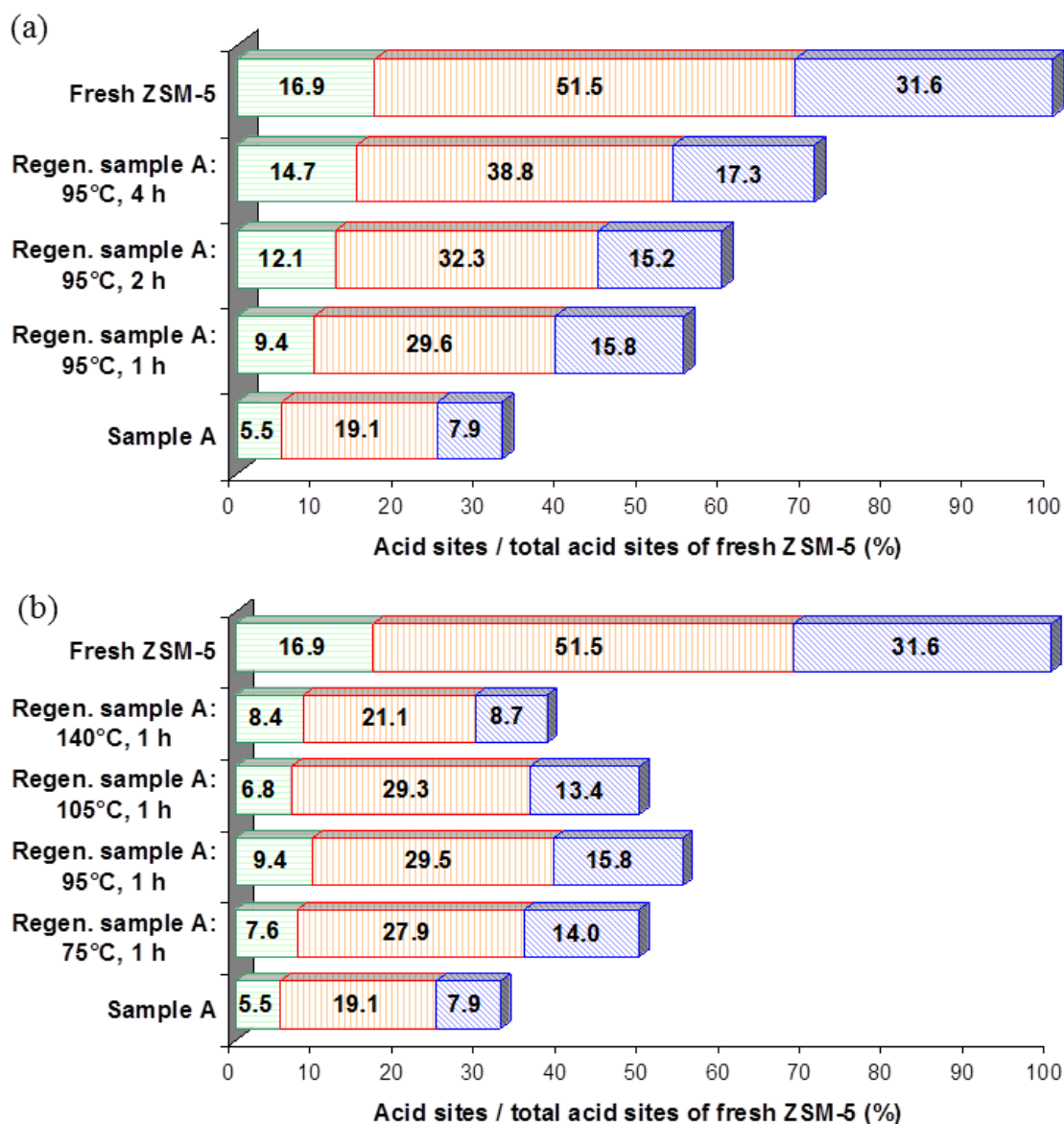


Figure 5.18 Distribution of acid sites for fresh zeolite, coked and regenerated ZSM5-A: (a) influence of regeneration duration and (b) influence of regeneration temperature.

Table 5.4 Acid properties of fresh and regenerated catalysts by pyridine adsorption method

Pyridine desorption temperature (°C)	Fresh zeolite extruded		ZSM5-A		(Partially) regenerated ZSM5-A (~100°C, 2 h)	
	Brønsted sites ($\mu\text{mol}\cdot\text{g}^{-1}$)	Lewis sites ($\mu\text{mol}\cdot\text{g}^{-1}$)	Brønsted sites ($\mu\text{mol}\cdot\text{g}^{-1}$)	Lewis sites ($\mu\text{mol}\cdot\text{g}^{-1}$)	Brønsted sites ($\mu\text{mol}\cdot\text{g}^{-1}$)	Lewis sites ($\mu\text{mol}\cdot\text{g}^{-1}$)
150	599	219	374	136	562	202
250	529	151	325	104	498	128
350	419	124	273	94	396	107

These results also suggest that both Brønsted and Lewis acid sites (estimated from desorption at 150°C) were in similar amounts on the partially regenerated catalyst at 95°C and on the fresh one (less than 10% difference). Moreover the strength of the Brønsted sites, that can be estimated from the ratio between the concentrations of pyridinium ions after desorption at 350°C and 150°C (Meloni et al., 2001), appeared also almost the same for both samples. This too optimistic results might be explained by a partial desorption of coke molecules from acid sites caused by pyridine, as previously reported (Meloni et al., 2001).

Noticeably the amount of total acid sites measured by pyridine adsorption/desorption method (estimated from desorption at 150°C) was lower than that from NH_3 -TPD. The difference between both techniques might be explained by the fact that the accessibility to pyridine of the microporous material was limited due to the large molecular size of pyridine. The underestimation of amount of acid sites by pyridine adsorption was previously mentioned by many researchers (Lee and Rhee, 1997; Wichterlová et al., 1998; Lü et al., 2003). Moreover the pyridine method

measured the remaining acid sites after desorption at 150°C, while for NH₃-TPD desorption started at a lower temperature (around 50°C) and therefore weaker acid sites were accounted for by the integration of the desorbed NH₃ amount.

5.3.2. PMMA degradation results

As previously described in chapter III, PMMA cracking tests of regenerated zeolites were performed in the 100 mL batch reactor (Mini Bench Top Reactor 4560) instead of the 250 mL batch reactor (High Pressure/High Temperature Reactor 4576) used in section 3.1.2.3. The reason for using of the 4560 reactor is that it shows several advantages, such as i) its compact size allows the experiment to be done with less materials (catalyst and PMMA), ii) its well-designed agitator with larger impeller (4-blade 45° pitched blade, see dimensions in Figure 3.10) in comparison with that of 4576 reactor enhances catalyst/PMMA mixing quality. Figure 5.19 compares the distribution of products from PMMA cracking obtained when using the different zeolites: fresh, coked (ZSM5-A and B), and after regeneration (varying TOS, as well as outlet temperature). After drying, the weight of solid (including catalyst) was in the range 0.39-0.43 g for all experiments: solid products accounting for less than 0.1% of the initial PMMA weight were not accounted for in the balance. These negligible solid contents obtained in this part (in comparison with those obtained in section 4.3) confirm the better mixing performance of 4560 reactor. The conversion of PMMA was thus considered total. The light fraction was mainly composed of MMA, while heavier liquid products were C6-C16 (consisting in aliphatic, alicyclic as well as aromatic compounds, most of them being oxygenated: dimethyl esters, carboxylic acids).

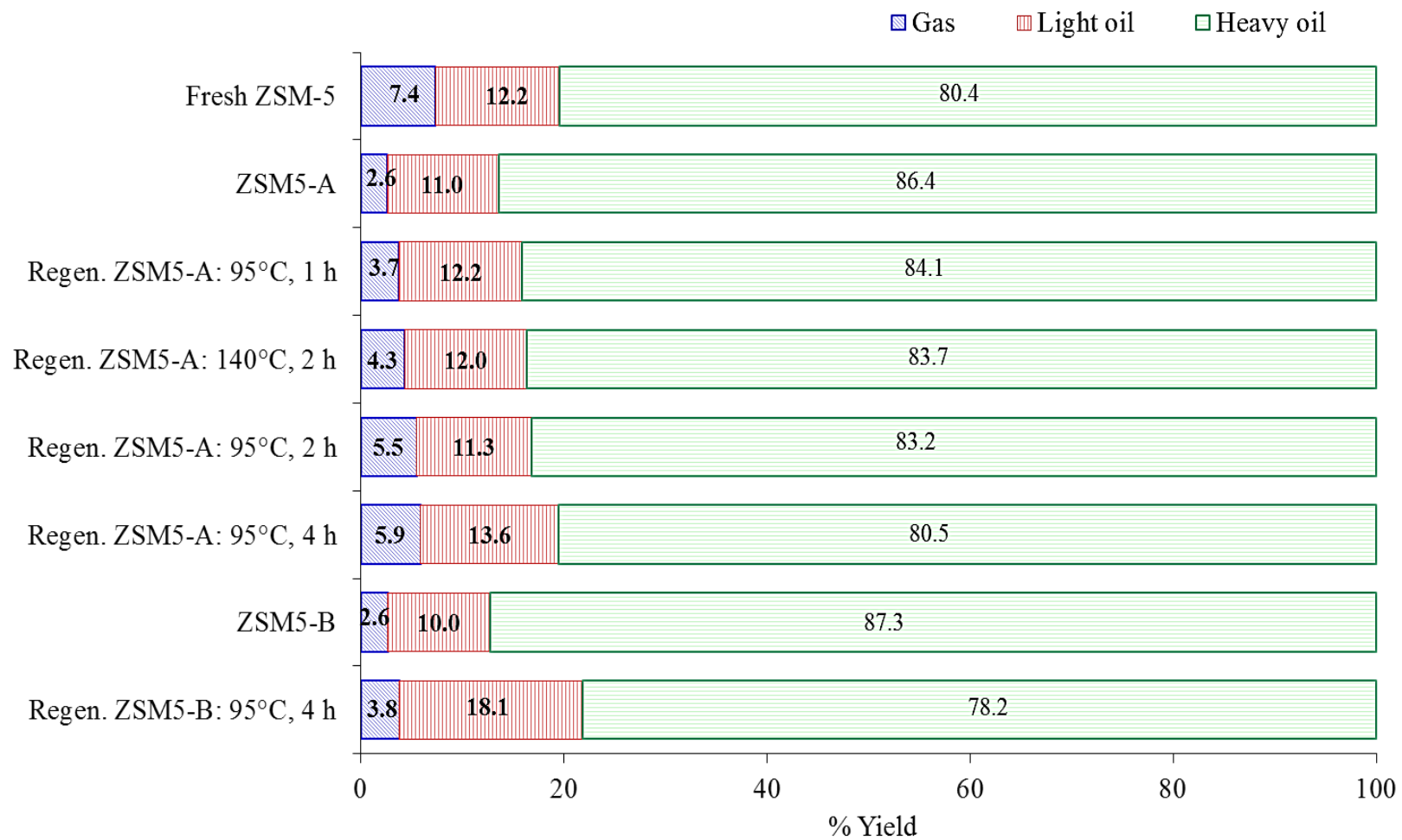


Figure 5.19 PMMA degradation yields: distribution of gas and liquid products.

As expected from the acidity and carbon removal results, increasing the regeneration duration improved the zeolite selectivity towards light hydrocarbons. After 4 h ozonation at 95°C, the regenerated zeolite gave almost the same (gas + light liquid) yield as the fresh one, yet with a smaller contribution of the gaseous compounds (especially for ZSM5-B). As previously shown, a temperature of 95°C was better than 140°C to restore the catalyst activity, but again main change was found in the gas yield. Therefore the differences in medium and strong acid sites observed between fresh and best regenerated zeolites affected only the ultimate stages of the cracking process, what should not be detrimental for the continuous process.

CHAPTER VI

CONCLUSIONS AND RECOMMENDATIONS

6.1 Degradation of PMMA by zeolite

Degradation of PMMA with various kinds of zeolite was successfully accomplished at investigated conditions (temperature range 300°C, 2 h with autogenous pressure in batch experiment, and 200°C to 300°C, 2-240 h at atmospheric in continuous experiment). Physicochemical properties of the samples were characterized by several techniques: thermogravimetry (thermal properties of PMMA), elemental analysis ($\text{SiO}_2/\text{Al}_2\text{O}_3$ ratio of zeolite), porosimetry (surface area and pore size of zeolite), X-ray diffraction (zeolite crystallinity), ammonia temperature-programme desorption (zeolite acidity).

In batch experiment, the thermal degradation of PMMA at 320°C is not suitable since it does not provide liquid product, but only non-condensed gases and jelly-like solid residue. The use of zeolites as catalyst can enhance the degradation of PMMA by reducing the reaction temperature and time. The product yield is mainly dependent on the acid properties of catalyst, both amount of acid sites and acid strength. The composition of the liquid product is directly related to the shape selectivity. In qualitative analysis, light fraction contains MMA monomer as a main component. Conversely heavy fraction contains various compounds, from C4 to C16, depending on the structure of zeolitic framework.

In continuous experiment, the increase of reaction temperature in the range of 200°C to 270°C shows a positive effect on liquid product yield. However, a further increase in reaction temperature above 270°C is not beneficial since the light product can be further cracked on catalyst active sites. The reaction temperature of 270°C appears as the most suitable for PMMA degradation. The light product obtained from this process is mainly MMA monomer as confirmed by GC-MS. This process is well workable over the PMMA feed rates studied - 0.2 to 0.8 $\text{g}\cdot\text{g}^{-1}_{\text{cat}}\cdot\text{h}^{-1}$ - with quite constant liquid product yield. The gaseous products obtained from the catalytic degradation of PMMA in continuous reactor are mostly MMA vapor due to the inadequate performance of condenser in this process.

6.2 Regeneration of used catalyst by ozonation

Regeneration of coked ZSM-5 extudates of 3 mm diameter was successfully achieved using ozone-enriched oxygen at temperature below 150°C. Physicochemical properties of the samples were characterized by several techniques: thermogravimetry (nature of coke deposit), elemental analysis (carbon content), porosimetry (surface area and pore size of zeolite), ammonia temperature-programme desorption and pyridine adsorption followed by infrared spectroscopy (zeolite acidity).

Reactions were carried out at various temperatures, gas hourly space velocities and inlet concentrations of ozone. They showed that partially coked samples (containing 3 wt.% of C) were successfully regenerated by ozone with carbon removal up to 80%, restoring specific surface area and 70% of acid sites. No dealumination was also observed. Carbon removal is improved by increasing the inlet ozone concentration in the range 16 to 50 $\text{g}\cdot\text{m}^{-3}$, with almost linear trend, and by

increasing time on stream despite the conversion seems to plateau after 2 h. Coke oxidation with O_3 starts at low temperature and exhibits an optimum at about 100°C . At high temperatures, the rate of ozone decomposition becomes much faster than its diffusion rate, so that radical species are no longer available for the coke deposit deep in the particles and the overall oxidation yield decreases. Indeed, catalytic decomposition of ozone is found to occur significantly above 100°C : O_3 decomposition reaches 90% with fresh ZSM-5 catalyst. Thus regeneration of coked zeolite particles involves both complex chemical reactions (coke oxidation and O_3 decomposition to active but instable species) and transport processes (pore diffusion to the internal coked surface).

Ozonation can restore both textural and acidic properties, allowing the catalyst to almost recover its initial activity in poly (methyl methacrylate) cracking. The activity results are well correlated with the carbon removal efficiency.

6.3 Recommendations

i) Since the degradation of PMMA by zeolite in this study was carried out in fixed bed reactor, it would be interesting to develop the process by applying fluidization technique which provides better heat / mass transfer and has a high capability to handle massive amounts of waste PMMA. In addition, this process could lessen the pore-clogging problem caused by the molten polymer, and could maintain the reaction temperature throughout the reactor. Moreover, in industrial applications, a fluidized bed system is often used because it is very easy to combine the cracking procedure with a parallel running regeneration process. If the catalyst tends to be deactivated, it can be easily replaced by fresh particles.

ii) Generally, commercial grade MMA monomer is at least $\geq 98.5\%$ purity. However, as seen in product analysis section, light fraction contains only 93%. MMA So a further purification of the product is necessary to reach specifications.

iii) As previously mentioned in Chapter IV, the problem in MMA recovery encountered leads to the underestimation of MMA monomer yield. So, a specially-designed condensing unit with high effective surface area and/or the use of ultra-cold fluid i.e. liquid nitrogen as coolant are needed. They would permit better condensation of MMA vapor and improve the precision of process performance evaluation.

iv) This study also found a positive effect of ozone concentration on carbon removal, unfortunately, it could be conducted under a narrow range owing to the limitation of ozone generator. It therefore would be interesting to investigate the effect of higher ozone concentrations for better catalyst regeneration and better understanding of this process. In addition, size of pellets should be varied to better understand O_3 diffusion effects during decoking. Moreover, economic evaluation of catalyst regeneration by ozonation process should be investigated and compared with that of classical processes.

NOMENCLATURE

Y_i	Product yield (%); i can refer to gas or liquid or solid
M_{Pd}	Mass of product (g)
M_{PMMA}	Mass of initial PMMA (g)
C_{ref}	Carbon content on reference half pellets (%)
C_s	Carbon content on zeolite samples (%)
$C_{O_3,in}$	Inlet ozone concentration ($g \cdot m^{-3}$)
$C_{O_3,out}$	Outlet ozone concentration ($g \cdot m^{-3}$)
P	Pressure (1 atm)
Q_G	Gas volume flow rate ($l \cdot h^{-1}$)
R	Gas constant ($0.0821 \text{ L atm K}^{-1} \text{ mol}^{-1}$)
T_{max}	Temperature at the maximum in NH_3 desorption rate ($^{\circ}C$)
T_{m1}	Temperature at the maximum in NH_3 desorption rate from deconvolution curve 1 ($^{\circ}C$)
T_{m2}	Temperature at the maximum in NH_3 desorption rate from deconvolution curve 2 ($^{\circ}C$)
T_{m3}	Temperature at the maximum in NH_3 desorption rate from deconvolution curve 3 ($^{\circ}C$)

REFERENCES

- Abbas, S.H. et al. The isomerization of cyclopropane over modified zeolite catalysts. In B. Imelik et al. (eds.), Catalysis by Zeolites, pp. 127-134. Amsterdam : Elsevier, 1980.
- Abrevaya, H. Cracking of naphtha range alkanes and naphthenes over zeolites. Studies in Surface Science and Catalysis 170 (2007) : 1244-1251.
- Achyut, K.P., Singh, R.K., and Mishra, D.K. Thermolysis of waste plastics to liquid fuel A suitable method for plastic waste management and manufacture of value added products—A world prospective. Renewable and Sustainable Energy Reviews 14 (2010) : 233-248.
- Aguado, J., Serrano, D.P., and Escola, J.M. Fuels from. Waste Plastics by Thermal and Catalytic Processes: A Review. Industrial & Engineering Chemistry Research 47 (2008) : 7982-7992.
- Aguado, J., Sotelo, J.L., Serrano, D.P., Calles, J.A., and Escola, J.M. Catalytic conversion of polyolefins into liquid fuels over MCM-41: comparison with ZSM-5 and amorphous SiO₂-Al₂O₃. Energy & Fuels 11 (1997) : 1225-1231.
- Al-Quraish, S.I. Microwave spent catalyst decoking method. United States Patent US 7,745,366 B2, 29 June 2010.
- Al-Salem, S.M., Lettieri, P., and Baeyens, J. Recycling and recovery routes of plastic solid waste (PSW): A review. Waste Management 29 (2009) : 2625–2643.

- Amornsit M. et al. Principles and techniques of instrumental analysis spectroscopy. second edition. Bangkok : Chulalongkorn University Press, 2011.
- Arisawa, H., and Brill, T.B. Kinetics and mechanisms of flash pyrolysis of poly(methyl methacrylate) (PMMA). Combustion and Flame 109 (1997) : 415-426.
- Arthur A. G., Salmiaton Ali., Jesús H. M. and Aaron A. Feedstock recycling of polymer wastes. Current Opinion in Solid State and Materials Science 8 (2004) : 419–425.
- Audiosio, G., Bertini, F., Beltrame, P.L., and Carniti, P. Catalytic degradation of polyolefins. Makromolekulare Chemie. Macromolecular Symposia. 57 (1992) : 191-209.
- Baerlocher, C., McCusker, L., and Olson, D.H. Atlas of Zeolite Framework Types. Sixth Revised Edition. Amsterdam : Elsevier, 2007.
- Bair, H.E. Thermal Analysis of Additives in Polymers. In E.A. Turi (ed.), Thermal Characterization of Polymeric Materials, second edition, pp. 2276. San Diego : Academic Press, 1997.
- Barrett, E.P., Joyner, L.G., and Halenda, P.H. The determination of pore volume and area distributions in porous substances. I. Computations from nitrogen isotherms. Journal of the American Chemical Society 73 (1951) : 373-380.
- Bartholomew, C. Catalyst Deactivation and Regeneration. In Kirk-Othmer Encyclopedia of Chemical Technology volume 5 Fifth edition, pp.255-322. New York : John Wiley & Sons, 2004.

- Bauer, F., and Karge, H.G. Characterization of coke on zeolites. Molecular Sieves 5 (2007) : 249-364.
- Blazsó, M., and Jakab, E. Effect of metals, metal oxides, and carboxylates on the thermal decomposition processes of poly-(vinyl chloride). Journal of Analytical and Applied Pyrolysis 49 (1999) : 125-143.
- Boyle, J.P. Ozone regeneration of platinum, and polymetallic platinum reforming catalysts. United States Patent 5,183,789, 2 February 1993.
- Brunauer, S., Emmett, P.H., and Teller, E. Adsorption of gases in multimolecular layers. Journal of the American Chemical Society 60 (1938) : 309–319.
- Buekens, A.G. and Huang, H. Catalytic plastics cracking for recovery of gasoline-range hydrocarbons from municipal plastic wastes. Resources, Conservation and Recycling 23 (1998) : 163–181
- Chen, D. Rebo, H. P. Moljord, K. and A. Holmen. Influence of Coke Deposition on Selectivity in Zeolite Catalysis. Industrial Engineering Chemical Research. 36 (1997) : 3473-3479.
- Chester, A., Green, L.A., Dhingra, S.S., Mason, T., Cho Timken, H. K. Catalytic cracking processing using an MCM-68 catalyst. United States Patent. US 7198711. Apr 3, 2007.
- Chester, A.W., and Derouane, E.G. (eds.). Zeolite Characterization and Catalysis A Tutorial,. Heidelberg : Springer, 2009.

- Copperthwaite, R.G., Hutchings, G.J., Johnston, P., and Orchard, S.W. Regeneration of pentasil zeolite catalysts using ozone and oxygen. Journal of the Chemical Society, Faraday Transactions 1 82 (1986) : 1007-1017.
- Costa, C., Lopes, J.M., Lemos, F., and Ribeiro F.R. Activity–acidity relationship in zeolite Y: Part 2. Determination of the acid strength distribution by temperature programmed desorption of ammonia. Journal of Molecular Catalysis A: Chemical 144 (1999) : 221-231.
- Damjanović, L., and Auroux, A. Determination of Acid/Base Properties by Temperature Programmed Desorption (TPD) and Adsorption Calorimetry. In Chester A.W., and Derouane E.G. (eds.), Zeolite Characterization and Catalysis A Tutorial, pp.107-167. Heidelberg : Springer, 2010.
- Dempsey, E. A tentative model of Y zeolites to explain their acid behavior. Journal of Catalysis 39 (1975) : 155-157, Cited in, Abbas, S.H. et al. The isomerization of cyclopropane over modified zeolite catalysts. In B. Imelik et al. (eds.), Catalysis by Zeolites, pp. 127-134. Amsterdam : Elsevier, 1980.
- Dempsey, E. Acid strength and aluminum site reactivity of Y zeolites. Journal of Catalysis 33 (1974) : 497-499, Cited in, Abbas, S.H. et al. The isomerization of cyclopropane over modified zeolite catalysts. In B. Imelik et al. (eds.), Catalysis by Zeolites, pp. 127-134. Amsterdam : Elsevier, 1980.
- Dempsey, E. Aluminum ion distributions in zeolites. Journal of Catalysis 49 (1977) : 115-119, Cited in, Abbas, S.H. et al. The isomerization of cyclopropane over modified zeolite catalysts. In B. Imelik et al. (eds.), Catalysis by Zeolites, pp. 127-134. Amsterdam : Elsevier, 1980.

- Elordi, G. et al. Catalytic pyrolysis of HDPE in continuous mode over zeolite catalysts in a conical spouted bed reactor. Journal of Analytical and Applied Pyrolysis 85 (2009) : 345-351.
- Elordi, G., Olazar, M., Artetxe, M., Castano, P., and Bilbao, J. Effect of the acidity of the HZSM-5 zeolite catalyst on the cracking of high density polyethylene in a conical spouted bed reactor. Applied Catalysis A: General 415-416 (2012) : 89-95.
- Elordi, G., Olazar, M., Lopez, G., Castano, P., and Bilbao, J. Role of pore structure in the deactivation of zeolites (HZSM-5, H β and HY) by coke in the pyrolysis of polyethylene in a conical spouted bed reactor. Applied Catalysis B: Environmental 102 (2011) : 224-231.
- Ferriol, M. Thermal degradation of poly(methyl methacrylate) (PMMA): modelling of DTG and TG curves. Polymer Degradation and Stability 79 (2003) : 271–281.
- Franck, J.P., and Martino, G. Deactivation and regeneration of catalytic-reforming catalysts. In J. Figueiredo (ed.), Progress in Catalysts Deactivation, pp. 355-397. The Hague : Martinus Nijhoff, 1982, Cited in, Bartholomew, C. Catalyst Deactivation and Regeneration. In Kirk-Othmer Encyclopedia of Chemical Technology, volume 5, fifth edition, pp.255-322. New York : John Wiley & Sons, 2004.
- Fyfe, C.A., Kennedy, G.J., De Schutter, C.T., and Kokotailo, G.T. Sorbate-induced structural changes in ZSM-5 (silicalite). Journal of the Chemical Society, Chemical Communications 8 (1984) : 541-542.

GAGGIONE SAS. POLYACRYLIC OR ACRYLIC RESIN (PMMA) [Online].

2007. Available from : <http://www.gaggione.com/downloads/polyacrylicoracrylicresinpmma.pdf> [2012, August 10]

Gartside, R.J., and Greene, M.I. Process of treating an olefin isomerization catalyst and feedstock. United States Patent Application Publication US 2003/0004385 A1, 2 January 2003.

Gentilhomme, A., Cochez, M., Oget, N., and Mieloszynski, J.L. Thermal degradation of poly(methyl methacrylate) (PMMA): modelling of DTG and TG curves. Polymer Degradation and Stability 79 (2003) : 271-281.

Guisnet, M., and Ribeiro, F.R. Deactivation and Regeneration of Zeolite Catalysts. Catalytic Science Series 9. Singapore : Imperial College Press, 2011.

Guy, L., and Fixari, B. Waxy polyethylenes from solution thermolysis of high density polyethylene: inert and H-donor solvent dilution effect. Polymer 40 (1999) : 2845-2857.

Holland, B.J., and Hay, J.N. The effect of polymerisation conditions on the kinetics and mechanisms of thermal degradation of PMMA. Polymer Degradation and Stability 77 (2002) : 435-439, Cited in, Pielichowski, K., and Njuguna, J. Thermal Degradation of Polymeric Materials. Shropshire : Rapra Technology Limited, 2005.

Horvath, G., and Kawazoe, K. Method for the calculation of effective pore size distribution in molecular sieve carbon. Journal of Chemical Engineering of Japan 16 (1983) : 470-475.

- Hutchings, G.J. et al. A comparative-study of reactivation of zeolite- γ using oxygen and ozone oxygen mixtures. Applied Catalysis 34 (1987) : 153-161.
- Ivanov, D.P., Sobolev, V.I., and Panov, G.I. Deactivation by coking and regeneration of zeolite catalysts for benzene-to-phenol oxidation. Applied Catalysis A 241 (2003) : 113-121.
- Yun, J. H., Structure and reactivity of dehydroxylated Brønsted acid sites in H-ZSM-5 zeolite: Generation of stable organic radical and catalytic activity for isobutene conversion. Thesis submitted to the Faculty of the University of Delaware in partial fulfilment of the requirements for the degree of Master of Chemical Engineering. (2011).
- Jolly, S., Sausey, J., and Lavally, J.C. FT-IR characterization of carbenium ions, intermediates in hydrocarbon reaction on H-ZSM-5 zeolites. Catalysis Letters 24 (1994) : 141-146.
- Kaminsky, W., and Franck, J. Monomer recovery by pyrolysis of polymethyl methacrylate (PMMA). Journal of Analytical and Applied Pyrolysis 19 (1991) : 311-318.
- Kaminsky, W., Predel, M., and Sadiki, A. Feedstock recycling of polymers by pyrolysis in a fluidised bed. Polymer Degradation and Stability 85 (2004) : 1045-1050.
- Kaminsky, W., Schmidt, H., and Simon, C.M. Recycling of mixed plastics by pyrolysis in a fluidized bed. Macromolecular Symposia 152 (2000) : 191-199.

- Kang, B.S., Kim, S.G., and Kim, J.S. Thermal degradation of poly (methyl methacrylate) polymers: Kinetics and recovery of monomers using a fluidized bed reactor. Journal of Analytical and Applied Pyrolysis 81 (2008) : 7-13.
- Kashiwagi, T. et al. Effects of weak linkages on the thermal and oxidative degradation of poly (methyl methacrylates). Macromolecules 19 (1986) : 2160-2168, Cited in, Ferriol, M., Gentilhomme, A., Cochez, M., Oget, N., and Mieloszynski, J.L. Thermal degradation of poly(methyl methacrylate) (PMMA): modelling of DTG and TG curves. Polymer Degradation and Stability 79 (2003) : 271-281.
- Krassimir, G. Ozone decomposition over silver-loaded perlite. International Journal of Civil and Environmental Engineering 3:3 (2011) : 202-205
- Lee, J.K., and Rhee, H.K.. Effect of metal/acid balance in Pt-loaded large pore zeolites on the hydroisomerization of n-hexane and n-heptane. Korean Journal of Chemical Engineering 14 (1997) : 451-458.
- Lin, Y.H., Hwu, W.H., Ger, M.D., Yeh, T.F., and Dwyer, J. A combined kinetic and mechanistic modeling of the catalytic of polymers. Journal of Molecular Catalysis A: Chemical 171 (2001) : 143-151.
- Liu, C. et al. Effect of ZSM-5 on the aromatization performance in cracking catalyst. Journal of Molecular Catalysis A: Chemical 215 (2004) : 195-199.
- López, A. et al. Deactivation and regeneration of ZSM-5 zeolite in catalytic pyrolysis of plastic wastes. Waste Management 31 (2011) : 1852–1858.
- Lowery, R.E., and Wright, J.L. Process for making magnesium oxide spheres. United States Patent 5,134,103, 28 July 1992.

- Lü, R., Tangbo, H., Wang, O., and Xiang, S. Properties and Characterization of Modified HZSM-5 Zeolites. Journal of Natural Gas Chemistry 12 (2003) : 56-62.
- Lutz, W. et al. Investigations of the mechanism of dealumination of zeolite Y by steam: Tuned mesopore formation versus the Si/Al ratio. Studies in Surface Science and Catalysis 154 (2004) : 1411-1417.
- Madorsky, S.L. Rates and activation energies of thermal degradation of styrene and acrylate polymers in a vacuum. Journal of Polymer Science 11 (1953): 491-506.
- Manring, L.E. Thermal degradation of poly(methyl methacrylate). 2. Vinyl-terminated polymer. Macromolecules 22(1989) : 2673-2677, Cited in, Pielichowski, K., and Njuguna, J. Thermal Degradation of Polymeric Materials. Shropshire : Rapra Technology Limited, 2005.
- Manring, L.E. Thermal degradation of poly(methyl methacrylate). 4. Random side-group scission. Macromolecules 24 (1991) : 3304-3309, Cited in, Ferriol, M. Thermal degradation of poly(methyl methacrylate) (PMMA): modelling of DTG and TG curves. Polymer Degradation and Stability 79 (2003) : 271–281.
- Marcilla, A., Gómez-Siurana, A., and Berenguer, D. Effect of regeneration temperature and time on the activity of HUSY and HZSM5 zeolites during the catalytic pyrolysis of polyethylene. Journal of Analytical and Applied Pyrolysis 74 (2005) : 361–369.

- Mariey, L. Lamotte, J. Chevreau T. and Lavalley, J.C. FT-IR study of coked HY zeolite regeneration using oxygen or ozone. Reaction Kinetics and Catalysis Letters Vol. 59, No. 2, (1996) : 241-246.
- Martens, J.A., and Jacobs, P.A. Introduction to Acid Catalysis with Zeolites in Hydrocarbon Reactions. In H. Van Bekkum, E.M. Flanigen, P.A. Jacobs, and J.C. Jansen (eds.), Introduction to Zeolite Science and Practice, pp. 633-671. Amsterdam : Elsevier, 2001.
- Martins, G.V.A. et al. Quantification of Brønsted Acid Sites in Microporous Catalysts by a Combined FTIR and NH₃-TPD Study. The Journal of Physical Chemistry C 112 (2008) : 7193-7200.
- Mathias, L.J. Poly (methyl methacrylate). The Macrogalleria level 2: Polymers Up Close and Personal [Online]. 2005. Available from : <http://www.pslc.ws/mactest/level2.htm> [2012, August 10]
- Meloni, D., Martin, D., Ayrault, P., and Guisnet, M. Influence of carbonaceous deposits on the acidity of a zeolite with two non-interconnected pore systems: MCM-22. Catalysis Letters 71 (2001) : 213-217.
- Michael, J. V. Thermal decomposition of ozone. The Journal of Chemical Physics 54 (1971) : 4455-4459
- Mohammed, A.H.A.K., Karim, S., and Rahman, A.M. Characterization and Cracking Activity of Zeolite Prepared from Local Kaolin. Iraqi Journal of Chemical and Petroleum Engineering 11 (2010) : 35-42.

- Monneyron, P., Mathe, S., Manero, M.H., and Foussard, J.N. Regeneration of High Silica Zeolites via Advanced Oxidation Processes—A Preliminary Study About Adsorbent Reactivity Toward Ozone. Chemical Engineering Research and Design 81 (2003) : 1193-1198.
- Montgomery, D.P. Regeneration of isomerization catalysts containing magnesium oxide. United States Patent 4,217,244, 12 August 1980.
- Ngamcharussrivichai, C. Wu, P. Tatsumi, T. Active and selective catalyst for liquid phase Beckmann rearrangement of cyclohexanone oxime. Journal of Catalysis 235 (2005) : 139-149
- Ngamcharussrivichai, C. Wu, P. Tatsumi, T. Liquid-phase Beckmann rearrangement of cyclohexanone oxime over mesoporous molecular sieve catalysts. Journal of Catalysis 227 (2004) : 448-458.
- Njuguna, J. Thermal Degradation of Polymeric Materials. Shropshire : Rapra Technology Limited, 2005.
- Oriňák, A., Halás, L., Amar, I., Andersson, J.T., and Ádámová, M. Co-pyrolysis of polymethyl methacrylate with brown coal. Fuel 85 (2006) : 12-18.
- Pecak, W.E. Reactivation of a magnesium oxide catalyst. United States Patent 3,962,126, 8 June 1976.
- Peterson, J.D., Vyazovkin, S., and Wigh, C.A. Kinetic Study of Stabilizing Effect of Oxygen on Thermal Degradation of Poly(methyl methacrylate). The Journal of Physical Chemistry B 103 (1999) : 8087-8092, Cited in, Pielichowski, K., and

Pfeiffer, P.W., Bronxville, N.Y., and Garrett, L.W. Staged fluidized catalyst regeneration process. United States Patent 3,563,911, 16 February 1971.

Pielichowski, K., and Njuguna, J. Thermal Degradation of Polymeric Materials. Shropshire : Rapra Technology Limited, 2005.

Read more: <http://www.faqs.org/patents/app/20110089081#b#ixzz2IA33oEkH>

Rozwadowski, M., Wojsz, R., Wisniewski, K.E., and Kornatowski, J. Description of adsorption equilibrium on type A zeolites with use of the Polanyi-Dubinin potential theory. Zeolites 9 (1989) : 503-508.

Salam, L.A., Matthews, R.D., and Robertson, H. Pyrolysis of polymethylmethacrylate (PMMA) binder in thermoelectric greentapes made by the tapecasting method. Journal of the European Ceramic Society 20 (2000) : 335-345.

Scheirs, J., and Kaminsky, W. Feedstock Recycling and Pyrolysis of waste Plastics: Converting Waste Plastics into Diesel and Other Fuels. Wiltshire : John Wiley & Sons, 2006.

Serrano, D.P., Aguado, J., and Escola, J.M. Catalytic cracking of a polyolefin mixture over different acid solid catalysts. Industrial & Engineering Chemistry Research 39 (2000) : 1177-1184.

Sidney, W. Benson AND Arthue, E. Axworthy, JR. Mechanism of the gas phase, thermal decomposition of ozone. The Journal of Chemical Physics 26 (1957) :1718-1726.

Smolders, K., and Baeyens, J. Thermal degradation of PMMA in fluidised beds. Waste Management 24 (2004) : 849-857.

Srinakruang, J. Process for producing fuel from plastic waste material by using dolomite catalyst. United States Patent US 2011/0089081A1, Apr. 21, 2011.

Stephen, R. Ely and Naperville. Ozone decomposition. United States Patent US 4,691,821 B2, Oct. 28, 1986.

Thai MMA Co., Ltd. คุณสมบัติทางกายภาพของ Shinkoilite DX [Online]. 2011. Available from : <http://www.thaimma.com/spec-shinkolite-dx.php> [2012, August 10]

Toju S. Kpere-Daibo, Plastic Catalytic Degradation Study of the role of external catalytic surface, Catalytic Reusability and Temperature Effects, A Thesis submitted for the degree of Doctor of Philosophy of the University of London, Department of Chemical Engineering University College London, London, WC1E 7JE, (2009).

Treacy, M.M.J., and Higgins, J.B. Collection of Simulated XRD Powder Patterns for Zeolites. Fourth Revised Edition. Amsterdam : Elsevier, 2001.

Van Bekkum, H., Flanigen, E.M., Jacobs, P.A., and Jansen, J.C. Introduction to Zeolite Science and Practice. Studies in Surface Science and Catalysis 137. Amsterdam : Elsevier, 2001.

Van Bokhoven, J.A. et al. An Explanation for the Enhanced Activity for Light Alkane Conversion in Mildly Steam Dealuminated Mordenite: The Dominant Role of Adsorption. Journal of Catalysis 202 (2001) : 129-140.

- Villaescusa, L.A., Barrett, P.A., and Cambor, M.A. ITQ-7: A New Pure Silica Polymorph with a Three-Dimensional System of Large Pore Channels. Angewandte Chemie International Edition 38 (1999) : 1997-2000.
- Vogelaar, B.M., Van Langeveld, A.D., Eijsbouts, S., and Moulijn, J.A. Analysis of coke deposition profiles in commercial spent hydroprocessing catalysts using Raman spectroscopy. Fuel 86 (2007) : 1122-1129.
- Wagner, P. et al. CIT-5: a high-silica zeolite with 14-ring pores. Chemical Communications 22 (1997) : 2179-2180.
- Wampler, T.P. Thermometric behavior of polyolefins. Journal of Analytical and Applied Pyrolysis 15 (1989) : 187-195.
- Wang, B., and Manos, G. A novel thermogravimetric method for coke precursor characterisation. Journal of Catalysis 250 (2007) : 121 - 127.
- Wichterlová, B., Tvarůžková, Z., Sobalík, Z., and Sarv, Z. Determination and properties of acid sites in H-ferrierite A comparison of ferrierite and MFI structures. Microporous and Mesoporous Materials 24 (1998) : 223-233.
- Wilkie, C.A. TGA/FTIR: an extremely useful technique for studying polymer degradation. Polymer Degradation and Stability 66 (1999) : 301-306, Cited in,
- Yan, Z. et al. On the acid-dealumination of USY zeolite: a solid state NMR investigation. Journal of Molecular Catalysis A: Chemical 194 (2003) : 153-167.
- Ylä-Mella, J. RECYCLING OF POLYMERS [Online]. 2005. Available from : <http://www oulu.fi/resopt/PlastRec.pdf> [2012, August 10].

APPENDICES

APPENDIX A

OZONE CONCENTRATION AND PRODUCTION

A laboratory ozone generator (HTU-500 ozone generator, Azcozon) was used to produce ozone from pure oxygen, in the range of concentration 16 to 50 $\text{g}\cdot\text{m}^{-3}$. This ozone generator produces the gas by corona discharge methods. In this method, oxygen gas was passed through an electrically charged chamber which electrically converts the oxygen into ozone. Figure A-1 shows ozone concentration and production provided by HTU-500 ozone generator (Voltage: 120V/60Hz).

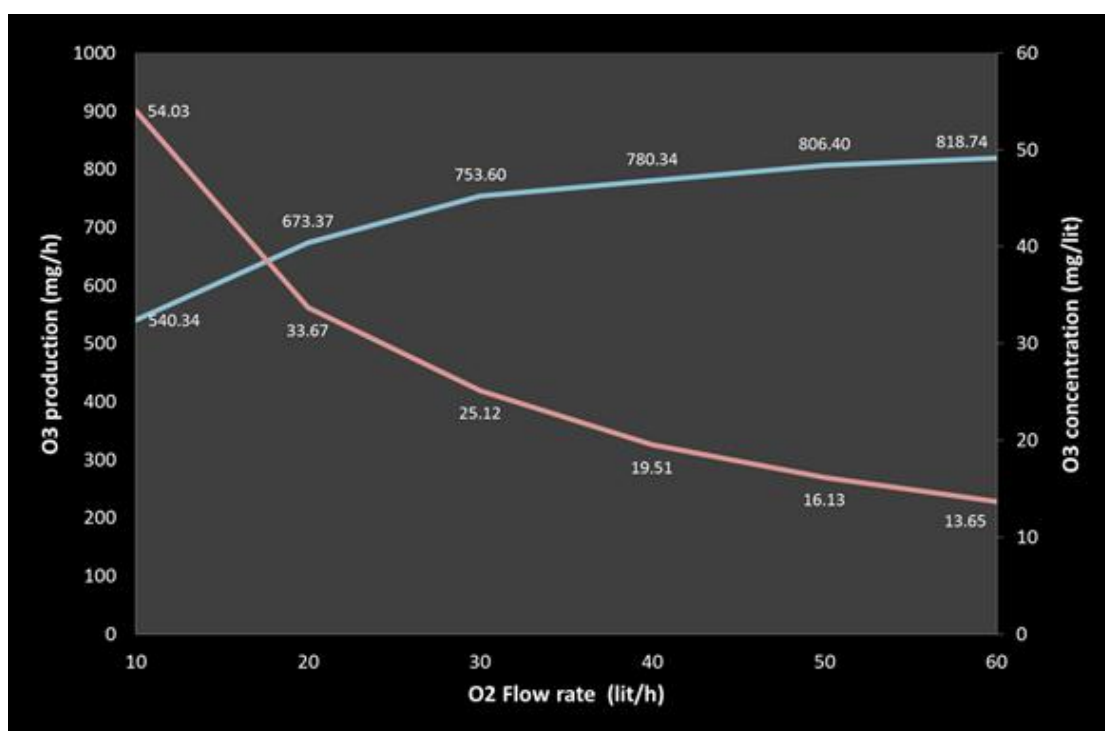


Figure A-1 Ozone concentration and production at various flows rate (20°C).

APPENDIX B

DECONVOLUTION OF TPD CURVE

Deconvolution technique was used to interpret the data which difficultly resolved from TPD curve of coked sample. The evaluation of the total free acid sites was done by subtraction of TPD profile of TPD with/without NH_3 using software Origin Pro 8.5.

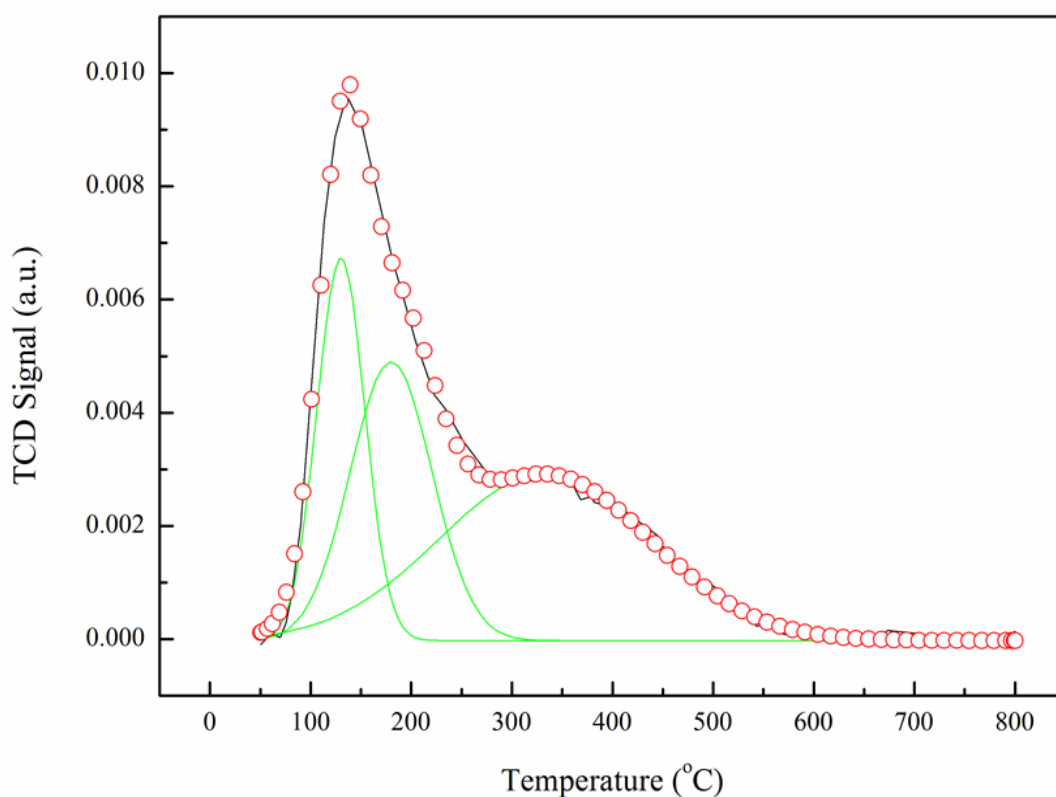


Figure B-1 NH_3 -TPD profile of amorphous silica-alumina (ASA) and its deconvolution curve.

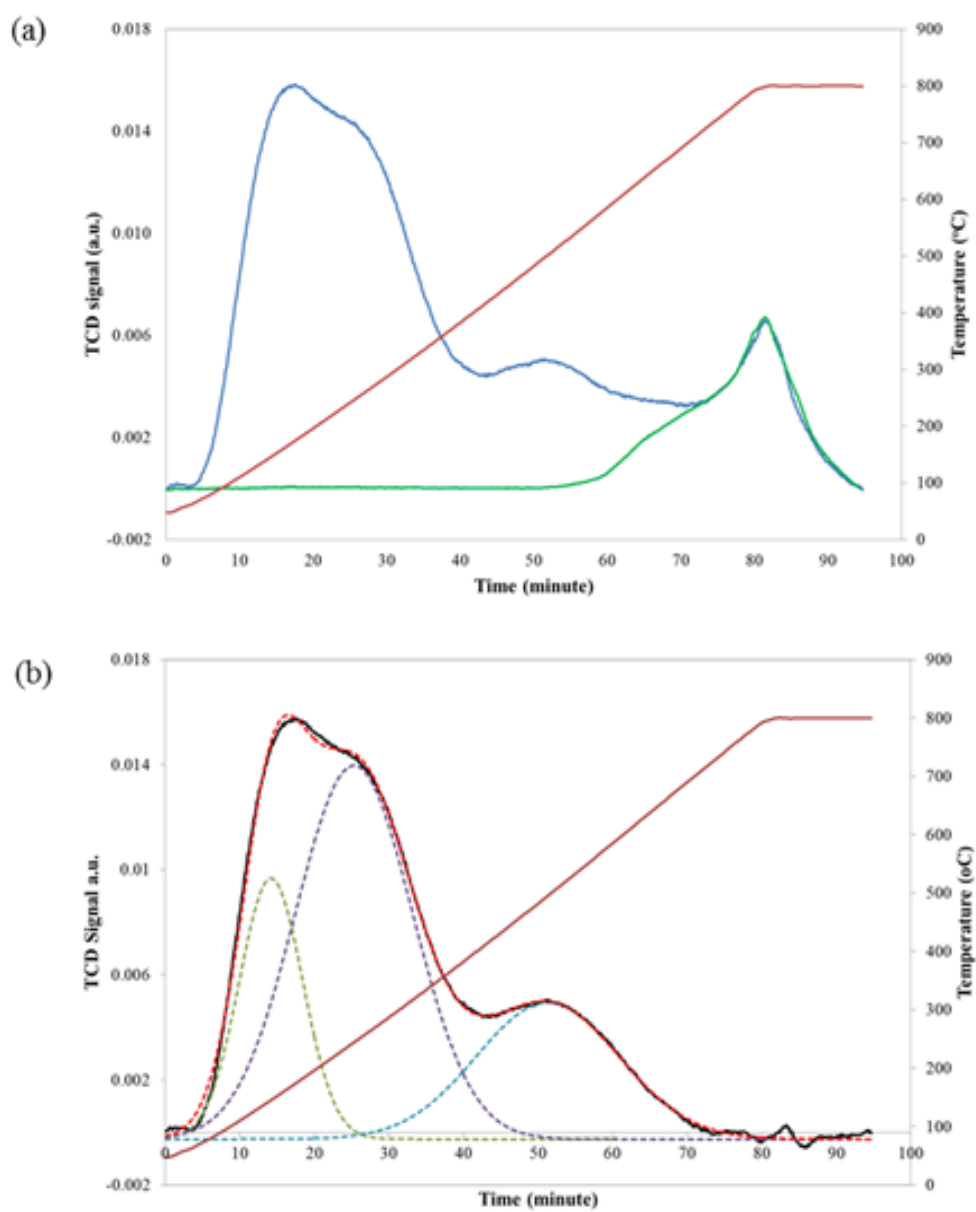


Figure B-2 NH_3 -TPD profile of used ZSM-5; (a) raw TCD signal and signal from blank test and (b) subtracted TPD profile and its deconvolution curve.

Publications and conferences:

KHANGKHAM, S., NGAMCHARUSSRIVICHAI, C., AND DAMRONGLERD, S., “PROCESS DEVELOPMENT FOR USED MOLECULAR SIEVE REGENERATION”, Technology and Innovation for Sustainable Development Conference, TISD 2006, Khon Kaen, Thailand, January 25-26, 2006.

KHANGKHAM, S., NGAMCHARUSSRIVICHAI, C., AND DAMRONGLERD, S., “PROCESS DEVELOPMENT FOR USED MOLECULAR SIEVE REGENERATION”, The 10 th Asian Conference on Fluidized-Bed and Three-Phase Reactors., ASCON 2006., Busan, Korea, November 26-29, 2006.

WORAMANKARAT, S., KHANGKHAM, S., NGAMCHARUSSRIVICHAI, C., AND DAMRONGLERD, S., “SYNTHESIS OF ZSM-5 ZEOLITE FROM NATURAL KAOLIN” ASCON – IEECE., 1st Asian Conference on Innovative Energy & Environmental Chemical Engineering – A New Paradigm Emerging from Fluidized-Bed and Three-Phase Reactors., Hokkaido University, Sapporo, Japan, August 31 – September 3, 2008.

BOONSONGPRASERT, M., KHANGKHAM, S., NGAMCHARUSSRIVICHAI, C., AND DAMRONGLERD, S., “SYNTHESIS OF NA-X ZEOLITE FROM NATURAL KAOLIN” ASCON – IEECE., 1st Asian Conference on Innovative Energy & Environmental Chemical Engineering – A New Paradigm Emerging from Fluidized-Bed and Three-Phase Reactors., Hokkaido University, Sapporo, Japan, August 31 – September 3, 2008.

KHANGKHAM, S., NGAMCHARUSSRIVICHAI, C., AND DAMRONGLERD, S., “CATALYTIC OXIDATION OF VOLATILE ORGANIC COMPOUNDS (VOCS) ON ZEOLITE CATALYSTS SYNTHESIZED FROM NATURAL KAOLIN”, CHE-USDC CONGRESS I, Chonburi, Thailand, September 5-7, 2008.

KHANGKHAM, S., JULCOUR C., DAMRONGLERD, S., NGAMCHARUSSRIVICHAI, C., MANERO, M-H, DELMAS, H., “REGENERATION OF COKED ZEOLITE BY OZONATION” IOA-EA3G Conference & Exhibition, Toulouse, France, June 4-6, 2011.

Abstract: Catalytic degradation of PMMA was successfully performed at temperatures below 300°C. The use of zeolite catalyst could reduce reaction temperature in comparison with an ordinary thermal degradation process. It was found that the product distribution obtained from batch experiments depends on zeolite acid properties whereas the composition of the liquid fraction is directly related to the shape selectivity of the catalyst. A continuous fixed bed process was designed that allowed to obtain MMA monomer as main product. The increase of reaction temperature from 200 to 270°C showed a positive effect on the liquid product yield. However, at higher temperatures, the light product was further cracked into gaseous products. Significant deactivation of ZSM-5 catalyst due to coking was observed after 120 hours of operation, resulting in a decrease in liquid product yield.

Regeneration of the coked ZSM-5 extrudates was achieved by oxidation with ozone at low temperatures, below 150°C. The effects of temperature, GHSV and inlet concentration of ozone on carbon removal efficiency were studied. Carbon removal with ozone started at 50°C and reached a maximum of 80% at 100°C. Higher temperatures were not beneficial due to the strong limitation of ozone diffusion which confines radical production then the regeneration process to the outer surface. In optimal conditions, ozonation almost fully restored the zeolite activity without damaging the texture and active sites of zeolite, as shown from the results of regenerated catalyst in PMMA cracking.

Résumé : La dégradation catalytique du PMMA a été réalisée avec succès à des températures inférieures à 300°C. L'utilisation de zéolithe comme catalyseur a permis de réduire la température de réaction par rapport aux procédés classiques de dégradation thermique. La distribution des produits de réaction obtenus en réacteur discontinu dépend des propriétés acides du catalyseur, tandis que la composition de la fraction liquide est directement liée à la sélectivité de forme du catalyseur. Un procédé continu à lit fixe a été développé qui a permis d'obtenir le monomère MMA comme produit principal. L'augmentation de la température de réaction de 200 à 270°C a montré un effet positif sur le rendement en produit liquide. Cependant, des températures de réaction supérieures ont favorisé le craquage du monomère en produits gazeux. Une désactivation significative de la zéolithe ZSM-5 a été observée après 120 heures d'opération, entraînant une diminution du rendement en produit liquide.

La régénération des extrudés de ZSM-5 cokés a été obtenue par oxydation à l'air ozoné à des températures basses, inférieures à 150°C. Les effets de la température, de la vitesse spatiale de gaz et de la concentration en ozone sur l'efficacité d'élimination du carbone ont été étudiés. Le décokage par l'ozone débute dès 50°C et montre un optimum à 100°C (avec une conversion de 80%). Des températures plus élevées ne sont pas bénéfiques, en raison de la forte limitation de la diffusion interne de l'ozone qui confine la production de radicaux, et donc le processus de régénération, à une mince couche externe. Dans les conditions optimales, l'ozonation a presque complètement restauré l'activité de la zéolithe sans en endommager la texture et les sites actifs, comme le montrent les résultats de craquage du PMMA obtenus avec le catalyseur ainsi régénéré.